THE PROCEEDINGS OF
THE PHYSICAL SOCIETY

VOL. 50, PART 4 *July* 1, 1938 NO. 280

THE ELASTIC PROPERTIES OF SODIUM WIRES BETWEEN – 183° AND 90° C.

BY RALPH H. V. M. DAWTON, B.SC., Davy Faraday Laboratory
of the Royal Institution, London

Received 20 *January* 1938. *Read* 25 *March* 1938

ABSTRACT. The elastic properties of single-crystal wires and of polycrystalline sodium are investigated. The results obtained with single crystals are found to be in good agreement with a theory recently given by Fuchs. The characteristic temperature Θ is calculated from the data obtained with the polycrystalline material. A comparison is made with the authors recent X-ray measurements.

§ 1. INTRODUCTION

THE present paper deals with the elastic properties of sodium wires at various temperatures including a close approach to the melting-point. Certain parts of the work are linked up with the author's recent X-ray investigation of sodium(1), in the course of which some numerical data were obtained for the characteristic temperature Θ. This temperature is closely connected with the elastic constants, as is well known from the Debye theory. It can be obtained independently from experiments on elastic properties and thus affords a check on the X-ray data. The second part of the paper, dealing with the elastic properties of single crystals in different crystallographic directions, is interesting in connexion with a theory recently given by Fuchs(2).

A few months after the experiments had been started, two short notes dealing with the elastic constants of sodium at 80° K. appeared in the *Physical Review*(3). The first of these furnished evidence of a considerable discrepancy between the experiments and Fuchs's theory. In the second note the authors rectified an error in their calculations and claimed to have found a good agreement between theory and observation; such agreement is found in the present work also. The agreement between the experimental data is particularly satisfactory in view of the differences in the experimental technique. The American authors worked with ultrasonic vibrations, whereas the present measurements were made with comparatively slow oscillations whose frequencies lay between 20 and 200 c./sec.

§ 2. EXPERIMENTAL DETAILS

The torsion modulus. A cylindrical magnet attached to the free end of a vertical sodium rod or wire is set into resonant oscillation by means of a variable speed alternator connected to a pair of Helmholtz coils. The torsion modulus of a polycrystalline rod is given by

$$\frac{8\pi lI}{r^4p^2} \qquad \text{......(1),}$$

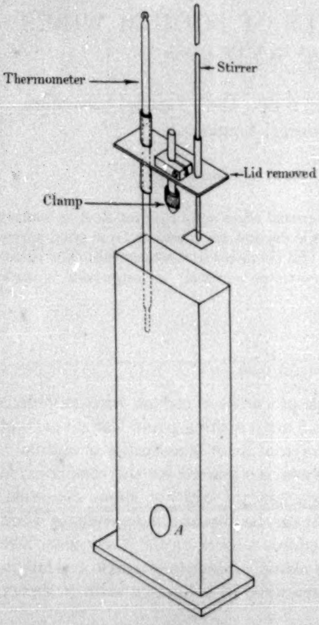

Figure 1.

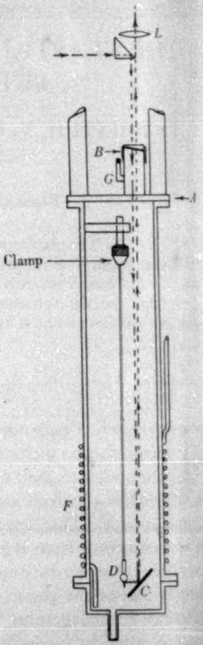

Figure 2.

where I is the moment of inertia of the magnet about the axis of oscillation, l and r are the length and radius of the rod, and p is the resonance period. The correction term due to the moment of inertia of the rod is negligible. Oscillatory current up to 60 c./sec. is obtained by reversing direct current with a commutator, and for frequencies between 30 and 500 c./sec. an alternator giving a sinusoidal output of 10 cycles per revolution is used. The speed of these machines is accurately controlled. The period of the vibrating magnet is deduced from the measured number of revolutions per second.

Measurements from 20 to 90° c. are made with the specimen immersed in oil in a copper container measuring 22 × 8 × 2½ cm. (figure 1). The lid of the container has a stirrer, a thermometer and a serrated four-jawed clamp which holds the upper end of the torsion rod. *A* is a glass window for the beam from the mirror. Purified thin paraffin oil is used, and a correction for its effect on the oscillator is applied. The outside of the container is fitted with flat electrical heaters, not shown on the drawing. For the measurements between 20 and − 183° C. the specimen is placed in an atmosphere of an inert gas. The gas-container, figure 2, which fits inside a Dewar flask, is a brass tube whose top end is bolted to a plate *A* and whose lower end contains a mirror *C*, adjustable by means of three screws which can be made to have a gas-tight fit.

The vibrations are made visible with the aid of light reflected from a small mirror at the free end of the oscillator. The light passes through a window *B*, is reflected at *C* on to the mirror of the oscillator *D*, and travels back along its own path. An image ¼ mm. wide is formed 80 cm. away by the lens *L*. When necessary a Dewar vessel, sliding in guides and containing either solid carbon dioxide and alcohol or liquid oxygen, is raised from below. To protect the sodium and promote temperature-equilibrium an inert gas, either argon or nitrogen, precooled by a spiral *F*, enters the lower end and leaves the upper end of the vessel by the non-return valve *G*. Oxygen and moisture are removed from the gas by causing the latter to pass first through a vessel containing about 15 ft. of sodium wire, then over 3 ft. of sodium wire in a tube heated to 75° C., and finally through a liquid-air trap.

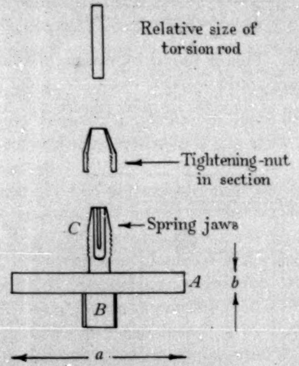

Figure 3.

The sodium specimen is made to vibrate by the action of the alternating field on a steel rod *A* (figure 3). This rod is attached to the free end of the sodium wire by a clamp with two serrated jaws which fit the diameter of the wire. The mirror *B* enables the vibrations to be observed. Five different clamps and rods are used, each having a different moment of inertia (see table 1). Uniform results are obtained so that, in view of column 7, we infer that the longitudinal stress to which the rod is necessarily subjected does not affect the torsion modulus. The resonance frequency is easily observable at all temperatures.

Table 1

Oscillator	*a* (cm.)	*b* (cm.)	Total weight *W* (g.)	Moment of inertia (g.-cm²)	Diameter of torsion rod (cm.)	Stress on torsion rod due to *W* (g./mm²)	Range of periods used (sec.)
No. 1	3·45	0·27	3·3	1·25	0·11	3·5	0·048 to 0·064
No. 2	3·25	0·35	4·1	2·20	0·2	1·3	0·023 to 0·04
No. 3	4·17	0·42	5·78	8·54	0·23	1·4	0·024 to 0·04
No. 4	3·0	0·48	5·1	3·24	0·24	1·1	0·015 to 0·025
No. 5	3·1	0·5	6·1	3·28	0·33	0·72	0·010 to 0·012

The extension modulus. This is found by means of transverse vibrations of the sodium specimen. The apparatus consists of a rectangular gas-container measuring 14 × 5 × 2·5 cm. with one of its sides of glass (figure 4). A beam or rod of sodium is held by a clamp *A*. An iron wire 2 mm. long is pushed into the sodium at the free end. Vibrations of the specimen are caused by the intermittent pull exerted on this iron wire by the magnet *B*, and are observed with a microscope. An estimate of the temperature factor is made by surrounding the beam (except at its extreme free end) with a concentric copper tube (not shown) fixed to the copper back of the container. This back forms part of a box, shown dotted, which is filled

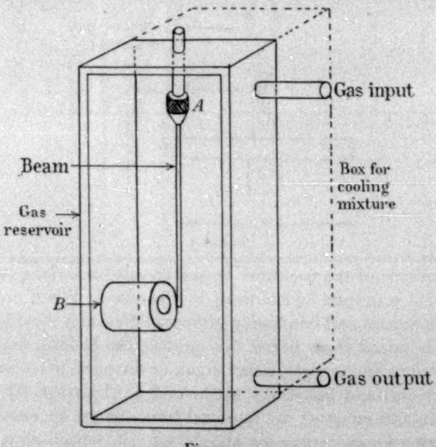

Figure 4.

with solid carbon dioxide and alcohol. The temperature of the copper tube is measured by a thermocouple. The resonance period of the beam is excited when the period of the alternating current is 2, 4, 6, ... times that of the beam. The extension modulus is given by the well-known expression

$$Y=\frac{4\pi^2 l^3}{3Ip^2}\left(M_0+\frac{33}{140}M\right) \qquad \text{......(2),}$$

where l is the length of the beam, I its moment of inertia, M its mass, M_0 the weight of the load at the extreme end, and p the resonance period.

Production of sodium rods. The polycrystalline rods are extruded from a sodium press. They vary from 1 to 3·3 mm. in diameter, and appear to be uniform in thickness if prepared with care. Single-crystal rods are formed by sucking molten sodium up a glass tube which is then cooled along its length. When cold the sodium rods can easily be ejected. They usually have a slight taper. The accidental bending of the rod during mounting is nowhere sufficient to give a radius of curvature less than 10 cm. During the process of mounting the oil apparatus is filled with purified paraffin; for the gas-container purified petroleum ether with a boiling-point of 40 to 60° is used, the container being filled with the liquid until the mounting is complete and the apparatus is gas-tight. The petroleum ether is then replaced by the inert gas.

Performance of apparatus. The determination of the torsion modulus requires a knowledge of (*a*) the moments of inertia of the oscillators, (*b*) the resonance period, (*c*) the effective length of the torsion rod, and (*d*) the radius of the torsion rod. (*a*) The moments of inertia are calculated and checked by comparing their ratios. (*b*) The amplitude of the resonance vibration, at 20° c., falls to half its value if the motor-speed is changed by 2½ per cent. At − 183° c. the peak is sharper, and a beat is often observed when the motor is just off resonance speed. The specimens continue their vibrations when the external field is switched off. They perform about 10 oscillations at room temperature and about 70 oscillations at − 180° c. before the amplitude falls to half its value. The periods of the vibrations of square-topped wave-form, determined by the reversing commutator, and of those of sinusoidal wave-form, determined by the alternator, are the same. The period is independent of the amplitude provided the amplitude does not exceed ½°. The effect of the oil is found by comparing the periods of a copper torsion wire in air and in oil. The oil increases the period by 5·4 per cent at 20° c. and by 5·3 per cent at 90° c. The correction is almost independent of the oscillator and of its frequency. (*c*) With an error not exceeding 1·5 per cent the distance between the clamps may be taken as the length of the rod, if this is greater than 6·5 cm. In general lengths between 11 and 15 cm. are used. For rods shorter than 6·5 cm. the square of the period is no longer proportional to the length, the apparent reason being that in order to produce an observable amplitude the short rods are strained beyond the elastic limit. (*d*) Except for the smallest wire the values of r^4 as determined by microscope readings and by weighing usually agreed to 1·5 per cent. For the smallest fibre the discrepancy is doubled. The measurements of the extension modulus are less accurate than those of the torsion modulus. The force maintaining the oscillation is not a push-pull, as in the torsion experiments, but an intermittent pull. The mass of the last 1 mm. of the beam, which contains the iron wire, is considered to be the M_0 in equation (2), and l is the full length less 1 mm. Beams are circular in section and between 1·1 and 3·3 mm. in diameter. The period is constant up to amplitudes of 0·5 mm., the smallest observable being 0·05 mm. An apparent decrease in the modulus occurs for the beams of largest diameter if their lengths are less than 4 cm. Such specimens are probably strained beyond their elastic limit even at small amplitudes. Higher harmonics of vibration are absent and there is no difference between vertical and horizontal beams. A rotation of the beam round its axis does not affect its period.

§ 3. RESULTS AND CONCLUSIONS

Polycrystalline rods; torsion modulus. The experiments show that the torsion modulus often varies by from 5 to 10 per cent. These variations are most probably due to the variation in the microstructure of the rods. It is well known that the individual crystals in polycrystalline sodium are much larger than those found in other metals, as is shown clearly in the typical Laue photograph, figure 5*a*. In a material consisting of a comparatively small number of individual units oriented at random, the statistical fluctuations are bound to be more pronounced than in a very fine-grained material. The temperature coefficients of the individual rods vary very little. The investigation of the torsion modulus is therefore carried out in the neighbourhood of 20° c. The modulus does not appear to be altered by bending the rods to a radius of 5 cm. and straightening or even giving them a permanent twist of 180°. The maximum error for any one experiment does not

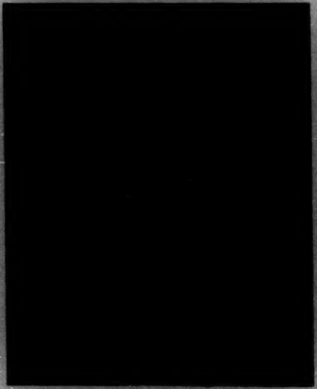

Figure 5*a*.

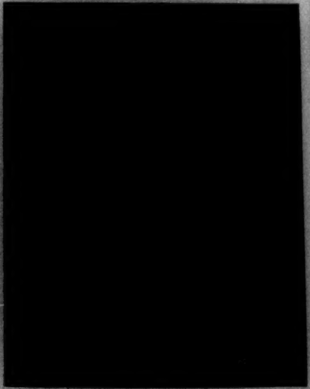

Figure 5*b*.

exceed ± 8 per cent for the rods 1·1 mm. in diameter, and is about 6 per cent for the other rods. The data observed at room temperature are given in table 2.

Table 2

Diameter of torsion rod (cm.)	Sample of sodium	Torsion modulus at 20° C. (10^9 dyne/cm^2)
0·115	Commercial	9·0
0·115	,,	9·7
0·17	,,	8·9
0·17	,,	9·9
0·17	,,	10·8
0·20	,,	9·7
0·20	,,	7·8
0·20	,,	10·3
0·20	,,	9·6
0·20	,,	9·4
0·24	,,	8·6
0·24	,,	10·0
0·24	,,	9·7
0·24	,,	9·0
0·24	,,	9·5
0·24	,,	8·9
0·33	Hopkins and Williams commercial	9·6
0·33	,,	9·4
0·33	,,	9·3
0·24	,,	9·7
0·24	,,	10·0
0·33	Hopkins and Williams; analytical reagent purity	9·8
0·24	Kahlbaum; analytical reagent purity	9·9
0·24	,,	10·8
0·24	,,	11·3
		Mean = 9·6

Oxidation of a rod causes a serious error at low temperatures; a 3-per-cent oxidation results in a 13-per-cent increase in the temperature coefficient. The oxidation was estimated by comparing the weight of the rod with that of an unused portion from which it was cut. The final results, for which the oxidation is less than 1 per cent, are given in table 3 and in figure 6. The torsion modulus is nearly a linear function of the temperature. The large value of the temperature coefficient is consistent with the considerable thermal expansion of sodium.

Polycrystalline rods; the extension modulus. The values of this are given in table 4; they vary with the diameter of the rod. The measurements become more consistent as the diameter decreases, but the experiments obviously do not yield an accurate value. Rough measurements from 20 to −70° C. indicate that the temperature coefficient is about 10 per cent greater than that of the torsion modulus. The extension modulus as calculated from the bulk modulus and the torsion modulus of table 2 is 28×10^9. This value, which is almost independent of the bulk modulus, may be compared with the experimental values in table 4.

Table 3

Temperature (° C.)	Torsional modulus in terms of its value at 20° C.
90	0·81 0·815 0·79 0·805 0·814
− 79	1·23 1·19 1·21
− 183	1·5 1·51 1·48 1·47

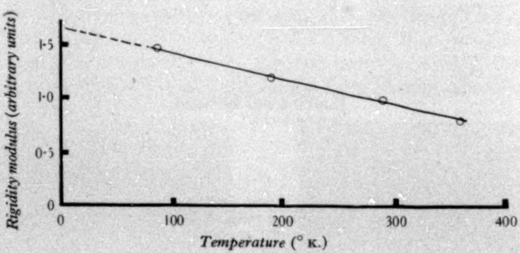

Figure 6.

Table 4

Diameter of beam (mm.)					
2·2		2·0		1·1	
Length (cm.)	Extension modulus (10⁹ dyne/cm²)	Length (cm.)	Extension modulus (10⁹ dyne/cm²)	Length (cm.)	Extension modulus (10⁹ dyne/cm²)
7·1	35	7·1	29·5	4·0	22·5
7·0	35	7·2	22·6	7·0	22·9
3·8	29	3·7	23·6	7·0	23·4
6·0	31	7·2	35·6	7·0	26·0
7·3	41	5·3	36·4	6·6	27·0
6·8	29	4·0	32·2	6·9	29·0
				7·0	29·0
	Mean, 33		Mean, 30		Mean, 26

Polycrystalline rods; the characteristic temperature Θ. The characteristic temperature is calculated in accordance with the theory of Debye(4). Assuming the validity of the standard relationships between the elastic moduli, the Debye formula may be transformed into one in terms of the torsion modulus and extension modulus. It is seen that the extension modulus contributes only about 2 per cent of the result, and hence an approximate value for this modulus is sufficient. Θ depends roughly on the square root of the torsion modulus. A close agreement between the values determined from X-ray measurements and from the elastic constants is not to be expected at higher temperatures, but for lower temperatures the agreement is better. The two curves are shown in figure 7. The values extrapolated to absolute zero are reasonably consistent with the theoretical figure given by Fuchs.

Single-crystal rods. The material is examined by the aid of X rays to ensure that the specimen is a single crystal; a typical Laue photograph is shown in figure 5*b*. No great care seems necessary in handling these crystals: a rod deliberately bent to a radius of 5 cm. and straightened had its torsion modulus reduced from $17{\cdot}0 \times 10^9$ to $15{\cdot}3 \times 10^9$, and the accidental bending is far less than this. The resonance vibrations do not damage the crystals.

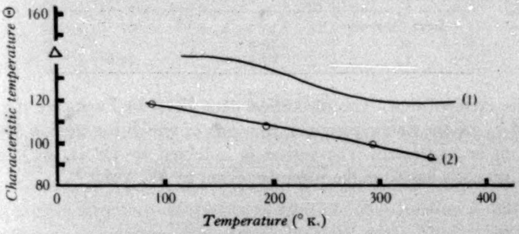

Figure 7. Δ, theoretical point found by Fuchs; (1), author's previous X-ray curve; (2), author's points from elastic constants.

The torsion modulus at 20° c. varies between 9×10^9 and 35×10^9, while the extension modulus varies between 31×10^9 and 14×10^9. In table 5 the results are classified in two groups (*a*) and (*b*). In group (*a*) the axis of the rod is parallel to the 100 direction. One of the values is questioned because the rod after being cooled to −79° c., and reheated for 20° c., shows resonance for two speeds of the alternator. These periods give the torsion modulus as 31×10^9 (the original value) and as 22×10^9. The cause of this double resonance is not understood; it happened only once in about 40 experiments.

The variations of the temperature coefficient as a result of successive cooling and heating amount sometimes to 30 per cent, and are caused chiefly by changes in the torsion modulus at room temperatures. Within 10 per cent no systematic difference is found between single crystals and the polycrystalline material.

In order to compare the theoretical values of Fuchs with the experimental data an extrapolation to absolute zero of temperature is carried out by drawing a straight line through the observed points. The procedure gives probably too high a value for the elastic constants, but the error is not likely to be large considering the small

Table 5A

Displacement of axis of rod from 100 direction (degrees)	Torsion modulus at 20° C. (10^9 dyne/cm.^{2})	Extension modulus at 20° C. (10^9 dyne/cm.^{2})
3	35	14·5
10	30 (?)	—
11·5	20	14
17·5	17	—
20·5	17	—
33	12	29

Table 5B

Displacement of axis of rod from 110 direction (degrees)	Torsion modulus at 20° C. (10^9 dyne/cm.^{2})	Extension modulus at 20° C. (10^9 dyne/cm.^{2})
Less than 2	9·0	31
10	10·4	—
11	11·5	24·6

range of the extrapolation. The theoretical data given by Fuchs are the constants c_{11}, c_{12} and c_{44} of the elastic potential, in terms of which the torsion and Young's modulus can be expressed. The author is indebted to Dr H. A. Jahn for this calculation which is based on the formulae given by W. Voigt$^{(5)}$.

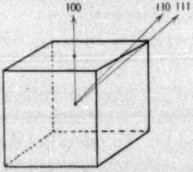

Figure 8.

Table 6

Direction of axis	Young's modulus (10^9 dyne/cm.^{2})		Torsion modulus (10^9 dyne/cm.^{2})	
	Theoretical	Experimental (extrapolated to absolute zero)	Theoretical	Experimental (extrapolated to absolute zero)
111	144	—	10	—
110	58	56	—	15
100	20·6	26	58	59

On comparison of the observations with Fuchs's theoretical data there seems to be no doubt that the theory can not only account for the order of magnitude of the elastic constants but also give their correct variation with direction in the anisotropic medium.

§ 4. ACKNOWLEDGEMENTS

The author is glad to express his indebtedness to the Managers of the Royal Institution and to Sir William Bragg for permission to carry out this work. He expresses his thanks to Dr A. Müller for suggesting it and for continuous interest and advice.

REFERENCES

(1) Dawton, R. *Proc. Phys. Soc.* **49**, 294 (1937).
(2) Fuchs, K. *Proc. Roy. Soc.* **157**, 444 (1936).
(3) Siegel, S. *Phys. Rev.* **51**, 1015 (1937).
Quimby, S. L. and Siegel, Sidney. *Phys. Rev.* **52**, 665 (1937).
(4) Debye, P. *Ann. Phys., Lpz.*, 4 F., **39**, 789 (1912).
(5) Voigt, W. *Ann. Phys., Lpz.*, 4 F., **16**, 398 (1882).

DISCUSSION

Dr A. Müller. It is to be expected that the elastic properties of a metal are structure-insensitive. Mr Dawton's experimental data are in reasonably good agreement with theoretical predictions, and show that the present-day theory of metal lattices can explain structure-insensitive properties. The situation is quite different when structure-sensitive properties are to be dealt with. The author's previous experiments on the hysteresis effect observed with X-ray reflection from sodium are still unexplained.

Dr R. M. Davies. One minor criticism of the paper relates to nomenclature; with the one exception of figure 6, the author consistently uses the term "torsion modulus" instead of the well-established "rigidity modulus". Apart from other considerations, this terminology has the disadvantage of clashing with the usage of engineers, who use the term "torsion modulus" to denote the ratio of the so-called "torsional rigidity" (torque per twist per unit length) to the rigidity modulus.* In the case of a rod of circular cross-section, the rigidity modulus of the engineers is thus $\frac{1}{2}\pi$ (radius)^4, and, in general, it is a quantity of the fourth power of a linear dimension.

The author's statement that the period of forced torsional vibration was independent of the amplitude "provided that the amplitude does not exceed $\frac{1}{2}^\circ$" is probably connected with the fact that, in the case of the forced vibration of a bar loaded with a magnet and driven by an alternating magnetic field, the period p_a corresponding to maximum amplitude will depend on (i) the magnetic moment of the magnet, (ii) the peak value of the driving field.* Alternatively, one may say that p_a will depend on the amplitude of forced vibration of the bar, since the amplitude depends on the magnetic moment and upon the driving field. However, when the amplitude approaches zero, p_a approaches p, the free period, corresponding to zero magnetic moment and zero driving field, and in accurate measurements of Young's modulus and the rigidity modulus by the alternating field method it is necessary to extrapolate the observed p_as to conditions of vanishingly small amplitudes as shown in the papers quoted above.

---

* R. V. Southwell, *Theory of Elasticity*, p. 323 (Oxford 1936).

Another point which may be mentioned is the restricted validity of equation (2), which is used to calculate Young's modulus from experimental observations. In the notation of equation (2), the general equation for Y in the case of the transverse vibrations of a loaded bar may be written

$$Y=\frac{4\pi^2 M}{Ip^2}\frac{l^3}{z^4} \qquad \ldots\ldots(1a),$$

where z is a numeric determined by the ratio M_0/M.

Equation (2), which is Rayleigh's approximation, may be derived from equation (1a) by writing

$$\frac{1}{z^4}=\frac{1}{3}\left(\frac{M_0}{M}+\frac{33}{140}\right) \qquad \ldots\ldots(2a),$$

and this approximation is valid only when $M_0 \gg M$.

In general, the value of the parameter z is given by the transcendental equation†

$$1+\cosh z\cos z=\frac{M_0 z}{M}(\cosh z\sin z-\sinh z\cos z);$$

an explicit solution of this equation, suitable for numerical calculation, has been given.‡

The data given in the present paper are insufficient to determine the value of the ratio M/M_0, but it appears that M_0 is comparatively small in comparison with M, and, under these conditions the Rayleigh approximation can be seriously in error. For the purpose of illustration, assume that M_0 is negligible in comparison with M; equation (2a) gives $\frac{1}{z^4}=\frac{11}{140}=0{\cdot}07857$, whereas the true value is $(1/12{\cdot}36)$, equal to 0·08090; the value is thus 3 per cent in error, and consequently the value of Y calculated from equation (2) will be 3 per cent too small.

Another possible source of error in equation (2) is due to neglect of the effect due to the rotation and shearing of the elements of the bar when in vibration.§ The correction for this effect becomes appreciable only when the length of the bar is not negligible in comparison with its cross-sectional dimensions, and calculation shows that the maximum value of the correction amounts to about ½ per cent in the experiments described in the paper. In the present instance, the correction is probably less than the experimental error, but in certain cases it may become important.

---

* R. M. Davies and E. G. James, *Phil. Mag.* **18**, 1023 and 1053 (1934); R. M. Davies and I. H. Thomas, *Phil. Mag.* **23**, 361 (1937).

† J. Prescott, *Applied Elasticity*, p. 213 (London, 1924).

‡ R. M. Davies, *Phil. Mag.* **22**, 892 (1936).

§ R. M. Davies, *Phil. Mag.* **23**, 1129 (1937).

Prof. ALLAN FERGUSON said that the constant $\frac{33}{140}$ used in the calculation of Young's modulus assumes that the shape of a cantilever is the same during vibration as during statical deflection. He asked whether the assumption was justifiable in the present case and suggested that the constant $\frac{33}{140}$ might need correction.

AUTHOR's reply. The points raised by Dr Davies do not appear to necessitate any alteration which would affect the results, except for the 3-per-cent correction which may be applied to the values of Y. I must thank him for this, and also for the calculation of the $\frac{1}{2}$-per-cent error due to the rotation and shearing of the elements of the bar in vibration.

On account of the difficulty in determining the shape of the bent beams I regret that I cannot answer Prof. Ferguson's question.

THERMIONIC EMISSION FROM CARBON

By A. L. REIMANN, Ph.D., D.Sc.

Communication from the Research Staff of the M.O. Valve Co. Ltd.,
at the G.E.C. Research Laboratories, Wembley, England

Communicated by Dr C. C. Paterson. Received 18 *February* 1938. *Read in title* 27 *May* 1938

ABSTRACT. Observations of the thermionic emission from a carefully outgassed filament of graphitic carbon were made at a series of temperatures between 1665° and 2191° K. The corresponding values of the constants A and ψ in the empirical emission formula

$$i = AT^2 \epsilon^{-\psi/kT}$$

were found to be 30 amp./cm.^{2}-deg.^{2} and 4·34 eV. respectively.

§ 1. INTRODUCTION

Carbon is one of the elements for which the thermionic data hitherto obtained are somewhat unsatisfactory. Thus for the constants A and ψ in the emission formula

$$i = AT^2 \epsilon^{-\psi/kT}$$

Langmuir$^{(1)}$ in 1913 obtained the values

$$\rho A = 5 \times 10^{-4} \text{ amp./cm.}^2\text{-deg.}^2, \quad \psi = 2\cdot 5 \text{ ev.},$$

where ρ represents the roughness factor for the emitting surface. Such a small value for ρA is altogether improbable in view of the values that have been obtained for other clean emitters, and it seems likely that the surface of Langmuir's specimen was not really clean. A few years later, Langmuir$^{(2)}$ obtained a value of 3·88 ev. for ψ, as against his previous 2·5 ev., but no value was given for A. At about the same time, Lester$^{(3)}$ measured the internal latent heat of evaporation of electrons, which, as Becker and Brattain$^{(4)}$ have pointed out, must be the same as ψ. For this he found the value of 4·52 ev. Finally, Langmuir$^{(5)}$, in yet another determination, has obtained the values

$$\rho A = 5\cdot 93 \text{ amp./cm.}^2\text{-deg.}^2, \quad \psi = 3\cdot 94 \text{ ev.}$$

This value of ρA is much nearer the expected order of magnitude than is Langmuir's first value, but it still appears to be somewhat low. All this earlier work was carried out at a time when the need for prolonged outgassing of the filament for the removal of impurities was not realized as it is now, and so it appeared desirable to undertake a fresh study of the emission from this element.

§ 2. THE EXPERIMENTAL TUBE

The electrode system is shown in figure 1. F is a straight carbon filament 0·31 mm. in diameter and 10 cm. long, held taut by the spring S. L is a flexible lead of stranded copper wire, which carries the bulk of the filament current, only an inappreciable fraction of it passing through the spring. Two previously outgassed nickel cylinders *C* are welded to the heavy nickel wires (also previously outgassed) to which the ends of the filaments are joined. Not only do these help to keep the nickel wires cool, but they enable them to be given a subsidiary outgassing while the tube is on the pump, by high-frequency induction heating of the cylinders. *A* is an outgassed molybdenum electron-collecting electrode of coarse mesh, 5 cm. long and of oval section measuring 3 cm. by 1·2 cm. This is separated by 5-mm. gaps at each end from two similar guard electrodes *B*, each 1 cm. long. *G* is an outgassed nickel getter cup, which holds a copper-clad barium getter pellet.

By holding the electrodes *B* as much negative with respect to the centre of *F* as *A* is positive, electrons are collected from a length of 5·5 cm. in the central region of the filament, while the emission from the remainder, near the ends, is suppressed. The object of using mesh, and not sheet, electrodes was to facilitate the escape of radiant energy from the filament and to ensure that during operation the collecting and guard electrodes should keep as cool as possible. The gaps between *A* and *B* were made relatively large with the intention of viewing the filament through one of the gaps in finding its brightness temperature as a function of heating current with the optical pyrometer. This, however, was not possible, after all, owing to the considerable blackening suffered by the walls of the tube in consequence of the deposition of nickel from the cylinders *C* during their induction heating, and so the temperature calibration was carried out subsequently, with the filament in a fresh bulb.

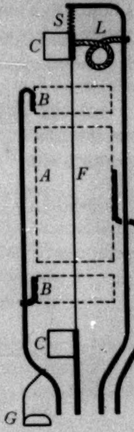

Figure 1. The electrode system.

The carbon filament was prepared according to standard practice in the carbon-filament-lamp industry in which cellulose in the form of pure white blotting paper is dissolved in a strong solution of zinc chloride, and the viscous syrup so produced is squirted through a glass die of appropriate size into a jar of acidified alcohol. Under these conditions the cellulose is regenerated in the form of a thread, which coils itself in the alcohol. The thread is left to harden for some days and washed repeatedly until it is free from zinc chloride, and is then wound on to a large drum to dry. The dried thread is tough, and feels like a violin string. It is now set into its final shape by means of a carbon former, and the complete assembly is packed in graphite powder in a crucible and baked in a furnace to a temperature approaching 1500° c. The carbonized filament is then mounted on its nickel support wires. The ends of these are hollowed out to take the ends of the filament, and an electrically sound joint is made by passing a current through the joints while they are immersed in a bath of a hydrocarbon. The joints become very hot and the carbon deposited on them from the hydrocarbon completes the joint.

In order to ensure that the filament shall be uniform in diameter, it is next flashed, that is, heated by a current in a hydrocarbon atmosphere; heavy petroleum vapour is used. In this way irregularities are removed, since the thinner parts of the filament are raised to a higher temperature than the rest and so receive a thicker deposit of carbon from the vapour. In this flashing process, the filament as a whole is heated to a temperature of 1600° to 1800° C., and it is left with a thin superficial coating of deposited carbon.

§ 3. TEMPERATURE CALIBRATION

After the thermionic measurements (to be discussed below) had been carried out, the tube was broken open and the filament was mounted in a fresh bulb, also provided with a barium getter. This was pumped, baked, gettered and sealed off in the usual manner, and then used for temperature calibration. Both brightness temperature (for a wave-length of 0·66μ.) and colour temperature were determined as a function of heating current. To increase the accuracy of the former measurements

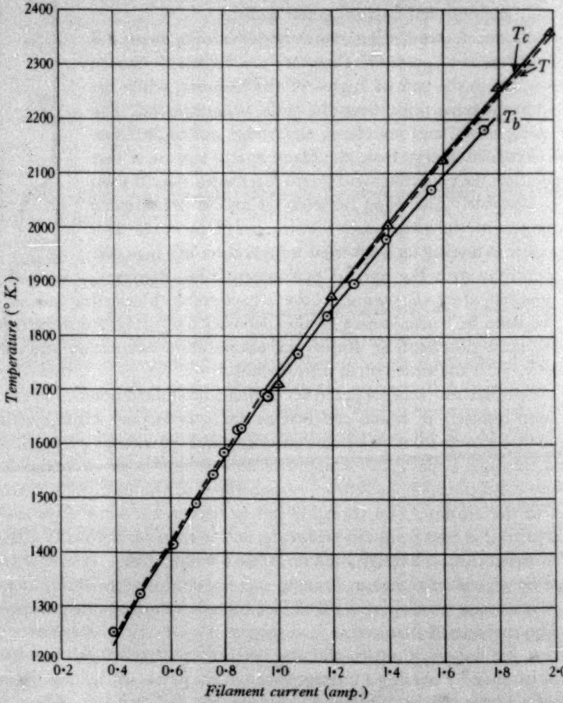

Figure 2. Temperature calibration.

the filament of a tungsten strip lamp, heated to various temperatures, was used as a background for the carbon filament, and the proper allowance was made for absorption and reflection by the carbon-filament bulb.

The results are shown in figure 2. The curves for brightness and colour temperature are marked T_b and T_c respectively. The true temperature is represented by the dashed curve marked T. This was obtained from the T_b curve and the spectral emissivity of graphitic carbon as found by Prescott and Hincke(6). The T_c curve serves as a rough check on the curve for T. It is a general rule that the true temperature is much closer to the colour temperature than it is to the brightness temperature, and this applies to the present curves.

Furthermore, for some metals at least, for instance, tungsten(7), molybdenum(8), tantalum(8), and niobium(9), T is intermediate between T_b and T_c. It is interesting to note that the T curve in figure 2 divides the interval between T_b and T_c everywhere in very nearly the same ratio as it does in the case of these four metals.

§ 4. THERMIONIC EMISSION

The tube used for thermionic emission measurements was baked for 30 min. at 400° C. on the pump. Then, with the filament running at about 2000° K., the molybdenum electrodes and the nickel cylinders were heated by high-frequency induction to bright redness, and at the same time the getter cup G was heated just not sufficiently strongly to disperse the getter. The filament was left burning for a total of 30 min. after the induction heating, and then it was flashed for a few minutes at 2300° K. Finally, the molybdenum electrodes and the nickel cylinders were again heated to redness for a few seconds, the getter was dispersed, and the tube was

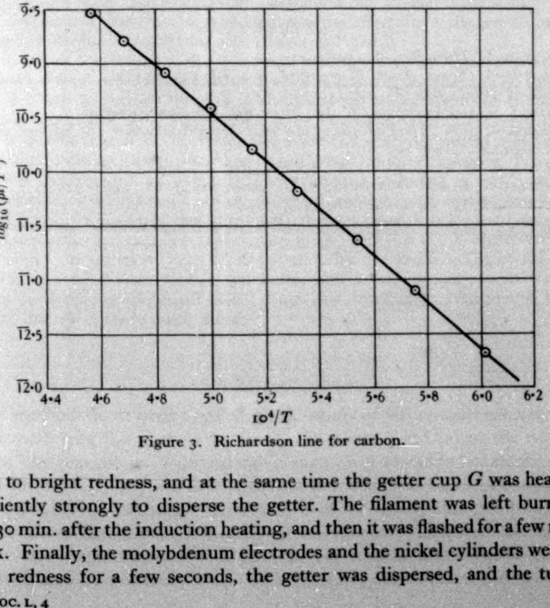

Figure 3. Richardson line for carbon.

sealed off from the pump. The filament was now heated for 16½ hours at 2150° K., while, to promote the clean-up of residual gas and of any gas that might be liberated from the filament, all three molybdenum electrodes were held at 50 volts positive to its negative end, collecting an electron current of 6ma. This last heating did not bring about any important change in the thermionic activity of the filament, and so it was assumed to have attained its final, gas-free condition and the thermionic measurements were proceeded with. The emission was measured at a series of temperatures between 1665° and 2191° K. and with different applied fields at each temperature. The corresponding zero-field emissions were then calculated, Schottky's relation between emission and field being used. The results are plotted in the usual manner in figure 3. The intercept and slope of the Richardson line correspond to the values of the thermionic constants

$$\rho A = 30 \text{ amp./cm.}^2\text{-deg.}^2, \quad \psi = 4{\cdot}34 \text{ ev.}$$

§ 5. ACKNOWLEDGEMENTS

In conclusion, the author wishes to tender his acknowledgements to the General Electric Company and the Marconi Company, on whose behalf the work was done which has led to this publication.

REFERENCES

(1) Langmuir, I. *Phys. Rev.* **2**, 450 (1913).
(2) Langmuir, I. *Trans. Amer. Electrochem. Soc.* **29**, 125 (1916).
(3) Lester, H. *Phil. Mag.* **31**, 197 (1916).
(4) Becker, J. A. and Brattain, W. H. *Phys. Rev.* **45**, 694 (1934).
(5) Richardson, O. W. *The Emission of Electricity from Hot Bodies*, 2nd edition, p. 81 (1921). (Longmans, Green and Co.)
(6) Prescott, C. H. and Hincke, W. B. *Phys. Rev.* **31**, 130 (1928).
(7) Forsythe, W. E. and Worthing, A. G. *Astrophys. J.* **61**, 126 (1925).
(8) Worthing, A. G. *Phys. Rev.* **28**, 190 (1926).
(9) Reimann, A. L. and Kerr Grant, C. *Phil. Mag.* **32**, 34 (1936).

AN X-RAY STUDY OF LATTICE-DISTORTION IN RHODIUM

By G. W. BRINDLEY, M.Sc., Ph.D., Mackinnon Student
of the Royal Society

AND

P. RIDLEY, B.Sc., Physics Laboratories, University of Leeds

Received 14 *February* 1938. *Read in title* 13 *May* 1938

ABSTRACT. Measurements of the intensities of X-ray reflections from filed and chemically prepared specimens of rhodium powder are made relatively to each other and are then converted to absolute units by comparison with suitable aluminium reflections. The scattering factors, f_T, obtained experimentally for both types of powder agree satisfactorily for the higher order reflections, with a theoretically estimated scattering factor, but for the lower order reflections the experimental values are markedly low, which suggests the existence of appreciable primary extinction. Detailed calculation shows that the variation of $[f_{T(\text{filed})}/f_{T(\text{chem.})}]$ with $(\sin\theta)/\lambda$ can be accounted for almost entirely in terms of primary extinction, and that there is very little residual effect due to lattice-distortion of the kind found in similar experiments with copper and nickel.

Measurements of the widths of the reflections are made for both types of powder; for the filed powder a total of 23 reflections for five radiations are measured. The results are discussed in relation to various theories of the nature of lattice distortion produced in metals by cold-work. The results are shown to be incompatible with the view that the broadening is due to smallness of crystal-size since the observed widths when plotted against θ fall on or near a mean curve, whereas with small crystal broadening there should be a separation according to wave-length. The difficulties attendant on any explanation in terms of periodic or semiperiodic lattice-distortion which have been discussed by Boas are briefly outlined. It is shown that the observed results may be explained in terms of a variation of the lattice spacing about the normal mean value due to the stresses caused by the filing process. Assuming a Gaussian distribution for the variation $(\delta a/a)$, the spread of the distribution is calculated. In this calculation there is only one adjustable parameter and this fixes the spread of the distribution. From this distribution a calculation is made of the internal energy of the worked metal.

§1. INTRODUCTION

X-RAY methods have been applied to the study of lattice-distortion in metals by considering the changes (*a*) in the intensities, and (*b*) in the widths of the X-ray reflections. A considerable amount of work has been done on this subject but hitherto, in any one investigation, attention has been focused mainly on one or other of these methods. A comparison of the results obtained by different investigators shows that conclusions drawn from intensity measurements alone as to the nature and magnitude of lattice-distortion in certain metals cannot easily be reconciled with conclusions based solely on line-width measurements; furthermore, estimates of the latent energy in a worked metal based on the conclusions drawn from the measurements of intensities and of line-widths do not agree with each other even as regards the order of magnitude of the effect, nor do they agree with direct calorimetric measurements of the latent energy. These difficulties have been discussed in two recent papers by Boas(2, 3). The conflicting nature of these conclusions points to the desirability of a wider experimental study of the subject, and this we are attempting to supply for a selected group of metals by making both intensity measurements and line-width measurements on the same sample of metal. By making absolute measurements of the reflected intensities, we are able to obtain more definite information than is obtainable from relative measurements; in the majority of previous experiments, relative measurements only have been made.

Rhodium was chosen for detailed investigation because preliminary results had shown that, compared with a number of other metals, it gave particularly broad lines when cold worked. Moreover, since the *K* absorption edge of rhodium lies well on the short-wave side of the wave-lengths usually employed in experiments of this type, the intensity of the general scattered radiation is small compared with the intensities of the reflected lines, which thus stand out prominently against a relatively weak background.

The results of an investigation of lattice-distortion in copper and nickel by one of the writers and F. W. Spiers(6) by means of X-ray intensity measurements have now been supplemented by measurements of the line-widths of the reflections carried out under the same conditions as for the rhodium measurements. These results, together with some measurements for aluminium and silver, will be discussed in relation to the rhodium results in a subsequent paper.

Throughout these experiments we have examined the distortion produced by filing the metal and have used the finest filed particles selected by a sieve with 350 meshes to the inch. In intensity measurements, filing has an important advantage over other methods of producing distortion since a specimen composed of filed particles shows little or no preferential orientation of the reflecting planes; other methods of producing distortion may result in a marked orientation which will probably have a far greater effect on the reflected intensities than the distortion itself.

The criticism may be made that filing cannot be controlled sufficiently well to justify any comparison between results from different metals. As regards the line-widths, we find that for any particular metal they are practically independent of the manner in which the filing is carried out, e.g., whether a coarse file or an almost dead smooth file is used. In view of the conclusion drawn by Wood(20, 21) that distortion produced in a metal by cold work has a limiting value which is not exceeded by continuing the cold-working process, it seems probable that the filed particles have suffered the maximum distortion possible at room-temperature. We also find that the line-widths of reflections from filed metals are comparable with the widths from metals which have been strongly worked in other ways. As regards the intensities of the reflections, they appear to depend to a small extent on the type of file used, but not to such an extent as to prevent a significant comparison of the results obtained from different metals.

§ 2. EXPERIMENTAL

The intensities of the reflections have been measured absolutely by the method of substituted powder layers described in a previous paper in these Proceedings by one of the writers and F. W. Spiers⁽⁷⁾; absolute values of the intensities have been obtained by comparison with suitable reflections from aluminium.

For the line-width measurements, photographs were taken with a camera of the type previously described having a collimator 27·5 mm. long and 0·58 mm. in diameter; the divergence of the incident radiation, measured photographically, was found to be 0·0339 radian (1·94°). In order to distinguish more satisfactorily between various possible causes of the broadening, photographs were taken with the $K\alpha$ radiations of five metals, zinc, copper, nickel, cobalt and iron; the $K\beta$ radiations were removed by suitable filters. The plate of powder was set at an angle α equal to 50° with the incident radiation; this setting gave a convenient range of reflections with all the radiations employed and was used for all the line-width measurements.

The filed rhodium was prepared from a fused button of the metal supplied by Messrs Johnson, Matthey and Co. Ltd. The line-widths and intensities corresponding to the undistorted metal were obtained from measurements on a fine powder produced by chemical reduction. The files used were of Swiss make of no. 4 and no. 6 grades of fineness; the no. 4 file is moderately smooth, the no. 6 almost dead smooth.

The X-ray photographs were measured with a Cambridge microphotometer by a null method. Readings were taken of the density of photographic blackness at intervals apart equal to 0·0185 mm. over each reflection and 0·0370 mm. along the background at each side of the reflection. For each reflection 20 or 30 readings were taken on the background at each side of the line, and 50 or more readings over the line. Two or three independent runs were made for each reflection on each film, and usually about 10 films were taken to obtain a final average value. As measures of the widths of the lines we have taken (*a*) the width at half the maximum intensity, and (*b*) the width as defined by von Laue⁽¹⁷⁾, namely the integrated intensity divided by the maximum intensity. These widths will be termed "half-widths" and "Laue widths" respectively.

§ 3. RESULTS OF THE INTENSITY MEASUREMENTS

Two series of measurements have been carried out. In the first the intensities from the filed powders were compared with the corresponding intensities from the powder prepared chemically. In the second series the intensities from the chemically prepared powder were placed on an absolute scale by comparison with suitable aluminium reflections. The results are conveniently expressed in terms of the atomic scattering factor f_T (the suffix T denotes a measurement at room-temperature T) which is derived from the integrated intensity, I_r, of a reflection by the following relation:

$$I_r/A = C \, . \, pF^2 \, . \, \phi(\theta),$$

where F, the scattering factor per unit cell, is equal to $4f_T$ for face-centred cubic metals,

$$\phi(\theta) = (1+\cos^2 2\theta)/(\sin\theta \, . \, \sin 2\theta)$$

and

$$A = [\sin(2\theta-\alpha)]/[\sin(2\theta-\alpha)+\sin\alpha],$$

where θ is the angle of reflection and α the angle between the incident radiation and the powder-surface, p is the multiplicity factor, and C is a constant.

Table 1 gives the measured values of the ratio of the scattering factors of the filed and chemically prepared powders calculated from the relation

$$f_{T\,(\text{filed})}/f_{T\,(\text{chem.})} = [I_{r\,(\text{filed})}/I_{r\,(\text{chem.})}]^{\frac{1}{2}}$$

for the two specimens of filed powders. The results are plotted against $(\sin\theta)/\lambda$ in figure 1 where the circles and squares correspond to powders prepared with grade 4 and grade 6 files respectively; the vertical line attached to each point indicates the mean deviation of the observed values from the mean value. The dashed lines are mean curves through the experimental results.

Table 1. Ratio of the scattering factors of filed and chemically prepared rhodium powders

Reflections	$(\sin\theta)/\lambda$	$f_{T(\text{filed})}/f_{T(\text{chem.})}$	
		no. 4	no. 6
111	0·228	0·93$_1$	0·96$_4$
200	0·263	0·84$_2$	0·85$_4$
220	0·373	0·87$_5$	0·92$_1$
311	0·437	0·88$_9$	0·93$_4$
331	0·574	0·93$_3$	0·94$_3$
420	0·589	0·92$_7$	0·95$_3$

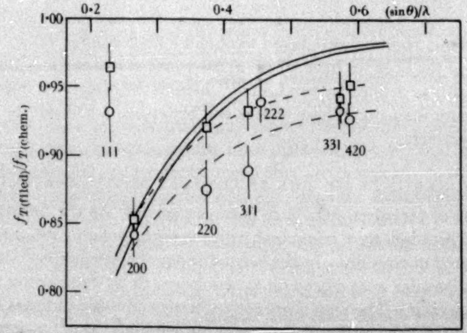

Figure 1. Dashed lines show the observed variation of $f_{T\,(\text{filed})}/f_{T\,(\text{chem.})}$ with $(\sin\theta)/\lambda$; the full lines show the calculated variation assuming primary extinction in the powders. The circles are the observed values for the no. 4 powder, obtained with the coarser file, and the squares for the no. 6 powder.

Absolute values of f_T* were obtained for all the specimens and are set out in table 2. Column 3 of the table gives the values of f_T for the chemical rhodium powder together with the aluminium reflections used as standards. The values of f_T assumed for the aluminium reflections are those given previously by the writers; see column 4 of table 1 in reference (8). The calculation of the results is based on equation (3) of the paper by Brindley and Spiers(7). In columns 4 and 5 are given the values of f_T for filed rhodium calculated from the ratios in table 1 and the values of f_T for the chemical powder in column 3.

Table 2. Absolute values of f_T for filed and chemically prepared rhodium powders, and theoretical values of f_T for the rhodium atom

1	2	3		4	5	6
		Absolute values of f_T, experimental				
Reflections	$(\sin\theta)/\lambda$	Chemical rhodium	Aluminium reflections used as standards	Filed rhodium no. 4	Filed rhodium no. 6	Theoretical $f_T=(f-\Delta f)\,e^{-\tilde{M}}$
111	0·228	28·5	111, 200	26·5	27·5	32·2
200	0·263	$27{\cdot}4_5$		23·1	$23{\cdot}4_5$	30·2
220	0·373	$23{\cdot}5_5$	220, 311	20·6	21·7	24·7
311	0·437	21·8		19·4	$20{\cdot}3_5$	22·2
222	0·456	21·3		—	—	$21{\cdot}5_5$
331	0·574	18·7		$17{\cdot}4_5$	$17{\cdot}6_5$	18·2
420	0·589	18·3		$16{\cdot}9_5$	$17{\cdot}4_5$	17·8
422	0·645	$16{\cdot}6_5$		—	—	$16{\cdot}4_5$

§ 4. THEORETICAL SCATTERING FACTOR OF RHODIUM

To ascertain whether the values of f_T for the chemically prepared powder are affected by extinction, we have estimated a theoretical scattering factor, f, in the following way. The only element near rhodium for which the electron-distribution has been calculated by Hartree's method is Ag^+ for which the calculations have been made by Miss Black(1). In table 3, column 2, values of f are given for Ag^+ calculated from Miss Black's results, and in column 3 are given the more approximate Thomas-Fermi values for neutral silver; the ratio of the Hartree to the Thomas-Fermi values is given in column 4 and differs from unity by less than 3 per cent between $(\sin\theta)/\lambda = 0{\cdot}1$ and $0{\cdot}7$. We have therefore estimated f values of the Hartree type for rhodium by multiplying the Thomas-Fermi values for rhodium by the ratio of the Hartree to the Thomas-Fermi values for silver. This procedure is admittedly lacking in rigour but it probably gives a better approximation to the true values of f than the unmodified Thomas-Fermi values.

---

* It has previously been pointed out that a weakness of the so-called substitution method of obtaining absolute values of f_T arises from the necessity of knowing the coefficients of linear absorption, μ, of the radiation in the two substances and this difficulty is apparent in the present case for no measurements of μ for rhodium for copper $K\alpha$ radiation have been made. To test the reliability of Jönsson's method of estimating absorption coefficients for elements in this region, we have compared the values given by Jönsson's method for silver with the following experimental values for the mass absorption coefficient μ/ρ: 217 (Allen), 212 (Jönsson), 214 (Barkla and Sadler); the mean of these, 215, is probably correct to about 1 per cent. Jönsson's interpolation method gives $\mu/\rho = 223$, which is about 4 per cent higher than the mean experimental value. We have therefore assumed that the method will give a value for rhodium also 4 per cent too high and have therefore taken μ/ρ equal to 190 for rhodium for copper $K\alpha$ radiation. For the density ρ we have taken 12·41 as given by Owen and Yates. Since f_T depends on $\sqrt{\mu}$, the percentage error in f_T will be only half that in μ, and since μ for rhodium is unlikely to be in error by more than 2 per cent, the error in f_T on this account is unlikely to be more than 1 per cent.

To compare the theoretical values of f with the measured values of f_T, we must make allowance for the heat motion in the lattice and for the effect of dispersion. With the usual notation we have*

$$f_{T,\,\mathrm{Cu}K\alpha}=(f_{\lambda\to 0}-\Delta f)\,e^{-M}$$

where $f_{\lambda\to 0}$ is the theoretical scattering factor valid for short waves, Δf is the dispersion term which for rhodium and copper $K\alpha$ radiation has the value 1·27 according to Hönl's method of calculation(14), and e^{-M} is the heat-motion factor calculated from the characteristic temperature Θ which for rhodium is 370° K. The values of f_T for copper $K\alpha$ radiation obtained in this way are given in column 6 of table 2.

Table 3. Values of f for silver and rhodium

1	2	3	4	5	6
$(\sin\theta)/\lambda$	f for silver			f for rhodium	
	Hartree	Thomas-Fermi	$\frac{\text{Hartree}}{\text{Thomas-Fermi}}$	Thomas-Fermi	Hartree (estimated)
0·0	46·0	47·0	—	45·0	—
0·1	43·4	43·0	1·010	41·1	41·5
0·2	37·5	36·9	1·016	35·1	35·7
0·3	31·7	31·3	1·015	29·8	30·2
0·4	27·1	26·8	1·014	25·4	25·7$_5$
0·5	23·9	23·7	1·005	22·6	22·7
0·6	21·4	21·3	1·006	20·2	20·3
0·7	19·5	19·0	1·027	18·0	18·5
0·8	17·8	17·0	1·047	16·1	16·8$_5$

§ 5. DISCUSSION OF THE RESULTS OF THE INTENSITY-MEASUREMENTS

The data in columns 3 and 6 of table 2 show that the measured values of f_T for the chemical powder agree well with the theoretical values for the higher-order reflections but fall below the theoretical values for the lower-order reflections. This effect is almost certainly due in part, if not wholly, to primary extinction. Darwin(10) has shown that to a close approximation primary extinction reduces the reflected intensity according to the relation

$$\frac{I_{r\,(\text{with extinction})}}{I_{r\,(\text{without extinction})}}=\frac{\tanh xq}{xq},$$

where

$$q=\frac{n\lambda}{\sin\theta}\,\frac{Fe^2}{mc^2}.$$

In these expressions, q is the reflected amplitude per lattice plane, n the number of unit cells per unit area, x the number of planes taking part in the reflection, and the remaining symbols have their usual significance. If d is the spacing of the planes and N the number of cells per unit volume, then $n = Nd$. Further, if L is the thickness of the crystal normal to the reflecting planes and a the side of the unit cube of the structure, then $x = L/d$ and $N = 1/a^3$; also $F = 4f_T$. Hence

$$xq = \frac{4f_T e^2}{mc^2 a^3}\left(\frac{\lambda}{\sin\theta}\right) L.$$

We wish to consider first how far the observed variation of $f_{T\,(\text{filed})}/f_{T\,(\text{chem.})}$ with $(\sin\theta)/\lambda$ shown by the broken curves in figure 1 can be accounted for in terms of primary extinction. Since f_T is proportional to $\sqrt{I_r}$, we have

$$\frac{f_{T\,(\text{filed})}}{f_{T\,(\text{chem.})}} = \left(\frac{\tanh xq}{xq}\right)^{\frac{1}{2}}_{\text{filed}} \Big/ \left(\frac{\tanh xq}{xq}\right)^{\frac{1}{2}}_{\text{chem.}}.$$

To evaluate the right-hand side of this equation, we require to know the crystal-sizes L of the powders, and also f_T. Values of L may be obtained by assuming for one particular reflection that the whole of the drop of f_T below the calculated value of f_T is due to primary extinction. In calculating xq we must use values of f_T which are free from extinction, and we have therefore used the theoretical values. When the quotient of $(\tanh xq)/xq$ for the filed and chemical powders is taken, small errors in f_T and L will tend to cancel out and the final result will therefore be more accurate than the values of $(\tanh xq)/xq$ for the separate powders.

The mean crystal sizes L calculated from the data for the 200 reflection, are as follows:

For the chemically prepared powder	$3{\cdot}4_5 \times 10^{-5}$ cm.
For the filed powder, grade 6	$6{\cdot}3_5 \times 10^{-5}$ cm.
For the filed powder, grade 4	$6{\cdot}6_5 \times 10^{-5}$ cm.

The calculated results for $f_{T\,(\text{filed})}/f_{T\,(\text{chem.})}$ plotted against $(\sin\theta)/\lambda$ are shown by the full lines in figure 1; their general run is similar to the run of the experimental points, but the latter fall below the calculated curves as $(\sin\theta)/\lambda$ increases. The percentage difference between the observed and calculated values is, however, small for all reflections except the 111. The agreement between them could be improved by making some allowance for the distribution of crystal-sizes about the mean values given above, but it would not be profitable in the present case to carry out such calculations in detail because the agreement is already fairly close when average values of L are used; and, secondly, the accuracy of the measurements, although as high as can reasonably be expected under the conditions imposed by the breadth of the lines from the filed powders, is not so high as to justify a more detailed calculation. It seems reasonable to conclude from these results that the major part of the variation of $f_{T\,(\text{filed})}/f_{T\,(\text{chem.})}$ with $(\sin\theta)/\lambda$ can be attributed to primary extinction.

The abnormal values obtained for the 111 and 222 reflections are almost certainly connected with the fact that the {111} planes are the planes on which slip occurs most readily in face-centred cubic metals. This might result in L being less for the {111} planes than for the other planes and might also give rise to a tendency for the {111} planes of the filed powder to be aligned parallel to the powder surface.

Measurements were not at first made on the relatively weak 222 reflection from the filed powders but the peculiarity of the results for the 111 reflection led us afterwards to measure the 222 reflection from the no. 4 filed powder, but it was not deemed necessary to make the measurement for the no. 6 powder also.

The fact that the experimental results for the powder obtained with the no. 6, the smoother, file are higher than for the no. 4 file also points to primary extinction being the cause of the difference between the values of f_T for the filed and chemical powders. The finer file required a very much greater expenditure of energy to yield sufficient powder; presumably the crystal-size of the powder was reduced more by this file than by the no. 4 file, but there is no evidence for any greater distortion in the no. 6 powder.

A comparison of the present results with those previously obtained by Brindley and Spiers(6) for copper and nickel will be considered in detail in a subsequent paper, and it will be sufficient to mention briefly here that there is a marked difference between the rhodium results and those for copper and nickel. Whereas for copper and nickel, $f_{T\,(\text{filed})}/f_{T\,(\text{chem.})}$ decreased as $(\sin\theta)/\lambda$ increased and there appeared to be little or no primary extinction, with rhodium practically the whole of the variation of $f_{T\,(\text{filed})}/f_{T\,(\text{chem.})}$ with $(\sin\theta)/\lambda$ can be explained in terms of primary extinction, and there seems to be little or no residual effect which might be attributed to lattice distortion.

§ 6. RESULTS OF LINE-WIDTH MEASUREMENTS

Preliminary measurements with copper $K\alpha$ radiation showed that there was no measurable difference between the widths of the reflections from the two specimens of filed powder; a full set of measurements with the $K\alpha$ radiations of zinc, copper, nickel, cobalt and iron were therefore made for the grade 4 powder only. For the chemically prepared powder it was found unnecessary to use more than two radiations; zinc and copper $K\alpha$ radiations only were used.

The results are summarized in table 4. Both the Laue widths and the half-widths of the reflections were measured, but as they differ only slightly one series of widths only is recorded; the Laue widths are given since theoretical calculations involving widths of reflections are almost invariably based on Laue's definition of line-width. As would be expected, the Laue widths are slightly larger than the half-widths, being 10 per cent larger for reflections from the filed powder and 5 per cent larger for reflections from the chemical powder.[*] Photographs obtained with the filed and chemically prepared powders for the various radiations are reproduced in plate 1.

Each reflected line contains two components, $K\alpha_1$ and $K\alpha_2$, the separation of which varies with the $K\alpha$ radiation used and with the angle θ. By differentiation of the Bragg equation, we have for the linear separation of the two components

$$\delta = 2R\,.\,\Delta\theta = 2R\tan\theta\,\Delta\lambda/\lambda,$$

[*] If we assume a reflected line to have a Gaussian distribution of intensity of the type $I = I_0 e^{-a^2x^2}$, then it is easily shown that the half-width is $2\sqrt{\log_e 2}/a$ and the Laue width is $\sqrt{\pi}/a$, so that the ratio of the Laue width to the half-width is $(\pi/\log_e 2)^{\frac{1}{2}}/2$, which is 1·064.

(*a*) Filed rhodium.

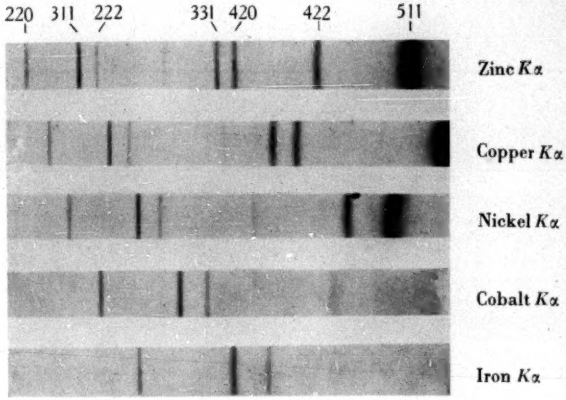
220
311
222
331
420
422
511
Zinc $K\alpha$
Copper $K\alpha$
Nickel $K\alpha$
Cobalt $K\alpha$
Iron $K\alpha$

(*b*) Chemically prepared rhodium.

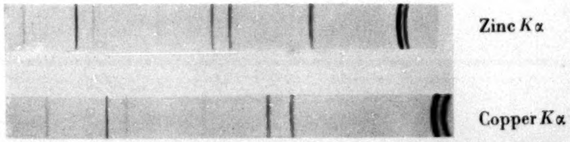
Zinc $K\alpha$
Copper $K\alpha$

Plate 1. Reflections from filed and chemically prepared rhodium powders for various radiations.

where R is the radius of the film, $2\Delta\theta$ is the angular separation of the reflected components, and $\Delta\lambda$ is the difference in the wave-lengths of the components. Values of δ are given in millimetres in column 5 of table 4 and are calculated for $R = 30{\cdot}5$ mm.

Table 4. Laue widths of X-ray reflections from filed and chemically prepared rhodium powders

1 Radiation	2 Reflection	3 θ (degrees)	4 Laue width (mm.)	5 Separation of $\alpha_1\alpha_2$ components, δ (mm.)	6 Correction for $\alpha_1\alpha_2$ separation	7 Corrected Laue width (mm.)
(*a*) Filed rhodium powder						
Zinc $K\alpha$	220	32·3	0·71	0·104	0·978	0·69
	311	38·8	0·68	0·132	0·958	0·65
	222	40·9	0·61	0·142	0·938	0·57
	331	55·4	0·92	0·238	0·925	0·85
	420	57·6$_5$	1·02	0·259	0·928	0·95
	422	67·7	1·39	0·400	0·908	1·26
	511	79·0	2·90	0·844	0·906	2·63
Copper $K\alpha$	220	35·0	0·66	0·106	0·972	0·64
	311	42·2$_5$	0·69	0·138	0·955	0·66
	222	44·6$_5$	0·64	0·150	0·937	0·60
	331	62·1$_5$	1·14	0·288	0·927	1·06
	420	65·0$_5$	1·34	0·327	0·933	1·25
Nickel $K\alpha$	220	38·1	0·63	0·111	0·965	0·61
	311	46·4	0·73	0·149	0·952	0·69
	222	48·1	0·68	0·158	0·940	0·64
	331	72·0	1·78	0·436	0·932	1·66
	420	77·4	2·63	0·634	0·934	2·45
Cobalt $K\alpha$	220	41·7$_5$	0·64	0·119	0·961	0·62
	311	51·3	0·87	0·166	0·958	0·83
	222	54·6	0·81	0·187	0·940	0·76
Iron $K\alpha$	220	46·1	0·73	0·129	0·964	0·70
	311	57·7	1·02	0·196	0·958	0·98
	222	62·0	1·05	0·234	0·942	0·99
(*b*) Chemically prepared powder						
Zinc $K\alpha$	220	32·3	0·49	0·104	0·949	0·46
	311	38·8	0·38	0·132	0·870	0·33
	222	40·9	0·35	0·142	0·822	0·29
	331	55·4	0·49	0·238	0·757	0·37
	420	57·6$_5$	0·51	0·259	0·746	0·38
	422	67·7	0·69	0·400	0·718	0·49$_5$
Copper $K\alpha$	220	35·0	0·45	0·106	0·937	0·42
	311	42·2$_5$	0·38	0·138	0·858	0·33
	222	44·6$_5$	0·38	0·150	0·831	0·31$_5$
	331	62·1$_5$	0·60	0·288	0·761	0·45$_5$
	420	65·0$_5$	0·66	0·327	0·751	0·49$_5$
(*c*) Widths of resolved lines from chemically prepared powder						
Zinc $K\alpha$	511 α_1	78·6	0·55	—	—	—
	511 α_2	79·4	0·53	—	—	—
Copper $K\alpha$	422 α_1	82·7	0·68?	—	—	—
	422 α_2	84·0	0·66?	—	—	—

An expression for correcting observed Laue widths for $\alpha_1\alpha_2$ separation has been calculated by Brill(4) on the assumption that the intensities of the α_1 and α_2 components are in the ratio of 2 : 1 and that the distribution of intensity in a reflected line has a simple triangular shape. Neither assumption is fully justified and the latter is especially doubtful. A graphical test of the accuracy of Brill's formula for lines of the shape obtained in our work was made and it was found that for small values of δ the formula gave corrected widths as much as 4 per cent too small, and for larger values of δ as much as 5 per cent too large; hence relative errors as large as 9 per cent might be obtained. In the meantime a more satisfactory method of correcting for $\alpha_1\alpha_2$ separation has been developed by F. W. Jones(15) and a short abstract describing it has appeared;* the method is a graphical one and the writers are much indebted to Dr Jones for supplying them with details of this work prior to their full publication. The correction factors given in column 6 of table 4 are based on the data supplied by Dr Jones and the corrected Laue widths are given in column 7 of the table.

Section (*a*) of table 4 refers to results for filed rhodium and section (*b*) to those for chemically prepared rhodium. Section (*c*) gives results for two high-order reflections from the chemical powder for which the α_1 and α_2 components are clearly resolved. These reflections also enable us to measure the intensities of the α_1 and α_2 components, which we find to be in the ratio 1·84 : 1 for zinc radiation and 1·80 : 1 for copper radiation. These are the ratios of the intensities recorded on the film which will be slightly different from the ratio of the intensities in the incident beam owing to the different absorption of the components. The Laue widths of the 422 α_1 and α_2 reflections with copper radiation are regarded as doubtful owing to a possible shielding of the background on one side of the lines by the collimator.

In figure 2 the Laue widths, after correction for $\alpha_1\alpha_2$ separation, are plotted against the angle θ; the results obtained with different radiations are shown by the use of different symbols. For the chemical powder the results lie close to a single mean curve. For the filed powders there is a greater divergence of the values from a mean curve, but with the exception of the results for the 222 reflections, which are consistently low, the great majority of the remaining points lie on or near a mean curve; as will be seen in the next section, this fact is of special importance in the interpretation of the results.

§7. DISCUSSION OF THE LINE-WIDTH MEASUREMENTS

We will now examine the results of the line-width measurements in relation to the various explanations which have been suggested to account for the broadening of the reflections caused by cold working. Since crystals of sizes approaching colloidal dimensions are known to give broadened lines, it has often been put forward as a possible explanation that cold working may produce crystals sufficiently small to yield broadening of this type. On the other hand the broadening might be explained by some type of lattice distortion such as that considered by Dehlinger(11) and Boas(3) in particular. A further possibility is that the stresses set up by the cold working may lead to extensions and compressions of small regions of the metal and so cause small deviations from the normal lattice spacing. We will consider these three kinds of explanation in turn.

---

* *Note added in proof*. The full account of Dr Jones' work has just appeared, *Proc. Roy. Soc.* A, **166**, 16 (1938).

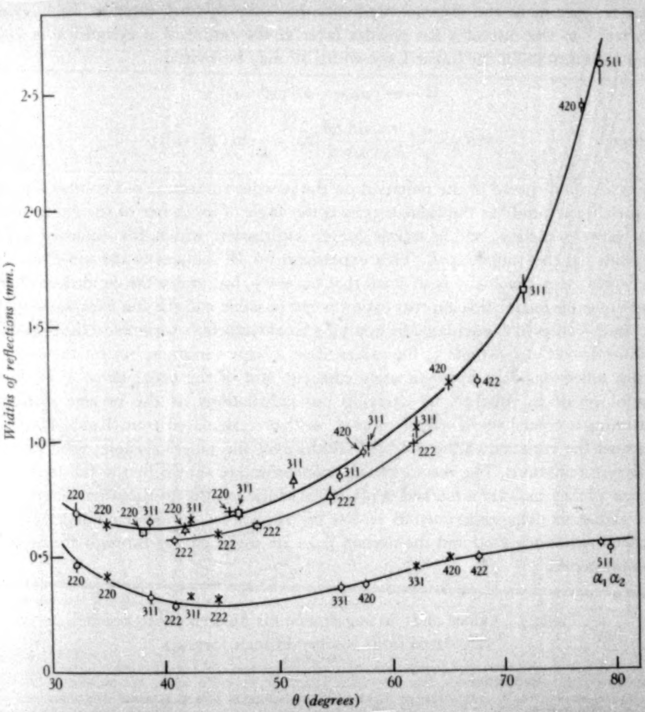

Figure 2. Laue widths of reflections, after correction for $\alpha_1\alpha_2$ separation, plotted against θ. The lower curve is for chemically prepared rhodium powder, the upper curves are for the filed powder. Except for the 222 reflections the widths from the filed powder lie on or near the mean curve; a slightly lower curve passes through the points representing the 222 reflections. The symbols indicate the radiations employed: ○, zinc $K\alpha$; ×, copper $K\alpha$; □, nickel $K\alpha$; Δ, cobalt $K\alpha$; +, iron $K\alpha$.

(*a*) ***Line-broadening due to small crystals.*** The theory of line-broadening by small crystals was first considered by Scherrer(18) who derived the following equation for cubic crystals and parallel or nearly parallel radiation:

$$\frac{W}{R}=2\,\frac{\lambda\sec\theta}{L}\sqrt{\frac{\log_e 2}{\pi}}+b,$$

where W is the linear half-width, R the camera radius, L the length of an edge of the crystal, and b a constant. From this it appears that the line-width should vary linearly with λ for a given value of θ, and it was to test this point that a number of radiations were used. A more general analysis by von Laue(17) for cylindrical powder specimens and divergent radiation has recently been extended by Kochendörfer(16) to the case of a flat powder layer at the centre of a cylindrical camera, and his formula for the linear Laue width W may be written

$$W = \pi r\,[\sin\alpha - \sin(2\theta - \alpha)]/\gamma$$

where
$$\tan\gamma = \frac{\omega}{4}\left(\frac{r}{R\eta}\right)\frac{\sin 2\theta}{\sin\theta}[\sin\alpha - \sin(2\theta-\alpha)];$$

$2r$ is the total spread of the radiation on the powder surface, ω is a constant in von Laue's theory and has the value 0·55, α is the angle of incidence of the radiation on the powder-surface, and η stands for an expression which for equiaxed cubic crystals has the value $\lambda/4\pi L$. This expression for W reduces to the same form as Scherrer's expression if γ is so small that $\tan\gamma \doteqdot \gamma$, but under the conditions of the present experiments this approximation is not possible and the full expression must be used. Values of L calculated by applying Kochendörfer's formula to the observed widths are set out in table 5; the values show a large variation, but for the higher-order reflections L is approximately constant and of the order of 90 A. A more useful result is obtained by carrying out calculations in the reverse manner; assuming a crystal size L equal to 90 A. we have calculated from Kochendörfer's formula the variation of the reflected widths over the range of angles used for the different radiations. The results of this calculation are shown by the full curves in figure 3; they indicate a marked dependence of the widths on the wave-length λ of the radiation. The experimental results are shown by different symbols for the various radiations used and the dashed lines are mean curves through the experimental points.

Table 5. Values of L, in angstroms, for filed rhodium powder calculated from Kochendörfer's formula

Reflection Radiation	220	311	222	331	420	422	511
Zinc $K\alpha$	*	490	271	86	84	93	80
Copper $K\alpha$	*	127	119	97	89	—	—
Nickel $K\alpha$	*	101	108	95	87	—	—
Cobalt $K\alpha$	185	95	117	—	—	—	—
Iron $K\alpha$	116	109	131	—	—	—	—

* For these reflections Kochendörfer's formula gives negative values.

Figure 3 shows that the experimental results are not dependent on wave-length as they would be if the broadening were due to small crystals, and hence provides strong evidence that the broadening arises from some other cause.

In addition to this evidence, we have the fact that if the crystal-size were really of the order of 90 A., then primary extinction would be negligible. The impossibility of reconciling the large extinction effect shown by the filed powders with a crystal-size small enough to produce broadening of the observed magnitude is additional confirmatory evidence that the broadness is not produced by small crystals.

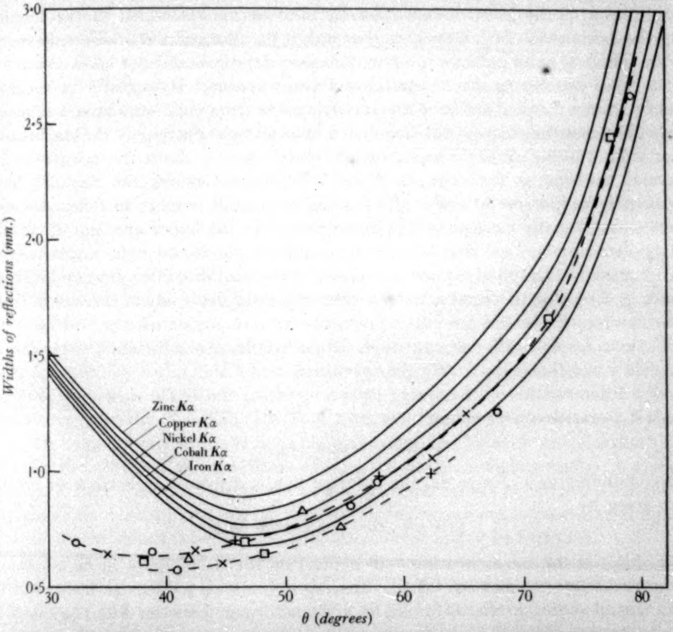

Figure 3. A comparison of the observed widths of reflections with calculated values derived from Kochendörfer's formula for the dependence of line-width on crystal size. The full lines show the calculated values for the five radiations employed and the symbols ○, ×, □, Δ and + show the observed values for the $K\alpha$ radiations of zinc, copper, nickel, cobalt and iron respectively. The point of particular importance shown by the figure is that there is no separation of the observed values with wave-length, of the kind obtained theoretically, and therefore that the broadening of the lines does not arise from smallness of crystal-size.

(*b*) *Line-broadening due to lattice-distortion*. The effect of various types of lattice-distortion on the widths and intensities of X-ray reflections has been studied by Dehlinger(11) and by Boas(3). Dehlinger showed that distortions of a strictly cosine type running throughout the lattice would give line-broadening of the magnitude observed. He also considered a type of deformation in which after each wave of distortion there is a region free from distortion; this type of deformation was shown to give no appreciable line-broadening. Boas considered a type of distortion in which equal blocks of the lattice at regular intervals are displaced normal to the reflecting planes, and this also was found to give no line-broadening. The transition from the simple cosine deformation which gives line-broadening to the other types which give negligible broadening is analysed by Boas by a method employing Fourier analysis; he shows that whereas broadening is produced by a single term of the Fourier expansion, as more terms are added the broadening rapidly diminishes. It is clear then that unless the distortion is of a strictly cosine form, which is most unlikely to occur, line-broadening would not be expected.*

(*c*) *Line-broadening due to variation of lattice spacing*. Haworth(13) has recently shown from a detailed study of the 311 reflections from cold-worked and annealed permalloy that the shape of the broadened line can be explained on the supposition that cold working causes a variation of lattice spacing about the normal value. Several workers, as for example Wood(20, 22, 23) and Caglioti and Sachs(9), have measured the increase of line-width for one or a small number of reflections and have correlated the increase with a mean change in the lattice spacing. Boas also has expressed the view that broadening might be connected with a variation of lattice spacing. Despite frequent reference to the possibility of a variation in lattice spacing, there does not appear to have been any extensive study of the widths from this standpoint. In the present experiments we have measured the widths of 23 reflections for five different radiations; these results are sufficiently extensive to provide a wide basis for testing the hypothesis.

By differentiation of the Bragg equation, taking the lattice spacing a and the angle θ as variables, we obtain

$$d\theta = -\tan\theta \, . \, da/a.$$

Corresponding to a change δa, the reflected line is displaced a distance δx on the film given by

$$\delta x = 2R \, . \, \delta\theta = -2R \tan\theta \; \delta a/a.$$

The shape of the broadened line will depend on the distribution of $\delta a/a$ about a mean value zero. Assuming that the distribution follows a Gaussian law, we have for the probability dp that $\delta a/a$ will lie in a small range between z and $(z+dz)$

$$dp = e^{-h^2z^2}\,dz \Big/ \int_{-\infty}^{+\infty} e^{-h^2z^2}\,dz = \frac{h}{\sqrt{\pi}}\, e^{-h^2z^2}\,dz.$$

If the distribution of intensity on the film for a reflection from the chemical powder is represented as a function $I(x)$ of x, then for the worked metal a fraction $I(x) \, . \, \delta p$ of this intensity will be displaced a distance δx and may be represented as $I(x') \, . \, \delta p$. For numerical calculation it is convenient to replace the continuous distribution of

---

* Boas(3) concludes, p. 368, "Wir glauben daher, dass die nach Deformation von Kristallen beobachtete Linienverbreiterung nicht von periodischen Gitterstörungen herrührt", and on p. 369, "Die nach plastischer Deformation auftretende Verbreiterung der Interferenzlinien ist mit periodischen Störungen des Gitters wohl nicht zu erklären. Die Linienverbreiterung dürfte zum wesentlichen Teil durch elastische Spannungen, die in grösseren Bereichen des Gitters ($\sim 0{\cdot}5\,\mu$) homogen sind, zustande kommen."

dp by a series of values of δp at close intervals. The intensity distribution in the broadened line is then obtained by summing the series of displaced lines of intensity $I(x')\,\delta p$.

When the breadth of the broadened line is being calculated as a function of θ, it must be borne in mind that the breadth varies with θ for two reasons; in addition to the broadening due to the variation of lattice spacing, which is approximately proportional to $\tan\theta$, there is also a broadening due to the focusing properties of the camera. We have investigated the latter by measuring the line-widths of the reflections from the chemical powder and the results are shown by the lower curve in figure 2. Using these results we can then calculate for each value of θ the width of the line resulting from any particular distribution of lattice spacings. It is to be emphasized that in calculating the widths of the broadened lines there is only one adjustable factor, namely the distribution curve, and if this is taken to be of the Gaussian type the only known quantity is h.

The result of such a calculation is shown in figure 4, where the widths are plotted against $\tan\theta$; the thin lines represent the best mean curves through the experimental points and the heavy line is the calculated curve based on a Gaussian distribution with h equal to 207. This distribution is shown in the inset of figure 4.

The agreement between the observed and calculated values is fairly close, particularly when it is considered that there is only one adjustable parameter, h. It seems justifiable to conclude that a major part at least of the broadening of the lines is caused by a variation of the lattice spacing. We have considered whether a better agreement could be obtained by modifying the distribution curve, and various departures from the Gaussian type have been examined, but it seems unlikely that any very considerable improvement could be obtained by such modification. The fact that the widths of all the reflections from the worked metal do not lie on a single curve indicates that the assumption of a single distribution curve is too simple to explain all the observations, and in view of this the agreement between the observed and calculated values is perhaps as good as can reasonably be expected.

It has been observed by Wood(21, 22, 24) in a number of instances that some reflections show greater broadening than others: for example, the 420 reflections from copper and from α brass are broadened more than the 331 reflections. It is of interest therefore to consider whether the present measurements indicate effects of this kind. The 222 reflections lie well below the mean curve, as has already been pointed out; this result is almost certainly a consequence of the fact that slip occurs most easily on the {111} planes so that these planes would be expected to show a smaller variation in spacing than other planes. The present results point to the 420 reflections being slightly broader than the 331 reflections when considered relative to the mean curve; there is, of course, a greater absolute broadening of the 420 reflections than of the 331 reflections, due to the larger value of $\tan\theta$ for the former. This illustrates very well a point of general importance, namely that incorrect conclusions may easily be drawn from measurements of the line-widths of a small number of reflections since part of the broadening of one line with respect to another arises from the difference of $\tan\theta$ and also from the difference in the focusing properties of the camera for the two reflections. The 311 reflections show a tendency to lie slightly above the mean curve. The 422 reflection falls well below the mean

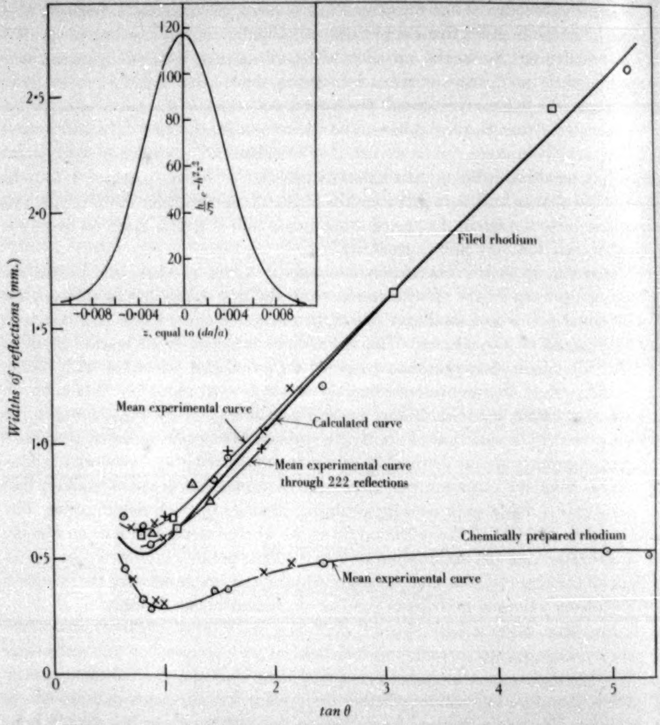

Figure 4. Reflected widths from filed and chemically prepared rhodium plotted against tan θ. The heavy curve running through the observations for the filed metal is calculated on the assumption of a Gaussian distribution of the lattice spacing about the normal mean value. The distribution is shown in the inset.

curve, but as we have only been able to measure this with zinc $K\alpha$ radiation we feel less certain of the result than in the case of the other reflections, which have been measured with several radiations.

§ 8. CALCULATION OF THE INTERNAL OR LATENT ENERGY OF DISTORTED RHODIUM

Having obtained the constant h in the Gaussian distribution, we easily obtain $|\bar{z}|$ and $\sqrt{\overline{z^2}}$, where z is written for $\delta a/a$.

$$|\bar{z}| = \frac{2h}{\sqrt{\pi}} \int_0^{\infty} e^{-h^2 z^2} z\, dz = \frac{1}{h\sqrt{\pi}} = 0{\cdot}00272$$

$$\sqrt{\overline{z^2}} = \left[\frac{h}{\sqrt{\pi}} \int_{-\infty}^{+\infty} e^{-h^2 z^2} z^2 dz\right]^{\frac{1}{2}} = \frac{1}{h\sqrt{2}} = 0{\cdot}00341.$$

These values are of the same order of magnitude as Haworth obtained from his study of the 311 reflection from permalloy. To calculate the internal or latent energy, Haworth uses the following formula derived by Stibitz(19):

$$V = 3E\overline{z^2}/[2\,(1 + 2\sigma^2)],$$

where V is the energy per unit volume, E Young's modulus, and σ Poisson's ratio. A somewhat similar formula has been given by Boas(2). Stibitz's formula assumes that the substance is elastically isotropic and that the stresses are independent and oriented at random with zero mean values. The experimental results themselves show that the stresses are not oriented entirely at random, so that the formula cannot strictly be applied, but nevertheless it may be used to obtain an estimate of the latent energy. Taking E as equal to $29{\cdot}4 \times 10^{11}$ dyne-cm.$^{-2}$, as given by Grüneisen(12), and assuming that $\sigma = 0{\cdot}3$, we obtain for the energy per gram

$$V = 0{\cdot}0834 \text{ cal./g.}$$

This value may be compared with the value found by Haworth for cold-worked permalloy, namely, 0·066 cal./g. It is considerably larger than values calculated by Boas for copper and nickel by a factor of the order of 20, but a larger value is to be expected for rhodium owing to its much greater hardness.

§ 9. CONCLUSIONS

The results of measurements of X-ray intensities reflected by filed and chemically prepared specimens of rhodium powder show that the change of intensity produced by working the metal may be largely explained in terms of primary extinction, and that there is little or no residual effect such as was previously found in similar experiments on copper and nickel, which might be attributed to lattice-distortion. The mean crystal-sizes of the filed powders calculated on the assumption that the whole of the variation of $[f_{T(\text{filed})}/f_{T(\text{chem.})}]$ with $(\sin\theta)/\lambda$ is due to primary extinction are found to be $6{\cdot}3_5 \times 10^{-5}$ cm. and $6{\cdot}6_5 \times 10^{-5}$ cm. respectively for the two filed powders investigated.

Measurements of the reflected widths are made for a total of 23 reflections for five radiations. It is shown that the results cannot be explained in terms of a small crystal-size, since the observed widths plotted against θ lie on or near a single mean curve, whereas if the broadening were due to small crystals a separation according to wave-length should be obtained. Moreover, the relatively large extinction effect shown by the intensity-measurements is incompatible with a crystal-size small enough to produce broadening of the observed magnitude; a size of the order of 90 A. would be necessary.

The observed widths are discussed in relation to other views of the nature of lattice-distribution, and it is shown that they can be accounted for reasonably well on the assumption that the lattice spacing varies about the mean normal value as a result of the internal stresses. Assuming a Gaussian distribution of the lattice spacings, a mean value of $|(\delta a/a)|$ of 0·272 per cent, and a root-mean-square value of 0·341 per cent are found. These lead to an estimate of the internal energy of the order of 0·083 cal./g., which is to be expected from previous estimates for other metals.

§ 10. ACKNOWLEDGEMENTS

Finally we wish to thank Prof. Whiddington for his interest in these experiments, the Government Grant Committee for a grant with which the rhodium and part of the necessary apparatus were purchased, and the Department of Scientific and Industrial Research for a maintenance grant allotted to one of us (P. R.).

REFERENCES

(1) Black, M. M. *Mem. Manch. Lit. Phil. Soc.* **79**, 29 (1935).
(2) Boas, W. *Z. Kristallogr.* **96**, 214 (1937).
(3) Boas, W. *Z. Kristallogr.* **97**, 354 (1937).
(4) Brill, R. *Z. Kristallogr.* **68**, 387 (1928).
(5) Brindley, G. W. and Spiers, F. W. *Proc. Phys. Soc.* **46**, 841 (1934); *Phil. Mag.* **20**, 865 (1935).
(6) Brindley, G. W. and Spiers, F. W. *Phil. Mag.* **20**, 882 (1935).
(7) Brindley, G. W. and Spiers, F. W. *Proc. Phys. Soc.* **50**, 17 (1938).
(8) Brindley, G. W. and Ridley, P. *Proc. Phys. Soc.* **50**, 96 (1938).
(9) Caglioti, V. and Sachs, G. *Z. Phys.* **74**, 647 (1932).
(10) Darwin, C. G. *Phil. Mag.* **27**, 675 (1914); **43**, 800 (1922).
(11) Dehlinger, U. *Z. Kristallogr.* **65**, 615 (1927).
(12) Grüneisen, E. *Ann. Phys., Lpz.*, **22**, 801 (1922).
(13) Haworth, F. E. *Phys. Rev.* **52**, 613 (1937).
(14) Hönl, H. *Ann. Phys., Lpz.*, **18**, 625 (1933).
(15) Jones, F. W. *Proc. Roy. Soc.* A, **163**, S 32 (1937).
(16) Kochendörfer, A. *Z. Kristallogr.* **97**, 469 (1937).
(17) v. Laue, M. *Z. Kristallogr.* **64**, 115 (1926).
(18) Scherrer, P. *Nachr. Ges. Wiss. Göttingen*, p. 98 (1918).
(19) Stibitz, G. R. *Phys. Rev.* **49**, 862 (1936).
(20) Wood, W. A. *Phil. Mag.* **14**, 656 (1932).
(21) Wood, W. A. *Phil. Mag.* **15**, 553 (1933).
(22) Wood, W. A. *Phil. Mag.* **19**, 219 (1935).
(23) Wood, W. A. *Proc. Phys. Soc.* **44**, 67 (1932).
(24) Wood, W. A. *Nature, Lond.*, **129**, 760 (1932); **131**, 842 (1933).

THE CRYSTAL STRUCTURE OF CADMIUM-INDIUM ALLOYS RICH IN INDIUM

By W. BETTERIDGE, Ph.D.

Received 21 *February* 1938. *Read in title* 8 *April* 1938

ABSTRACT. The solubility of cadmium in indium has been determined by X-ray diffraction methods as 14·5 ± 0·5 atomic per cent at 100° C. and 4·5 ± 0·5 atomic per cent at 20° C. The axial ratio of the face-centred tetragonal lattice of the indium-rich solid solution has been found to decrease with increasing cadmium-content, until at 4·5 atomic per cent the structure becomes face-centred cubic. No change in the volume of the indium atom is associated with the change in axial ratio.

---

§ 1. INTRODUCTION

The constitutional diagram of the cadmium-indium system of alloys has recently been determined by thermal and microscopic methods by Wilson and Wick (1). They found that indium dissolves cadmium, forming a solid solution; the limit of solubility is about 18 per cent at 122·5° C., the eutectic temperature, and falls to approximately 12 per cent at room temperature. The present investigation was undertaken with the object of confirming this portion of the diagram by crystallographic methods.

§ 2. PREPARATION OF ALLOYS

The indium was supplied by Messrs Johnson, Matthey and Company, Ltd., and was stated to be of 99·98 per cent purity, the impurities being traces of copper, tin, lead and zinc, with spectroscopically visible traces of aluminium, cadmium, calcium, sodium and silver. The cadmium was obtained from the National Smelting Company, Ltd., who very kindly made a special spectroscopic analysis of the sample used, the percentages of impurities present being estimated as follows: lead 0·015, zinc 0·0075, thallium 0·0075, copper 0·004.

Owing to the high cost of the indium the alloys were made in two series starting with pure indium, additions of cadmium being made to one alloy to produce the alloy next higher in cadmium-content. The metals were melted together in a pyrex tube under a layer of mineral oil and maintained at 200° C. in an oil bath for 10 min.; this is considerably below the melting point of cadmium (321° C.) but was found to be sufficiently high for the indium to take the cadmium into solution, and had the advantage of keeping the melting losses to a minimum. The molten alloy was allowed to cool slowly to 180° C., taking about 5 min., and the tube containing it was then removed from the oil bath and quenched in cold water, the freezing range of the alloy thereby being quickly traversed and segregation being minimized. The alloys were all very soft and in order to render them as homogeneous as possible they were severely cold-worked by hammering and subsequently annealed at 100° c. for 3 hours. The bar of metal was then cut in two, and filings were taken from the section for examination in the X-ray diffraction camera, the residue being used as the basis for the next alloy of the series. It was found to be unnecessary to anneal the filings to remove strain, for they annealed spontaneously at room temperatures and yielded sharp high-order lines in the X-ray diffraction pattern; this also proves that the treatment given to the block of metal was efficient in yielding a sample of uniform composition.

By starting with approximately 5 grams of indium and following the procedure described above, a series of alloys was prepared with the following nominal cadmium-contents: 4·75, 8, 12, 15, 20 and 25 per cent by weight. The loss of weight in melting was between 0·005 and 0·032 g. for each alloy, corresponding to percentage losses of from 0·1 to 0·6. If the losses are assumed to consist entirely of cadmium the composition of the final alloy will be 23·3 per cent, while if the losses are entirely indium the value will be 25·2 per cent. A chemical analysis of the final alloy was made by Mr N. L. Paddock, the cadmium being estimated by precipitation with β-naphthoquinoline and the indium by precipitation with hexamine and weighing after oxidation by ignition. Two individual analyses were made, the cadmium and indium contents totalling 99·8 per cent in the worst case, and the mean result was 25·3 ± 0·1 per cent of cadmium, which suggests that the melting losses were almost entirely of indium. A fine suspension remaining in the oil used to cover the molten alloy was also found to consist mainly of indium. On these grounds it was decided that the compositions of the alloys would be most accurately represented by the values calculated on the assumption that the melting losses were entirely indium, and these values are given in the table.

Cadmium		Structure at 100° c.		Structure at 20° c.	
Weight per cent	Atoms per cent	a_0 (A.)	c/a	a_0 (A.)	c/a
0	0	4·6122 ± 0·001	1·0679 ± 0·001	4·5888 ± 0·001	1·0756 ± 0·001
0·99	1·01	4·6116	1·0668	4·5953	1·0696
1·97	2·01	4·6212	1·0589	4·5973	1·0665
2·94	3·00	4·6334	1·0497	4·6055	1·0592
3·94	4·02	4·6451	1·0397	4·6170	1·0500
4·42	4·51	4·7038 ± 0·0005	1	—	—
4·79	4·89	4·7029	1	4·6310	1·0399
8·05	8·20	4·6939	1	4·6256	1·0434
12·06	12·28	4·6850	1	4·6302	1·0397
15·06	15·33	4·6789	1	4·6284	1·0411
20·1	20·5	4·6791	1	4·6296	1·0404
25·2	25·6	4·6799	1	4·6270	1·0424

After some results had been obtained with the first series of alloys it was found necessary to examine more alloys in the range 0 to 5 per cent of cadmium and accordingly a second series was prepared, starting with pure indium and adding the necessary amount of the 25 per cent alloy to produce alloys with the following nominal cadmium-contents: 1, 2, 3, 4 and 4·5 weight per cent. The last alloy of this series was also chemically analysed, the cadmium-content found being 4·53 per cent, while the composition calculated from the charged weights, allowing for the losses as before, was 4·42 per cent. The compositions given in the table were calculated similarly and are considered to be accurate to within 0·1 per cent; in subsequent reference to the composition of the alloys the atomic percentages, also given in the table, are used.

§ 3. X-RAY APPARATUS AND METHOD

The X-ray apparatus used was the Philips Metalix outfit, the tube employed having a cobalt target.* The camera was 5·76 cm. in diameter and could be used both for the ordinary powder method to give a complete spectrum or for the back-reflection focusing method for accurate measurement of the high-order lines. The Debye-Scherrer method was used in preliminary observations in order to identify the lines of the diffracted pattern, but all the parameters quoted have been deduced from planar spacings obtained from photographs taken by the focusing method. A brass frame was fitted to the camera which threw a shadow of two knife edges on the film, by means of which film-shrinkage was allowed for. The distance apart of the knife edges was determined from a photograph of the reflections of pure silver, the size of the unit cell of which was taken to be 4·0773 A.

In the case of the cubic lattice of the indium-rich solid solution the reflection of the cobalt Kα radiation by the {333} planes of the lattice is obtained at an angle of 80 to 83°, which enables accurate evaluation of the size of the unit cell to be made. For the tetragonal lattice, however, at least two reflections are required in order to obtain the two parameters, and the following method was found to be the most accurate. The reflections from the {422} and {224} planes occur at angles of approximately 70 and 65° respectively in the case of pure indium, and approach one another as the axial ratio of the tetragonal cell is reduced, finally merging into one reflection when the cell becomes cubic. These reflections were used to calculate the axial ratio, which was then used in conjunction with the accurately determined spacing of the {333} planes to calculate the separate parameters a_0 and c_0. The accuracy of the value of the axial ratio was twice as great when it was obtained by this method as when it was obtained by calculation from the {333} and {422} spacings, although the latter planes were those with the most accurately determined spacings.

The structures at room temperature were obtained by mounting the specimen in the form of fine filings in a uniform layer on a thin sheet of card with weak adhesive, and clamping this against the aperture in the wall of the camera. For the structures at 100° C. the filings were mounted in a similar manner on a thin metal foil, and steam was blown on to the back of the foil. No direct measurement of the temperature of the sample was made, but it has been shown by Owen and Yates (2) that a powder cemented to a metal sheet attains very closely the temperature of the sheet, and it is therefore assumed that the temperature of the sample was within 2° of 100° C. Care had to be taken to insulate the camera from the source of heat, and as a further precaution it was cooled with an air blast. It was found unnecessary to maintain the temperature of the sample for any lengthy period before commencing the exposure, for equilibrium, as judged by the sharpness of the lines in the X-ray pattern and the reproducibility of the results, was attained almost immediately. The procedure adopted was to pass steam for five minutes before commencing the exposure.

---

* The wave-lengths used were Kα_1 1·78529 and Kα_2 1·78919 A.

§ 4. STRUCTURES AT 100° C.

The parameters found for the indium-rich solid solution at 100° C. are given in columns 3 and 4 of the table, the values quoted being mostly the mean of two independent observations. It will be noticed that, with increasing cadmium-content, the axial ratio of the tetragonal cell falls, slowly at first and then suddenly, until at 4·5 atomic per cent of cadmium the cell becomes cubic. In figure 1 the axial ratio has been plotted against composition. The normal procedure for the determination of a solubility limit from a series of measurements such as those in the table is to plot the length of the side of the unit cell against the composition, but in the present case, in order to embrace the observations both of tetragonal and cubic lattices, the volume of the unit cell has been plotted, as shown in figure 1. From the fact that the line shows no inflection at 4·5 per cent of cadmium, the composition at which the cubic structure supersedes the tetragonal, it is clear that a true change of phase

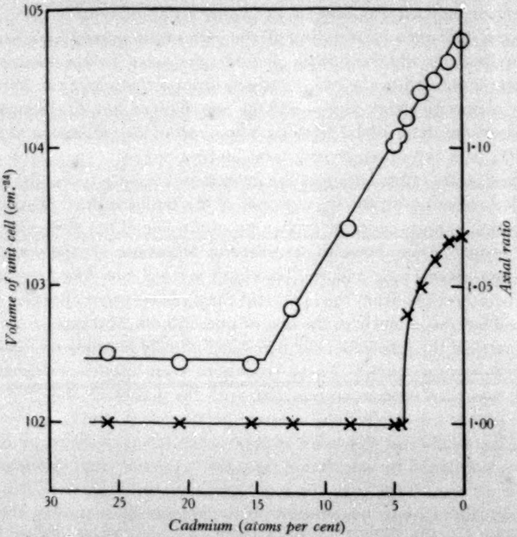

Figure 1. Cadmium-indium alloys at 100° C. ○, volume of unit cell; ×, axial ratio.

cannot be considered to occur there, and that the tetragonal structure is, as it is usually considered to be, merely a distorted form of the normal face-centred cube, as a result of some lack of symmetry (probably incomplete ionization) of the indium atom. The true solubility limit at this temperature is at 14·5 atomic per cent of cadmium, which agrees quite well with the value of 15·3 per cent taken from the diagram of Wilson and Wick, when it is remembered that the latter investigators drew their solubility line from microscopic observations of alloys of fairly widely separated compositions.

§ 5. STRUCTURES AT ROOM TEMPERATURE

Photographs taken immediately after the samples had been cooled from 100° C. to room temperature showed that, in general, a cubic structure did not change to tetragonal, but after ageing at room temperature for several hours the tetragonal structure appeared. A gradual and slight increase in axial ratio over the range 1·035 to 1·045 was observed to proceed for several days until equilibrium was attained after about 5 days. Columns 5 and 6 of the table give the parameters obtained after all samples had been aged at room temperature for at least a week, the photographs being taken at a temperature of 20 ± 2° C. All the alloys have a tetragonal structure, the axial ratio falling with increasing cadmium-content until the solubility limit is reached at 4·5 atomic per cent; this limit was ascertained by plotting the volume of the unit cell against composition as before. The value is considerably lower than the 12 per cent quoted by Wilson and Wick, and the discrepancy is almost certainly due to their microscopic method not being sufficiently sensitive to detect the precipitation which occurs at low temperatures; the precipitate would undoubtedly be in a very finely divided state.

It will be noticed that the axial ratios of the alloys still in the single-phase region are consistently higher than the corresponding ratios at 100° C., even in the case of pure indium. This cannot be assigned merely to a difference in thermal expansion in the directions of the a and c axes of the unit cell, for an actual contraction in the direction of the c axis is found to occur as the temperature is raised. The change appears to indicate a reduction in the asymmetry of the indium atom with increase in temperature, and a complete investigation of the phenomenon is desirable.

§ 6. CADMIUM-RICH PHASE

The phase precipitated from the indium-rich solid solution on crossing the solubility limit consists, according to Wilson and Wick, of cadmium with less than 1 per cent of indium in solution. The Debye-Scherrer photographs of the alloys containing more than 8 per cent of cadmium showed lines due to the precipitated phase, and these were all found to coincide with lines of the pattern for pure cadmium. In the photographs taken by the focusing method the reflection from the {212} planes of the cadmium lattice was recorded for these alloys, and it was measured in the case of the alloys 20·5 and 25·6; a similar photograph was taken with pure cadmium for comparison. The spacings found were: cadmium, 0·91912 ± 0·0002 A.; alloy 20·5, 0·91926 A.; alloy 25·6, 0·91930 A.

Since no change greater than the probable error in measurement was detected, the precipitated phase appears to have been almost pure cadmium, in agreement with the statement of Wilson and Wick, but no limit to the amount of indium in solution can be fixed, since the variation of the {212} spacing of the lattice with composition cannot be determined.

§ 7. DISCUSSION OF RESULTS

The determination of the solubility of cadmium in indium at 100° C. and at room temperature, which was the original object of this research, has been compared with the results obtained by microscopic methods in §§ 4, 5 and the most probable explanation of the discrepancy at room temperature has been given.

Perhaps the observation of greatest theoretical interest, however, is the transformation of the crystal structure of the indium-rich solid solution from tetragonal to cubic with increasing cadmium-content. The tetragonal nature of the lattice of pure indium has been advanced as evidence to show the incomplete state of ionization of the atoms, further evidence being afforded by the fact that the atomic diameter of the atom, determined from the closest distance of approach, is greater than would be expected from comparison with the preceding univalent element silver(3). The present investigation has shown, however, that the asymmetry of the atom, as evidenced by the tetragonal structure, can be destroyed by the presence of about 5 per cent of cadmium without there being any change in the atomic volume. The tetragonal lattice and the large atomic diameter are not, therefore, mutually related and equally dependent on incomplete ionization.

It is very probable that a change in axial ratio similar to that observed in the present case will explain the apparent discrepancy in the constitutional diagram determined for the lead-indium system(4). These two metals are stated to form an unbroken series of solid solutions, but doubt has been cast on this conclusion because of the different lattice structures of the pure metals. A gradual change from tetragonal to face-centred cubic at the indium end of the diagram would remove the difficulties.

Ageew and Ageewa(5) have found that the two metals do not form a continuous series of solid solutions, the structure of the indium-rich solid solution remaining tetragonal up to the phase boundary with no well-marked change in axial ratio. It is felt, however, that another examination of the system would be of value, the possibility of a transformation such as that described above being borne in mind.

§ 8. ACKNOWLEDGEMENTS

The author's thanks are due to the Bristol Aeroplane Company, in whose laboratories the work was conducted, for permission to publish these results.

REFERENCES

(1) Wilson, C. L. and Wick, O. J. *Industr. Engng Chem.* **29**, 1164 (1937).

(2) Owen, E. A. and Yates, E. L. *Proc. Phys. Soc.* **49**, 17 (1937).

(3) Hume-Rothery, W. *The Structure of Metals and Alloys* (1936). London.

(4) Hansen, M. *Der Aufbau der Zweistofflegierungen* (1936). Berlin.

(5) Ageew, N. and Ageewa, V. *J. Inst. Met.* **59**, 311 (1936).

A SIMPLE TYPE OF HELIUM CRYOSTAT

By J. G. DAUNT and K. MENDELSSOHN
Clarendon Laboratory, Oxford

Received 9 *March* 1938. *Read* 13 *May* 1938

ABSTRACT. Two simple cryostats for the temperature region of liquid helium are described; they have been found to facilitate experiments in that region greatly. The apparatus were constructed with the aim of combining the advantages of a small liquefier with those of an ordinary helium cryostat.

§ 1. INTRODUCTION

Two different techniques have been employed hitherto in handling liquid helium. One was developed in Leiden in close resemblance to experiments with liquid air and liquid hydrogen; helium is liquefied in a standard liquefying unit, and the liquid is transferred into a Dewar vessel in which it can be carried about. The specimen under investigation and the measuring apparatus are immersed in this bath of liquid helium. The other technique, which was developed by Simon and his collaborators, employs a compound apparatus in which a small helium liquefier is directly attached to each experimental unit(1).

The advantage of the helium bath is the comparatively simple arrangement of the apparatus, which makes it easy to change specimens. Its disadvantages are the high price made necessary by a big liquefaction unit, the necessity of using great amounts of helium, large pumps, and so on, and the difficulty of controlling temperature. The compound apparatus on the other hand is free from these disadvantages and is especially adapted to the conditions at very low temperatures, where it is possible to carry out practically all experiments with only a very small amount of liquid helium, since the latent heat of the cooling agent is very high in comparison with the heat capacities of most substances. A disadvantage of the compound apparatus, however, is the work imposed on the researcher, who, in order to insert a new specimen, has to take the apparatus to pieces and to resolder and test one or more vacuum cases. As these cases have to hold a vacuum of 10^{-6} cm. of mercury the reassembling requires much care and time. It is further necessary to warm up the apparatus to room-temperature in order to insert a new specimen, which is very uneconomic when a great number of specimens is to be investigated.

We have developed a type of apparatus which combines the advantages of the helium bath and the compound apparatus. As two of these cryostats have now been in use for two years and have proved extremely useful for various experiments at liquid helium temperatures, a detailed description of them seems justified.

The first apparatus, A, was so designed that the specimen was kept in the liquid helium itself and could be exchanged several times, the same helium, produced in one liquefaction, being used throughout. In the second apparatus, B, the specimen can be changed between two helium liquefactions without the apparatus having to be warmed above the temperature of liquid hydrogen.

§ 2. APPARATUS A*

In order to illustrate the principle of the liquefier, a simplified diagram is given in figure 1. The helium liquefaction was carried out by the expansion method[2] in which helium gas, compressed to a high pressure, is allowed to expand adiabatically from a low starting temperature produced by solid hydrogen.

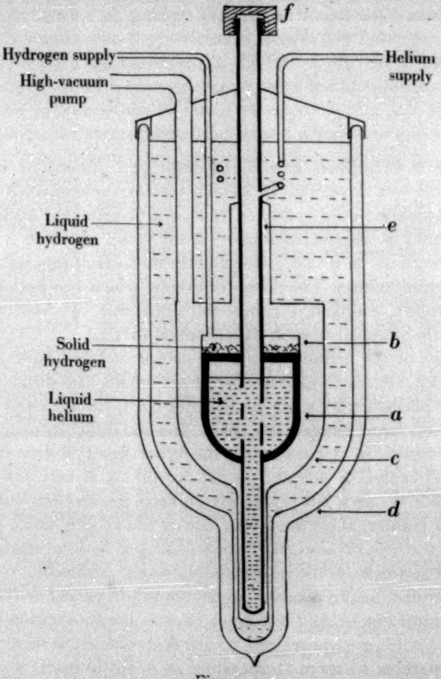

Figure 1

a represents a strong-walled high-pressure helium chamber to which the hydrogen container *b* is attached. *a* and *b* are kept in the vacuum jacket *c* which can insulate thermally the helium chamber from the liquid hydrogen in the glass Dewar vessel *d*, surrounding the whole apparatus. The helium chamber is suspended on a strong-walled tube *e*, extending to the top of the apparatus. This tube, which is of German silver, is closed at the top by a heavy nut *f* which can withstand the pressure of 150 atmospheres in the helium chamber before an expansion is made. The specimens were inserted in the helium chamber through this long tube and in the actual apparatus they were situated in a long tail-like projection of the helium chamber. This shape of the lower end of the apparatus served to facilitate magnetic experiments. After the compressed helium had been expanded and liquid helium obtained in the helium chamber, the nut *f* was unscrewed and replaced by a cap which could support any electrical or mechanical connexions to the specimen. It was found quite possible with this arrangement to change specimens when liquid helium was in the apparatus, so that several different specimens could be used during one run. In no case however was it necessary in changing specimens to disturb any vacuum-jacket joints, which are always left sealed.

---

* Apparatus A was constructed with the collaboration of Dr R. B. Pontius.

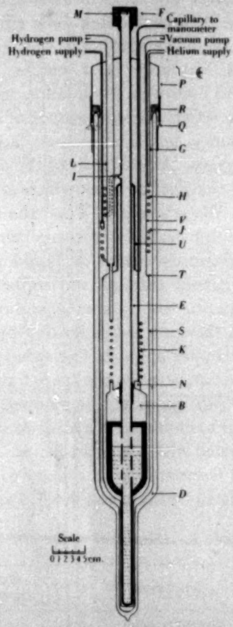

Figure 2

The temperature of the specimen was determined by measuring the vapour pressure of the surrounding liquid helium which was in actual contact with it.

A complete diagram is given in figure 2. The whole apparatus was suspended by the tube *e* from the brass cap *p*. The glass Dewar vessel *d* was joined to the cap by means of a rubber sleeve *q* with a packing of felt *r* between the metal and glass.

The vacuum jacket consists of the cylindrical copper tube *s* which is soldered with Wood's metal to the copper cap *t*. This cap is attached to the tube *e*, through the tower *u*. This tower was employed in order to increase the distance between the points at hydrogen temperature and at helium temperature along the tube *e*, in order to isolate thermally the helium chamber more effectively, without at the same time giving too large a volume to the vacuum jacket. The tower was made of thick-walled copper tubing which conducted heat well, so that towards the end of an experiment the level of liquid hydrogen could fall to the bottom of the tower while the tube *e* would continue to retain the temperature of liquid hydrogen at the place at which it enters the vacuum jacket. The vacuum jacket was shaped to surround the tail, as shown in the diagram. All the parts of the jacket were of copper, tinned on the outside to block up the porous holes which are found to exist in copper, and soldered together with Wood's metal. The exhaustion of the vacuum jacket was carried out through the thin-walled German-silver tube *v*.

High-pressure helium previously cooled in liquid air was led in through the German-silver tube *g* and passed through the copper spiral *h* immersed in the liquid hydrogen, before entering the helium chamber through the tube *e* at *i*. Hydrogen was condensed in the space *b* by allowing hydrogen gas at a small over-pressure to circulate in the copper spiral *j*. The spiral *k* was of German silver, in order to make the heat connexion between the space *b* and the hydrogen bath as bad as possible. The condensed hydrogen could be pumped off through the thin-walled German-silver tube *l*, in order to obtain solid hydrogen at about 10° K. in the space *b*. The joint on the cap *f* was sealed with a lead washer *m*. A small helium gas thermometer *n* was connected by a German-silver capillary to a dial vacuum manometer, in the manner described in detail by Mendelssohn(3). Particulars are given in table 1.

Table 1. *Details of apparatus A*

Part	Material	Inside diameter	Outside diameter
Tube *e*	German silver	1·1 cm.	1·6 cm.
Spirals *h* and *j*	Copper	$\frac{1}{8}$ in.	$\frac{3}{16}$ in.
Spiral *k*	German silver	3·6 mm.	4 mm.

The specimens were always connected to a long glass or German-silver tube which reached up to the cap *f*. This tube also carried the electrical connexions leading to the specimen. After the helium had been liquefied by expansion and while it was boiling under atmospheric pressure,* cap *f* was unscrewed and the electrical wires leading to the specimen were taken out† through the new cap which was fitted instead of *f* and which contained a wide tube. This tube could be connected to a strong pump to pump off the liquid helium. Owing to the great width of *e* and this connecting tube the liquid helium could be kept boiling at temperatures as low as 1·3° K.

---

* As the tube *i* was connected to a gasometer the helium was actually boiling at an over-pressure of 2 cm. of mercury.

† Of course only specimens which withstood the pressure of 150 atmospheres could be inserted before the liquefaction.

For different kinds of experiments different caps were employed. Figure 3 shows a cap that was employed for induction experiments. The German-silver tube

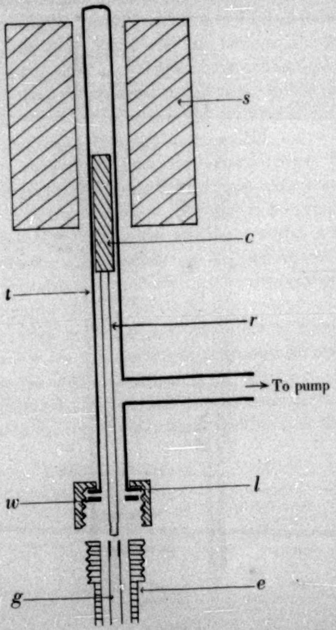

Figure 3

g, which bore the specimen at its lower end, was threaded at the upper end, and to this thread could be screwed a rod *r* which at its upper end bore a cylinder *c* of soft iron. Rod and cylinder were surrounded by the tube *t* sealed at the top and having at its lower end a flange *l*, which could be pressed on to the upper end of the tube *e* by a nut, a vacuum-tight joint being obtained by means of the washer *w*. By means of the solenoid *s* the soft-iron cylinder could be pulled up in *t*, in turn withdrawing the specimen from a search coil.

It was found that the rate of evaporation of liquid helium in this apparatus was approximately 7 cm^3 per hour. Consequently it was possible, if good conditions of pressure and temperature had been obtained before the expansion, to keep liquid helium temperatures for twelve hours or more.

Another alternative was to make experiments of a shorter duration and to use part of the liquid helium to cool a second or a third or even a fourth specimen. The procedure for changing the specimen was the following. After the cap had been unscrewed the old specimen was withdrawn and the new one, previously cooled in liquid air, was quickly inserted into the top of the tube *e*. But before the specimen was allowed to reach the liquid helium it was kept for some time high up in the tube *e*, above the tower *u*, where it could take up the temperature of the surrounding hydrogen bath. The evaporating helium acted as heat-exchanging medium between the specimen and the bath. When it was certain that the specimen had reached the temperature of the boiling hydrogen, it was gently lowered into the liquid helium. In order to avoid loss of helium or condensation of air into the apparatus during the exchange of the specimens, the outlet tube *e* was covered with a temporary cap of plasticine through which the long rod bearing the specimen was withdrawn or lowered. The evaporating helium left the apparatus through the high-pressure tubes and spirals via *i* and was collected in a gasometer.

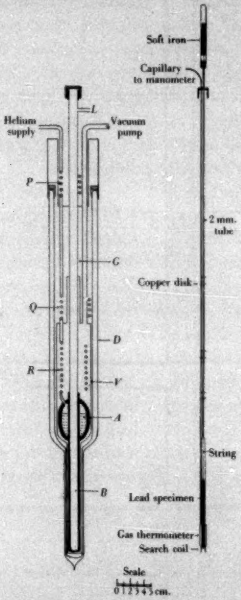
Soft iron
Capillary to manometer
L
Helium supply
Vacuum pump
P
2 mm. tube
G
Copper disk
Q
D
R
V
A
String
B
Lead specimen
Gas thermometer
Search coil
Scale
0 1 2 3 4 5 cm.

Figure 4

§ 3. APPARATUS B

Apparatus B, which also worked with the expansion method, was smaller than apparatus A and was employed when experiments of two hours' duration or less were carried out. It was also possible with this apparatus to make experiments in the temperature region between 4° and 10° K. A diagram is given in figure 4. The specimen was again introduced through the long German-silver tube *g*, which however did not communicate directly with the helium chamber. *g* had thin walls (0·1 mm. thick) and bore at its lower end the helium chamber *a*. Through the middle of *a* there was a strong-walled copper tube *b* which projected considerably beyond the lower end of the helium chamber and was closed at the bottom. *b* formed a continuation of *g*. The whole arrangement was suspended in the vacuum jacket *v*. Before *a* and *b* were embodied in the apparatus the whole unit was carefully annealed for twenty-four hours to ensure good heat-conduction along *b*. Helium was supplied to *a* by the tube *r* which before entering the vacuum space was coiled at *q* in order to precool the helium in liquid hydrogen. In order to minimize the evaporation of liquid hydrogen, the cap of the apparatus was constructed to form a container for liquid air, through which the tubes leading to the apparatus passed. The compressed helium entering the apparatus was precooled to the temperature of liquid air in the spiral *p*. The helium chamber had no hydrogen space attached to it as apparatus *A* had. As the hydrogen bath was small and the influx of heat was reduced by the liquid air in the cap, a low enough starting temperature for the expansion could be obtained by pumping the whole hydrogen bath with a good rotary pump. The temperature of *a* was indicated by a gas thermometer similar to the one in apparatus A, which was attached to the top of the helium chamber (not shown in the drawing).

Table 2. *Details of apparatus B*

Part	Material	Inside diameter	Outside diameter
Tail *b*	Copper	1·1 cm.	1·6 cm.
Spirals *p* and *q*	Copper	$\frac{1}{8}$ in.	$\frac{3}{16}$ in.
Spiral *r*	German silver	3 mm.	4 mm.

As the space containing the specimen was not subjected to high pressure, as it was in apparatus A, the specimen with its special cap and attachments was always inserted before the liquefaction. As an example, the arrangement which was employed to measure the induction in a lead rod is shown in figure 4*a*. The specimen can be withdrawn from the search coil by means of a string connected to a lump of iron at the top of the apparatus, which can be pulled up with a magnet. The temperature of the specimen is determined by means of a gas thermometer. Circular copper discs, which have the same diameter as the internal width of the German-silver tube *g*, prevent convection currents in the helium gas which could give an unwanted heat-exchange between the lower and upper ends of the tube. During the experiment helium gas of a few mm. of mercury was kept in the tube *g*.

To exchange a specimen for another after one liquefaction, without removing the bath of liquid hydrogen, *g* was connected through *l* to the gasometer, thus giving a slight over-pressure of helium and preventing the condensation of air in the tube. The exchange of specimens was carried out in very much the same way as that described for apparatus A.

In order to test the homogeneity of temperature along *b*, a preliminary experiment was carried out in which the bulb of a helium gas thermometer was allowed to travel up and down in *b*. It was found that the variation of temperature was less than 0·02°. The heat-influx into this apparatus was comparatively small, so that only 4·5 cm^3 of liquid helium evaporates in one hour.

When experiments between the temperature ranges of liquid helium and liquid hydrogen were to be carried out, the highly compressed gas in the helium chamber was expanded not to atmospheric pressure but only so far as to cool the apparatus to the desired temperature. Owing to the large heat-capacity of the gas remaining in the helium chamber *a*, the apparatus warmed up only very slowly; to keep the temperature constant it was only necessary to expand from time to time a little further. It was possible in this way to take readings to an accuracy of about 0·01° or less, and it was found that the same values were obtained for these temperatures when the temperature was attained by a preceding cooling or warming. This means that, with our method of keeping the temperature constant by allowing a little gas to escape from time to time, no temperature-difference of a higher order than 0·01° occurred in the apparatus.

In the temperature region of liquid helium the temperature of the cryostats could be kept constant to less than 0·003° by means of a device described by one of us(4).

§ 4. CONCLUSION

The cryostats were used for a great number of various electric and magnetic experiments; a list of publications in which results obtained with these cryostats have been communicated is given at the end of the paper(5). It is quite evident, however, that the cryostats can be used for other purposes also without much difficulty, for instance in optical experiments, determinations of thermal conductivities, gas absorption, and so on. The cryostats have been in constant use, sometimes twice a week, over long periods, and it was never necessary to disturb vacuum joints or any part of the liquefaction mechanism. Apart from the replacing of specimens and caps, they required no attention. They have proved especially time-saving when a series of experiments with a great number of specimens had to be carried out. As the exchange of specimens entailed practically no work, whereas in the ordinary small-scale liquefier such an exchange usually required a whole day, researches could be carried out in two or three liquefactions which otherwise would have taken several weeks.

REFERENCES

(1) For a fuller description of these techniques see, for instance, *Low Temperature Physics*, by M. and B. Ruhemann. Cambridge University Press.

(2) SIMON, F. "On the expansion method for the liquefaction of helium." *Proc. VIIth Int. Congress of Refrigeration*, **1**, 367 (1936).

(3) MENDELSSOHN, K. "Eine Apparatur nach dem Desorptions-verfahren für Messungen bis zu 2° abs." *Z. Phys.* **73**, 482 (1931).

(4) MENDELSSOHN, K. "The transition between the supraconductive and the normal state. I. Magnetic induction in mercury." *Proc. Roy. Soc.* A, **155**, 558 (1936).

(5) MENDELSSOHN, K. and DAUNT, J. G. "Supraconductivity of lanthanum." *Nature, Lond.*, **139**, 473 (1937).

DAUNT, J. G. and MENDELSSOHN, K. "Equilibrium curve and entropy difference between the supraconductive and the normal state in Pb, Hg, Sn, Ta and Nb." *Proc. Roy. Soc.* A, **160**, 127 (1937).

MENDELSSOHN, K., MOORE, J. R. and PONTIUS, R. B. "Threshold value, magnetic induction and free energy of supraconductors." *Proc. VIIth Int. Congress of Refrigeration*, **1**, 431 (1936).

MENDELSSOHN, K., DAUNT, J. G. and PONTIUS, R. B. "Some experiments on supraconductors." *Proc. VIIth Int. Congress of Refrigeration*, **1**, 445 (1936).

DAUNT, J. G. "Experiments on supraconductors in alternating magnetic fields." *Phil. Mag.* **24**, 361 (1937).

MENDELSSOHN, K. and PONTIUS, R. B. "Thermal conductivity of supraconductors in a magnetic field." *Phil. Mag.* **24**, 777 (1937).

PONTIUS, R. B. "Threshold values of supraconductors of small dimensions." *Phil. Mag.* **24**, 787 (1937).

"Magnetic experiments on tin, lead and vanadium", to be published shortly.

DISCUSSION

DR EZER GRIFFITHS. The authors have produced an extremely compact and adaptable apparatus for work at liquid-helium temperatures.

I should like to draw attention to the gas thermometer forming part of the apparatus shown on the table. It would be interesting to know the relative volumes of the gas-thermometer bulb and the dial gauge, what precautions have to be taken to maintain the purity of the helium, and what solders and fluxes are used in the construction of the apparatus.

AUTHORS' REPLY. The ratio of the volumes of the thermometer bulb to the dial gauge is about 1 : 10. At this ratio the temperature interval between 0 and 20° K. covers roughly two-thirds of the gauge scale.

The helium coming from the compressor passes an oil strainer and a trap containing charcoal that dips into liquid air.

The solders employed at consecutive stages in the building of the apparatus are silver solder with borax as flux, soldering-tin, and Wood's alloy with Baker's fluid as flux.

INTENSITY OF γ RADIATION PRODUCED BY SLOW NEUTRONS

BY R. D. HILL, M.SC., AND A. A. TOWNSEND, M.SC., Natural
Philosophy Laboratory, University of Melbourne

Communicated by Professor T. H. Laby, F.R.S., 28 January 1938.
Read in title 27 May 1938

ABSTRACT. Intensities of γ rays produced by absorption of slow neutrons have been measured for eleven elements. The results for thermal neutrons are used to calculate relative values of p, the probability of production of a γ-ray quantum by an absorbed neutron. In general, the values of p so found lie close to unity (which is the value assumed for cadmium). This observation is discussed in relation to the absolute magnitude of p, and it appears likely, in fact, that p is of the order of at least five in the elements investigated. Measurements have also been made of the γ-ray intensities as a function of the thickness of specimen for the elements silver, chlorine and mercury. These lead to approximate determinations of the absorption coefficients of thermal neutrons in these elements. For slow neutrons of greater than thermal energies, the γ-ray intensities have been used to obtain the relative cross sections for γ-ray production.

§ 1. INTRODUCTION

THE production of γ radiation when slow neutrons pass through certain substances has been observed and measured by many experimenters. This emission of γ rays is usually explained by supposing capture of the incident neutron into the nucleus; the energy assigned to the radiation being such that the total energy in the process is conserved. To interpret the capture process on the lines of the Bohr theory of the nucleus, we may say that the neutron and nucleus form a new intermediate nucleus, which may attain its ground state by one or more transitions. We will denote this number of transitions by p; thus p represents the number of γ-ray quanta emitted per absorbed neutron.

The question of the magnitude of p has been investigated theoretically by Bethe and Bacher(1), and experimentally by Fleischmann(2) and by Griffiths and Szilard(3). Theory indicates that the number of γ-ray quanta is probably quite large; but whereas the latter experimenters found for cadmium a value of p greater than or equal to 7, the former obtained the value 1. Both these absolute evaluations involved difficult estimates of tube-counter efficiency and of geometrical factors. Another method of obtaining some information of the magnitude of p is to compare the values of p for various elements. For instance, if the values were to fall into a definite integral relationship with one another, it would be clear that at least for some of the elements the absolute values of p are greater than 1.

Relative measurements of p for a number of elements have already been made by Griffiths and Szilard(3), who found that the values are reasonably constant.

The experiments to be described below determine relative values of p for eleven elements, thermal neutrons being used. For non-thermal neutrons, relative cross sections are calculated, since the information for obtaining p is unavailable.

§ 2. EXPERIMENTAL ARRANGEMENT

Figure 1 shows the arrangement of the apparatus used to investigate the emission of γ radiation. The γ radiation was detected by a tube counter, 6 cm. long and 3 cm. in diameter. The pulses were amplified and then counted by a scale-of-four counter of the type described by Wynn-Williams and Ward(4). The counter was placed in a lead cylinder whose walls were 2 mm. thick, this thickness being sufficient to prevent any β particles arising in the specimen from reaching the counter. The specimens in which γ radiation was induced were, in general, of rectangular cross section measuring 9×7 cm.^{2} and of sufficient thickness to produce a conveniently measurable effect. They were placed directly under the counter, and were completely covered on the top face by an absorber of boron carbide which totally absorbed the thermal neutrons scattered to the specimen from the surroundings. Absorbers of boron carbide could be placed immediately below the specimen.

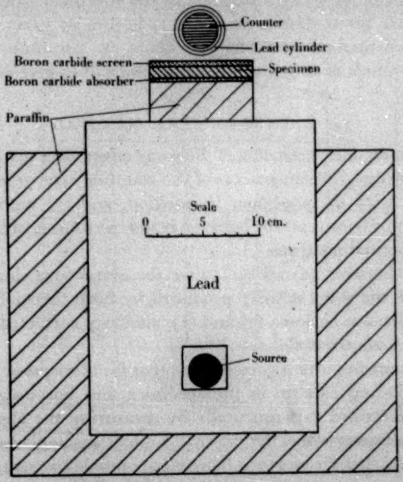

Figure 1. Experimental arrangement.

Cadmium, silver, copper and iron were measured in the form of solid blocks, mercury and chlorine (as carbon tetrachloride) as liquids in a thin iron container, and arsenic, vanadium, iodine, antimony, tin in the form of powder contained in small tins.

The remainder of the arrangement comprises a quantity of paraffin to produce the necessary slow neutrons and sufficient lead between the counter and the radon-beryllium source to reduce the background count to a reasonable figure.

§ 3. MAGNITUDE OF EFFECTS

With the counter used, the normal natural count was approximately 60 per min. The count with a 350-millicurie radon-beryllium source in position was 300 per min. A cylinder of cadmium surrounding the counter then increased the count to 700 per min. This effect of 400 per min. is the largest effect measured, the minimum being about 30 per min. This is the corrected effect as described in the next section, correction being made for γ-ray absorption in the specimen. In the tables, experimental activities are given relative to either cadmium or silver. The actual effect for silver with non-thermal neutrons was about 60 per min. With the smaller effects even long periods of counting were not sufficient to give very great accuracy.

§ 4. EXPERIMENTAL METHOD

For each specimen, measurements of the γ-ray effect were made for both thermal and resonance neutrons. Measurements of the counting rate were made (1) without the specimen, (2) with the specimen in position, and (3) with the specimen in position and a filter of boron carbide between it and the source, of sufficient thickness to eliminate the thermal neutrons.

The difference between (2) and (1), after the corrections described below had been applied, gave the γ-ray activity produced by both thermal and non-thermal neutrons. The difference between (3) and (1), similarly corrected, gave the activity due to non-thermal neutrons alone.

The first and most important correction is that for absorption of γ rays from the source and surrounding paraffin in the specimen and boron-carbide filter. This correction was determined experimentally by measuring the absorption of γ rays in the various specimens when the neutron-source was replaced by one of pure radon. It is assumed that the γ rays in this case are nearly the same as those incident on the counter when a neutron-source is in position. The γ rays in the latter case differ only by the addition of some γ radiation produced by the absorption of neutrons in the paraffin, and by the presence of the hard γ radiation produced during the α-particle-beryllium reaction in the source. The latter radiation is comparatively weak, while the γ rays arising from the neutron-proton reaction have nearly the same energy as the primary γ rays from the source(5, 6). The validity of this method was confirmed by subsidiary experiments in which the absorption in lead of the radiations from the neutron and pure radon sources were compared.

The second correction was for the different effective distances of the specimens below the counter. It was determined experimentally by measuring the effect due to a sheet of cadmium placed at different distances below the counter. To apply the correction a mean distance was first calculated from the absorption coefficients of thermal neutrons as given by Dunning and his co-workers(7).

§ 5. EXPERIMENTAL RESULTS

To compare the activities of the different specimens the relation

$$I=Np\,\frac{\mu_n}{\mu_n-\mu_\gamma}\,(e^{-\mu_\gamma l}-e^{-\mu_n l}) \qquad \ldots\ldots(1)$$

has been used in the reduction of the results. Here I is the total intensity of γ rays from the upper surface of the specimen, in quanta per unit time; N is the number of neutrons, thermal or non-thermal, incident on the specimen per unit time; p is the probability of production of a γ-ray quantum by an absorbed neutron; μ_n is the mass absorption coefficient of neutrons, thermal or non-thermal, in the specimen; μ_γ is the mass absorption coefficient of induced γ rays in the specimen; and l is the mass per unit area of the specimen.

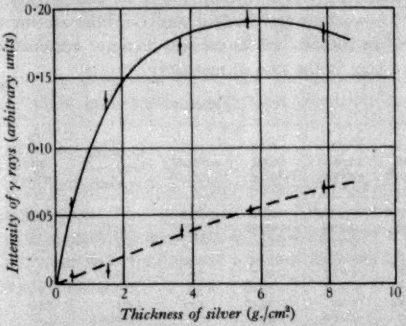

Figure 2. Excitation of γ rays in silver. —— Thermal neutrons; ---- resonance neutrons.

Thermal neutrons. In previous work thermal neutrons have been separated from those of non-thermal energies by placing a sheet of cadmium of thickness nearly 0·5 mm. in the neutron beam. The neutrons so absorbed have been defined by Fermi and Amaldi as C neutrons. This method of isolating thermal neutrons is unsuitable when γ rays are being investigated, owing to the intense γ radiation from the cadmium sheet. For this reason a boron-carbide filter has been used to absorb the thermal neutrons. Boron absorbs slow neutrons strongly, but produces only a weak γ radiation.

To correlate this work with results published by other workers who used cadmium to separate thermal neutrons, it is necessary to know the absorption coefficient of thermal neutrons in boron. The mass absorption coefficient has been measured by Livingston and Hoffmann(8), who obtain the value $\mu/\rho=36$ cm.²/g. Mitchell(9) as well as Goldsmith and Rasetti(10) give the value $\mu/\rho=28$ cm.²/g. All these determinations were made with detectors whose sensitivity varied inversely as the neutron-velocity. Measurements carried out by Burhop and others(11) by an entirely independent method support the higher value of μ/ρ. Their value, $\mu/\rho = 38$ cm²/g., will be used. From this, it is readily calculated that our boron-carbide filter (containing 0·0614 g./cm² of boron) absorbs 87 per cent of the *C* neutrons as detected by a v^{-1}-law detector.

The γ-ray activity as a function of the specimen-thickness has been investigated for the elements silver, chlorine, mercury. Figure 2 shows a typical curve, obtained for silver. As is indicated by equation (1), the activity *I* is given as a function of the thickness by the difference between two exponential terms, $\exp(-\mu_\gamma l)$ and $\exp(-\mu_n l)$, so that by assuming a value for μ_γ, a determination of μ_n can be made from the form of the curve.

The values of μ_γ for the absorption of the radiations in the specimens themselves have been calculated from the energies of the γ-ray quanta as determined by various workers$^{(5, 6)}$. These values are shown in column 4 of table I. The values of μ_n then determined as above, are given in column 5 and, for comparison, the values found by Dunning and co-workers and Szilard and Griffiths are included in the next columns. The present authors' values are seen to agree reasonably well with those of other workers except in the case of mercury.

Table 1

Element	Thickness (g./cm²)	Experimental activity	μ_γ calculated (cm²/g.)	μ_n authors (cm²/g.)	μ_n Dunning and co-workers	μ_n Griffiths and Szilard	p authors	p Griffiths and Szilard
(17) Chlorine	1·73	0·912	0·061	0·65	0·65	0·89	1·22 ± 0·16	0·95
(23) Vanadium	1·68	0·174	(0·033)	—	0·118	—	0·95 ± 0·10	—
(26) Iron	10·2	0·317	0·029	—	0·13	—	0·74 ± 0·18	—
(29) Copper	5·38	0·178	0·029	—	0·0713	—	0·60 ± 0·18	—
(33) Arsenic	3·61	0·162	0·035	—	0·070	—	0·78 ± 0·14	—
(47) Silver	5·25	0·211	0·0346	0·50	0·309	0·54	0·96 ± 0·11	0·75
(48) Cadmium	0·434	1·00	0·0340	—	15·5	24·4	1·00	1·00
(50) Tin	4·20	0·109	0·039	—	0·0204	—	1·48 ± 0·40	—
(51) Antimony	5·88	0·160	(0·04)	—	0·0403	—	0·85 ± 0·14	—
(53) Iodine	5·51	0·142	(0·04)	—	0·0448	—	0·72 ± 0·18	—
(80) Mercury	1·76	0·678	0·040	0·63	1·145	1·04	1·03 ± 0·10	1·05

In the majority of elements the γ-ray activity has only been found for one thickness of specimen. In these cases, the value of p has been calculated relatively to cadmium, for which p has been taken arbitrarily as 1. For this purpose a knowledge of both μ_γ and μ_n is necessary; μ_γ is obtained as described above, while μ_n is taken from Dunning's results. The resulting values of p are tabulated in column 8, while some values obtained by Griffiths and Szilard are given in column 9.

As can be seen from the table, the values of p lie reasonably close to unity. This observation may be interpreted in either of two ways. The departures from unity may be attributed to experimental error and the results taken as indicating that the values of p are the same for all elements. If this be the case, then, the simplest hypothesis to make is that the nucleus following the capture of the neutron reaches the ground state in a single transition. On the other hand, if the departures are considered as real the results indicate the existence of rather large values of p which are all of much the same order of magnitude for the elements here studied.

In this case, we may conclude that the average number of γ-ray quanta emitted per absorbed neutron is at least five. This conclusion is consistent with the observations of Griffiths and Szilard for cadmium and has the theoretical support of Bethe and Bacher.

Non-thermal neutrons. The γ-ray activity produced by non-thermal neutrons has been studied as a function of thickness for the element silver. The results are graphed in figure 2. In table 2 the experimental activities for single thicknesses of six elements relative to silver are shown and the corresponding relative cross sections tabulated. These cross sections have been calculated from the relation

Table 2

Element	Thickness (g./cm.^{2})	Experimental activity	σ_γ relative to A
(26) Iron	10·2	0·70 ± 0·25	0·13 ± 0·05
(29) Copper	5·72	0·83 ± 0·25	0·32 ± 0·10
(33) Arsenic	3·61	0·36 ± 0·13	0·26 ± 0·09
(47) Silver	3·68	1·00 ± 0·16	1·00 ± 0·16
(51) Antimony	5·88	0·46 ± 0·13	0·32 ± 0·09
(53) Iodine	5·51	0·76 ± 0·19	0·59 ± 0·15
(80) Mercury	20·7	1·59 ± 0·32	0·52 ± 0·11

$$\sigma_\gamma = \frac{IA}{l},$$

where σ_γ is the relative cross section, I the intensity of the γ rays, A the atomic weight of the specimen, and l the superficial mass of the specimen. The value of σ_γ is then reduced so as to make the cross section for silver unity. The use of the above relation is justified, since the experimental activities have been corrected for γ-ray absorption in the specimen.

§ 6. ACKNOWLEDGEMENTS

We take this opportunity of thanking Dr E. H. S. Burhop for his advice and help with the investigation. We are also indebted to the Commonwealth X-ray and Radium Laboratory for supplying us with the necessary radon to perform the experiment. Both authors were aided by research grants from the University of Melbourne.

REFERENCES

(1) Bethe and Bacher. *Rev. Mod. Phys.* **8**, 82 (1936).
(2) Fleischmann. *Z. Phys.* **100**, 307 (1936).
(3) Griffiths and Szilard. *Nature, Lond.*, **139**, 323 (1937).
(4) Wynn-Williams and Ward. *Proc. Roy. Soc.* A, **136**, 312 (1932).
(5) Fleischmann. *Z. Phys.* **103**, 113 (1936).
(6) Kikuchi, Aoki and Husimi. *Nature, Lond.*, **137**, 992 (1936).
(7) Dunning and co-workers. *Phys. Rev.* **48**, 265 (1935).
(8) Livingston and Hoffmann. *Phys. Rev.* **51**, 1021 (1937).
(9) Mitchell. *Phys. Rev.* **49**, 453 (1936).
(10) Goldsmith and Rasetti. *Phys. Rev.* **50**, 328 (1936).
(11) Burhop, Hill and Townsend. *Proc. Roy. Soc.* A, **165**, 116 (1938).

THE MOTION OF A MERCURY INDEX IN A CAPILLARY TUBE

By G. D. YARNOLD, M.A., D.Phil., Lecturer in Physics,
University College, Nottingham

Received 7 *February*, 1938. *Read* 8 *April* 1938.

ABSTRACT. The general case of the motion of an index of any liquid is considered theoretically and it is shown that the viscosity of the liquid can be determined by observation of the velocity of the index when different pressure-differences are applied between its ends. Experiments on the motion of mercury indexes are described; they lead to a value of the viscosity which is about 6 per cent higher than the accepted value. The discrepancy is attributed to the electrification of the walls of the tube which continues to increase slowly even after the index has made several excursions along it. It is found that the difference between the angles of contact at the two ends is practically independent of the velocity of the index.

§ 1. INTRODUCTION

It was shown many years ago by Jamin(1) that a liquid index in a tube is able to withstand quite a considerable difference in pressure between its ends without being caused to move along the tube. Jamin pointed out that the index adjusts itself so that the two end surfaces have different curvatures, and the angle of contact between the liquid and the wall of the tube is different at the two ends. The maximum pressure-difference which the index can withstand without moving was found to be independent of its length. When the index moves along the tube the end surfaces still have different curvatures but, so far as can be ascertained, the motion was not studied by Jamin.

More recently, the motion of a mercury index in a comparatively wide tube was investigated by Rankine(2) in connexion with his determination of the viscosities of the rare gases. In his experiments a short mercury index fell slowly in a vertical tube, driving the gas through a fine capillary tube. Rankine noted that the difference in curvature between the top and bottom surfaces causes a small reduction in the effective weight of the index, but he found the apparent reduction in weight to be independent of the length and velocity of the index. As will appear later, this is true only when the viscous forces within the index are negligible, and would not be true in a narrow tube.

The need for a more complete investigation of the motion of an index was suggested to the writer by some chance observations made with a Wilson capillary electrometer which was in use in the laboratory.

§ 2. MOTION OF AN INDEX OF ANY LIQUID

Let us consider an index of any liquid at rest in a horizontal tube which is sufficiently narrow for the end surfaces to be regarded as spherical, figure 1. Let the pressure of air in the tube be atmospheric at the right-hand end and greater than atmospheric by an amount p at the left-hand end. There is thus a tendency for the index to move from left to right, and the end surfaces adjust themselves as shown in the figure. Let us suppose that the angle of contact becomes θ_1 at the left-hand end and θ_2 at the right-hand end of the index. Then, if the surface tension of the liquid is denoted by T and the radius of the tube by a, the force opposing the pressure-difference p and keeping the index at rest is given by

$$2\pi a T (\cos\theta_1 - \cos\theta_2) = \pi a^2 p$$

and thus

$$p = \frac{2T}{a}(\cos\theta_1 - \cos\theta_2) \qquad \text{......(1).}$$

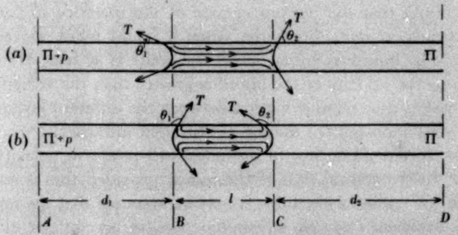

Figure 1. (*a*) Index of a liquid which wets the tube; (*b*) index of a liquid which does not wet the tube.

The maximum difference in pressure which the index can withstand without moving increases as the radius of the tube is diminished, and is ultimately governed by the extent to which the angle of contact can change without the occurrence of slip. When a liquid rests in contact with a solid surface and the angle of contact has its normal value θ, the following relation holds between the surface tension T of the liquid and the tensions T_{SA} and T_{SL} of the interfaces separating respectively the solid from the air and the solid from the liquid:

$$T\cos\theta = T_{SA} - T_{SL} \qquad \text{......(2).}$$

If the angle of contact departs from the normal value, then, for equilibrium, it is necessary to suppose that there is a frictional force(3) equal to F per unit length of the line of contact and acting at right angles to it, so as to oppose the motion of the liquid over the solid surface. Thus at one end we have

$$T\cos\theta_1 = T_{SA} - T_{SL} + F \qquad \text{......(3)}$$

and at the other

$$T\cos\theta_2 = T_{SA} - T_{SL} - F \qquad \text{......(4).}$$

Subtracting, we obtain $$T(\cos\theta_1 - \cos\theta_2) = 2F \qquad \text{......(5)}$$

and thus $$p = \frac{4F}{a}.$$

It is now seen that the maximum pressure-difference which the index can withstand depends on the limiting value of the friction F. In the case of most liquids the limiting friction varies widely, and in any case it depends on the state of both the solid and liquid surfaces.

When the pressure-difference between the ends becomes sufficiently great the limiting friction is exceeded and the index moves along the tube. The two end surfaces still have different curvatures, from which it follows that the frictional force F still acts when the liquid is in motion. It must not, however, be assumed that when the index is in motion F is either equal to the limiting friction or independent of the velocity of the index.

If a pool of mercury moving on a gently sloping plane surface is observed it appears to roll. The velocity of the top surface, as is shown by the movement of dust particles, is considerably greater than the velocity of the pool as a whole, while there is little doubt that the bottom surface of the mercury in contact with the solid is very nearly at rest. Similarly, when a liquid index moves in a tube it actually flows. The liquid in contact with the walls is at rest, or very nearly so, while on the axis the velocity of the liquid is greater than the velocity of the index as a whole. There is thus relative motion between the different layers of the liquid, and viscous forces opposing the motion are brought into play.

Let us now consider the flow of an index with uniform velocity in a tube of uniform bore. In the central part of the index, provided this is sufficiently long compared with the radius of the tube, it may be assumed that the motion approximates to the ordinary case of streamline flow in an infinite tube, to which Poiseuille's law applied. In this region the streamlines are parallel to the axis of the tube. Near the ends of the index, however, the streamlines cannot be parallel to the axis and it is reasonable to assume that the flow is somewhat as indicated in figure 1. Moreover, at the rear end of the index the liquid is being accelerated to the velocities characteristic of the Poiseuille distribution, while at the front end the liquid is decelerated. The kinetic energy of the index as a whole remains constant and, any dissipation of energy by turbulence being neglected, it will be supposed that the forces necessary to accelerate the liquid at the rear end are equal and opposite to the forces causing the deceleration at the front end. Thus, in the application of Poiseuille's equation, no correction will be made for the kinetic energy given to the liquid, but an end correction will be added to the length of the index to allow for the curvature of the streamlines near the ends.

The total pressure-difference between the ends of the tube when the index is in motion is now seen to be made up of three parts, (1) the term $(\cos\theta_1 - \cos\theta_2)\,2T/a$ arising on account of the difference in curvature between the two ends; (2) a pressure-difference due to the viscous forces brought into play by the relative motion of the different layers of liquid; and (3) the pressure-difference required to drive air along the sections AB and CD of the tube.

Poiseuille's equation for an incompressible fluid may be written in the form

$$p_1 - p_2 = \frac{8\eta l V}{\pi a^4},$$

where the symbols have their usual significance. The effective length of the index which must be used in calculating term (2) in the preceding paragraph is greater than the actual length l and may be taken as $(l+x)$, where x, the end correction, is some function of the radius of the tube. If v is the velocity of the index as a whole, the volume of liquid passing any cross-section of the tube per second is $\pi a^2 v$ and thus, in order to maintain the flow, there must be a pressure-difference $8\eta v\,(l+x)/a^2$.

Since the viscosity η' of air is small compared with the viscosity η of the liquid, and since the actual mean pressures of the air in the sections *AB* and *CD* of the tube, figure 1, are large compared with the pressure-difference p, we may use the same form of Poiseuille's equation for the flow of the air as for the flow of the liquid. Thus for the fall in pressure along the section *AB* of length d_1 we have $8\eta' v d_1/a^2$, and for the fall in pressure along the section *CD* of length d_2 we have $8\eta' v d_2/a^2$, an end correction being unnecessary in this case. If the total length of the tube is L these two pressure-differences may together be represented by the term $8\eta' v\,(L-l)/a^2$, which remains constant as the index moves along the tube. For the total pressure-difference between the ends of the tube we now have the expression

$$p = \frac{8v}{a^2}\left[(l+x)\,\eta + (L-l)\,\eta'\right] + \frac{2T}{a}(\cos\theta_1 - \cos\theta_2) \qquad \ldots\ldots(6).$$

It had been hoped that a method might be developed by which the viscosity of a small volume of a liquid might be determined by measurement of the velocities of indexes of different lengths with different values of the driving pressure p. However, in the case of liquids which wet the tube, it was found that the film of liquid left behind on the walls, which is inherently unstable, very quickly collects together to form a number of small indexes which complicate the motion. Experiments have in consequence only been made with mercury indexes, and these experiments will now be described.

§ 3. EXPERIMENTAL PROCEDURE

Some difficulty was experienced in obtaining uniform glass capillary tubes sufficiently long to enable accurate measurements of the velocity of the index to be made. Eventually, three soft-glass tubes were selected, each of length 150 cm.; their cross-sectional areas, as determined by measurement of a mercury index, did not vary by more than 2 per cent from the mean value. The mean radii of the tubes found from the weight of mercury required to fill them were respectively 0·0277, 0·0503 and 0·1014 cm. The tubes were mounted side by side on wooden supports screwed to the bench and adjusted so as to be accurately horizontal, their ends being bent as shown in figure 2 to facilitate the introduction at *A* and removal at *B* of the mercury indexes. Each end of each tube could be either opened to the atmosphere or connected to the reservoir *C* in which the pressure was raised above atmospheric. The reservoir was of about 6 litres capacity and contained calcium chloride. The manometer D contained xylene, of specific gravity 0·866. Each tube was carefully washed and dried before use, and only clean redistilled mercury prepared by Hulett's(4) method was used for the indexes.

In order to drive the index from left to right the stopcocks T_1 and T_3 were closed and T_2 and T_4 left open. To drive the index from right to left T_1 and T_3 were opened and T_2 and T_4 closed. With this arrangement an index could be driven backwards and forwards along the tube several times while the pressure of the air in the reservoir remained sensibly constant. The terminal velocity of the index corresponding to any particular difference in pressure between its ends was obtained by timing it in both directions with an accurate stopwatch, reading to one tenth of a second, over a distance of 80 cm. in the middle of the tube. The method of timing did not introduce any systematic error.

When an index was driven along a tube which had not been used for some time, it was found that the velocity acquired under any particular pressure-difference was less than on subsequent occasions when the index had already made several excursions along the tube. This is thought to be due to the fact that during the motion of the index the mercury and glass become oppositely charged. However, after several excursions the electrification of the tube remains practically constant and only increases slowly as the index continues to move to and fro. Thus, after several excursions very little work is done in separating the charges. For this reason an index was always driven backwards and forwards along the tube several times before its velocity was recorded.

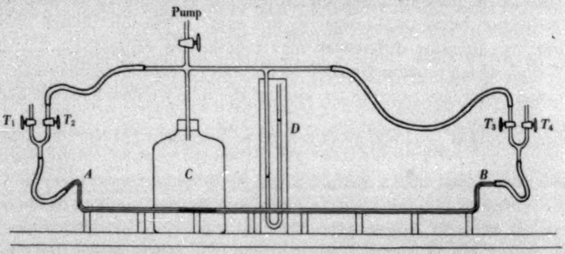

Figure 2. Arrangement of apparatus (only one of the three capillary tubes is shown).

Velocities greater than about 20 cm./sec. could not be measured with sufficient accuracy on account of the difficulties of timing, while at very low velocities the indexes were found to stick. The results obtained in the range in which accurate observations of the velocity are possible are shown by the curves in figures 3, 4 and 5, which refer respectively to capillary tubes of small, medium and large diameters. Each curve represents the variation of pressure-difference with velocity for an index of the length shown. The ordinates represent the pressure-difference in cm. of xylene, and the abscissae velocities in cm./sec. Figures 3, 4 and 5 are all drawn on the same scale to facilitate comparison of the results for the different tubes.

§4. DISCUSSION OF RESULTS

It will be seen that in each case the pressure-difference necessary to drive a particular index increases linearly with increase of velocity except when the critical velocity is exceeded. The critical velocities for the three tubes calculated from Reynolds's formula, with the value 0·0160 g./cm.-sec. for the viscosity of

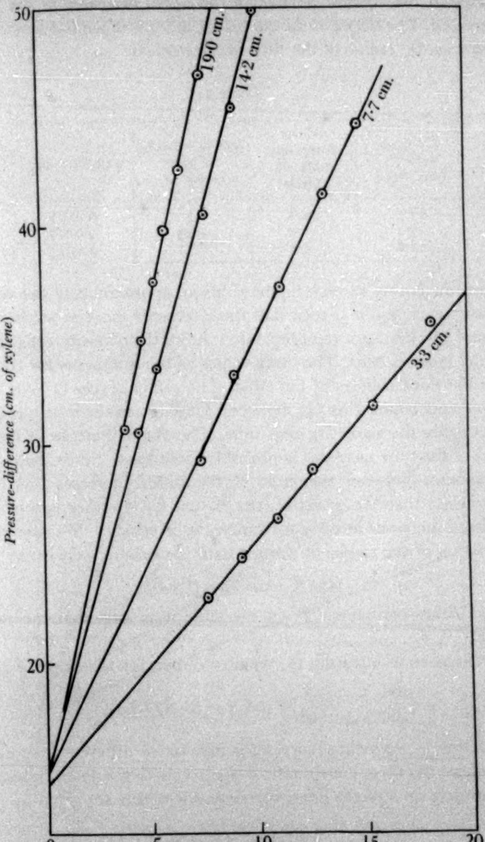

Figure 3. The variation of pressure-difference with velocity for indexes of various lengths in the tube of radius 0·0277 cm.

mercury at 15° C., are given in the second column of the table. The critical velocity is exceeded only in the experiments with the widest tube and, as would be expected, the rate of increase of pressure becomes more rapid beyond this point. With each tube the slope of the straight portion of the curve increases as the length of the index is increased. The slopes of the curves for indexes of similar lengths in different tubes increase as the radius of the tube is diminished.

Table 1

Radius of tube (cm.)	Critical velocity (cm./sec.)	Mean intercept (cm. of xylene)	$(\cos\theta_1-\cos\theta_2)$ at zero velocity	η (g./cm.-sec.)	$\left(\frac{8\eta}{a}x+2TB\right)$
0·0277	42·5	14·8	0·32	0·0171	2·1
0·0503	23·4	8·9	0·35	0·0169	3·4
0·1014	11·6	4·7	0·37	0·0173	11·7

Moreover, the curves in each figure all make approximately the same intercept on the pressure axis, and it is seen that the intercepts increase as the radius of the tube decreases. The intercept represents the value of the pressure-difference when the velocity of the index is zero. The mean values of the intercepts for the three tubes are given in the third column of the table. The values of $(\cos\theta_1-\cos\theta_2)$ calculated from the intercepts taking T as 547 dyne/cm. are given in the fourth column and are seen to be roughly the same for each tube. The slight increase in $(\cos\theta_1-\cos\theta_2)$ as the radius of the tube increases is probably fortuitous. Since, however, the total pressure-difference between the ends of the index increases linearly with the velocity it is clear that the quantity $(\cos\theta_1-\cos\theta_2)$ is either independent of the velocity or itself increases linearly with increase of velocity. We may represent the possible variation of the angles of contact with increase of velocity by writing

$$(\cos\theta_1-\cos\theta_2)=A+Bv,$$

where A and B are constants. From the table it is seen that the value of A is roughly 0·35.

By differentiation of equation (6) we now obtain for the slope of each curve

$$\left(\frac{dp}{dv}\right)_{l\ \text{const.}}=\frac{8}{a^2}[(l+x)\,\eta+(L-l)\,\eta']+\frac{2TB}{a} \qquad \text{......(7).}$$

The slopes of the experimental curves for indexes of different lengths are shown in figure 6, where the three curves refer respectively to the three tubes. The points lie quite accurately on straight lines, the slopes of which are given by

$$\frac{d}{dl}\left(\frac{dp}{dv}\right)=\frac{8}{a^2}(\eta-\eta').$$

The values of η calculated from the slopes of the curves in figure 6 are shown in the fifth column of the table.

Comparison with the accepted value 0·0160 g./cm.-sec. of the viscosity of mercury at 15° C. shows the experimental values to be too high by about 6 per cent. The errors of observation are not considered to be large enough to account for the difference, more particularly since the values of η obtained with the three tubes are consistent to within 2 per cent.

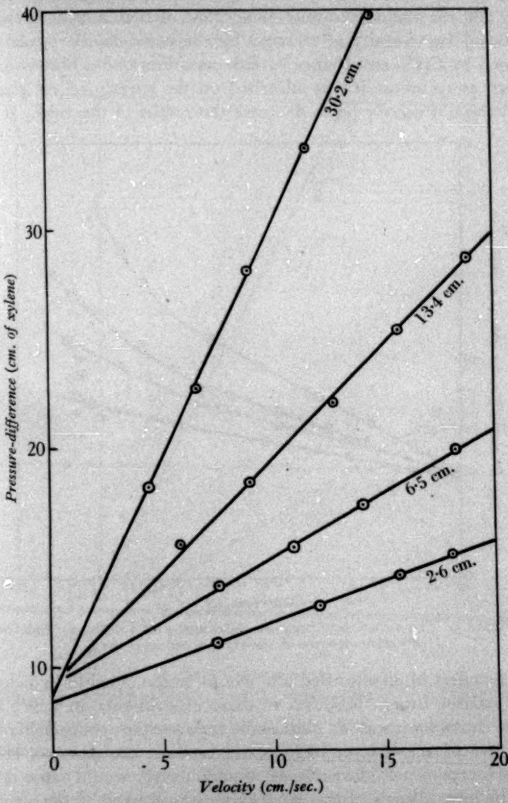

Figure 4. The variation of pressure-difference with velocity for indexes of various lengths in the tube of radius 0·0503 cm.

It seems probable that the discrepancy is due to the fact that work is always done in producing the small increase in the electrification each time the index traverses the tube. If the tube were of quartz it is likely that the electrification would become quite constant after several excursions of the index and that a more accurate value of the viscosity would be obtained. Experiments are being made to test this view.

Nevertheless, the mere fact of electrification suggests also that the outer layer of mercury may slide over the glass and that there may be a thin film of air between the mercury and the wall of the tube. The effect of such a layer in the case of the measurement of the viscosity of mercury by the usual capillary-tube method has been discussed by Erk(5) and Reiner(6). Erk considers that a film of air would be quickly swept away unless it was adsorbed on the surface of the glass, in which case its effect would merely be to decrease the radius of the tube. It is generally agreed that the effect of an adsorbed film would be too small to be detected except in extremely narrow tubes. However in these experiments, in which the moving mercury is in contact with air at both ends, it is perhaps conceivable that a layer thicker than the adsorbed layer might exist between the mercury and the glass without being swept away. The presence of such a layer would cause the measured value of η to be low. Clearly, if this error exists it is masked by the error due to the work done in electrification.

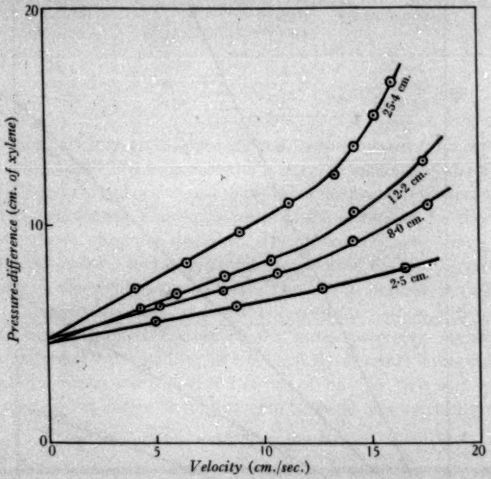

Figure 5. The variation of pressure-difference with velocity for indexes of various lengths in the tube of radius 0·1014.

It may be urged that the error is in part due to the fact that Poiseuille's equation has been used without any allowance for the kinetic energy given to the liquid. This would be a justifiable criticism if the value of η were derived from observation of a single index. That the correction is in any case small is evident from the fact that the experimental points lie accurately on the straight lines of figures 3, 4 and 5.

Schiller and Kirsten(7) have obtained a series of kinetic-energy corrections for the case of flow into a tube with a bell mouth; unfortunately, however, these corrections are not applicable to the experiments described here, and attempts to use them produced results of no value. With any one tube any kinetic-energy correction, if it were necessary, would be the same for indices of different lengths moving with the same velocity. It follows that the slopes of the curves in figure 6 would be unchanged by making the correction and the same value of η would be obtained.

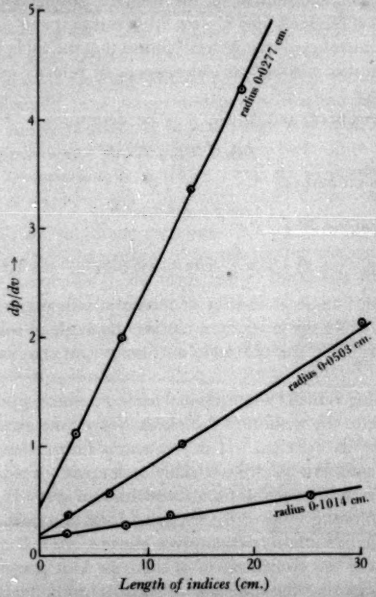

Figure 6. The variation of (dp/dv) with the length of the index for the three tubes.

We must now return to consider the possible effect of change of velocity on the angles of contact at the two ends of the index. The curves in figure 6 do not pass through the origin but make intercepts on the axis of (dp/dv). The intercepts, denoted by Y, are obtained by putting l equal to 0 in equation (7). Thus

$$Y=\left(\frac{dp}{dv}\right)_{l=0}=\frac{8}{a^2}(x\eta+L\eta')+\frac{2TB}{a}.$$

From this equation neither x nor B can be determined separately. However it may be written in the form

$$a\left(Y-\frac{8L\eta'}{a^2}\right)=\frac{8\eta}{a}x+2TB$$

and the quantity on the right-hand side can be calculated. The values obtained are given in the last column of the table. Although this quantity can be determined only very roughly, it clearly increases as the radius of the tube increases. It is hardly likely that B is a function of the radius and we can only suppose that the end correction x depends on some higher power of the radius. It then follows that the second term of the expression, namely $2TB$, is certainly less than 2·1, which means that B is less than 0·001. We may therefore conclude that the angles of contact at the two ends of the index are independent of the velocity throughout the range of the observations, and that the term $(\cos\theta_1 - \cos\theta_2)$ is constant and equal approximately to 0·35. It will be remembered that Ablett$^{(8)}$ found that the angle of contact between water and a paraffin wax surface was independent of velocity except at very small velocities.

The actual values of θ_1 and θ_2 can now be determined. From equations (2) and (3) we obtain

$$T(\cos\theta_1 - \cos\theta) = F,$$

and from equations (2) and (4)

$$T(\cos\theta - \cos\theta_2) = F.$$

Thus by equation (5)

$$\frac{F}{T} = (\cos\theta_1 - \cos\theta) = (\cos\theta - \cos\theta_2) = \tfrac{1}{2}(\cos\theta_1 - \cos\theta_2) = 0{\cdot}175.$$

If we take the normal angle of contact of mercury with respect to glass as 140°, it then follows that while the index is in motion the angle of contact θ_1 at the rear end is approximately 160°, and the angle of contact θ_2 at the front end is approximately 126°.

The corresponding value of the frictional force F, which acts at the ends of the index, in opposition to the motion of the mercury over the glass surface, is found to be approximately 96 dyne/cm. It is frequently found that the difference in pressure which is sufficient to drive a short index with a small velocity is not sufficient to start the index moving from its position of rest. It must therefore be concluded that the limiting value of the frictional force is usually somewhat greater than the value of the dynamical friction given above.

An investigation of the electrification of the tube is at present in progress and the effect both of degassing the tube and of substituting a quartz tube for a glass one will be tried.

§ 5. ACKNOWLEDGEMENTS

In conclusion I should like to thank Prof. L. F. Bates and Mr N. Davy for their interest in the work.

REFERENCES

(1) Jamin, J. *Cours de Physique*, 3rd ed. **1**, 230.
(2) Rankine, A. O. *Proc. Roy. Soc.* **83**, 265 (1910).
(3) Adam, N. K. and Jessop, G. *J. Chem. Soc.* **127**, 1863 (1925).
(4) Hulett, G. A. *Phys. Rev.* **33**, 307 (1911).
(5) Erk, S. *Z. Phys.* **47**, 886 (1928).
(6) Reiner, M. and Erk, S. *Z. Phys.* **79**, 139 (1933).
(7) Barr, G. *Monograph of Viscometry*, p. 34.
(8) Ablett, R. *Phil. Mag.* **46**, 244 (1923).

DISCUSSION

Dr G. D. **West**. I should like to call the author's attention to a paper by me "On the Resistance to the Motion of a Thread of Mercury in a Glass Tube" published in the *Proc. Roy. Soc.* **86**, 20 (1911). A very similar formula was there worked out (except that end corrections and the viscosity of the air were neglected), and the experimental procedure was not very different. Dr Yarnold's work, however, is clearly more accurate than my own done twenty-seven years ago, and many points are considered in much greater detail by him. I note also how much more uniform in diameter are his glass tubes. Rather striking, however, is the different value obtained for $(\cos\theta_1 - \cos\theta_2)$. My own value was some 30 per cent higher. It is possible that Dr Yarnold used cleaner mercury, or that the difference is accounted for by the use of different glass, or by a different condition of the glass surface. The suggested experiments with a quartz tube may throw some light on this matter. In fact the variations of $(\cos\theta_1 - \cos\theta_2)$ for different surfaces in contact with the mercury is a subject that the author might think worth investigation.

Professor L. F. **Bates**. Some time ago Dr C. J. Smith suggested that a neat modification of the Quincke method of measuring the magnetic susceptibilities of liquids might be practicable if one made use of the device invented by Professor Ferguson for measuring the surface tension of small quantities of liquid. Accordingly, Mr J. Deller made experiments in my laboratory with this object in view. He used a capillary tube, with one end ground flat, containing a strong solution of manganese sulphate of appreciable magnetic susceptibility. The tube was mounted with the ground end between poles of an electromagnet. The only magnet available at the time was of a lecture-room pattern and not powerful, and the magnetic force upon the column of liquid was not great. The motion of the column of liquid was observed on exciting the magnet, and the column was restored to its original position in several different ways, for instance by tilting the tube, by reducing the pressure on the curved surface of the column, and so on. The measurements of magnetic force thus obtained were most unsatisfactory. They were equally unsatisfactory when the experiments were repeated with the curved surface of the liquid column within the pole-gap. The method failed because the free surface was always deformed before the column moved. The experiments which the author has just described throw much light upon Mr Deller's work, for they show the enormous importance of this deformation of the surface before and during motion, and it is clear that, even if Mr Deller had used a much stronger field, reliable results could not have been obtained with this modification of the Quincke method.

Dr E. G. **Richardson**. I wonder whether the lines of flow in a water index could be investigated experimentally, in a somewhat wider tube; this might show whether energy was being expended in eddies within the index. I doubt whether any effect due to electrification will be found. I cannot recall any authenticated effect of electrification on viscosity. The wings of birds often acquire a static charge in flight, presumably as a result of friction; and I remember some experiments being done in the Aeronautics Laboratory at Queen Mary College to test whether an aerofoil charged to a high potential experiences a lessened resistance to an air current. The result was negative.

Dr L. HARTSHORN. I am very interested in the author's deduction of a frictional force between the mercury and the walls of the tube, which is independent of velocity. Experiments on the damping of mechanical vibrations in solid bodies and on the dissipation of energy in dielectrics in alternating electric fields also appear to demand for their explanation a force of this character, i.e. a force of the nature of soled friction rather than one of viscosity. Has the author any conception of the mechanism of such a force?

In connexion with the problem of the electrification of the tube, it might be worth while to use lead glass as this usually has a much higher electrical resistance than soda glass.

AUTHOR'S REPLY. In reply to Dr G. D. West: I am much obliged to Dr West for drawing my attention to his own work on a similar topic, which had, unfortunately, escaped my notice. I am particularly interested in Dr West's observation that the value of $(\cos\theta_1 - \cos\theta_2)$ deduced from the results of his experiments is some 30 per cent higher than the value I have given. The observations recorded in figures 3, 4 and 5 of my paper were all made with indexes freshly inserted in the tubes, but it was noticed that after an index had remained for 24 hours or more in a tube which was open to the atmosphere the pressure-difference necessary to drive it with a particular velocity was greater than it had been at first. The slope of the curve connecting pressure-difference and velocity was not appreciably different, but the intercept on the pressure axis was always greater than it had been when the index was freshly inserted. This suggests that $(\cos\theta_1 - \cos\theta_2)$ is increased by slight contamination of the mercury, which may be the cause of the discrepancy pointed out by Dr West. On the other hand, I agree with him that the nature of the glass must also affect the value of $(\cos\theta_1 - \cos\theta_2)$.

In reply to Dr E. G. Richardson: It would certainly appear to be worth while to investigate the lines of flow of the liquid in the index as suggested by Dr Richardson. I do not wish to suggest, however, that the viscosity of the mercury is any different from the normal viscosity on account of the electrification, but rather that, in so far as my method of measurement involves the performance of work against electrical forces, the value obtained for the viscosity should be greater than the true value. It does not by any means follow that the measurement of the viscosity of mercury by any of the usual viscometers, in which the liquid always fills the capillary tube, is similarly vitiated.

In reply to Dr L. Hartshorn: The suggestion that there may be some connexion between the frictional forces acting on a mercury index in a glass tube and the dissipation of energy in a dielectric is extremely interesting. I am afraid I have no conception, however, of the nature of the forces; in fact speculation seems premature until the mechanism of the normal angle of contact of a liquid is better understood.

THE PROPAGATION OF SUPERSONICS IN CAPILLARY TUBES

By J. MAY, M.Sc., King's College, Newcastle-on-Tyne

Communicated by Dr E. G. Richardson, 8 *December* 1937. *Read* 8 *April* 1938

ABSTRACT. The velocity and attenuation constants for the propagation of supersonic vibrations, of frequencies 40 to 115 kc./sec., in air contained in narrow tubes, of diameters 0·06 to 0·15 cm., are measured, the sources being monel needles in magnetostrictive oscillation. On comparison with Kirchhoff's theory, the results show that the absorption in the tubes is considerably greater in practice than in theory, though not markedly different from that observed at low frequencies.

§ 1. INTRODUCTION

MEASUREMENTS of the velocity and coefficient of absorption of sound in tubes have in the past been almost entirely confined to tubes of moderate areas of cross-section, in which the layer affected by viscosity can only be a small fraction of the radius. Although a considerable amount of work has been done on tubes several millimetres in diameter, one can mention only two cases in which the authors have made investigations with capillaries. The papers referred to are those by Richardson(1) and Penman and Richardson(2). In the former case the author used a rubber tube 1·7 mm. in diameter and frequencies from 390 to 940 c./sec. Under these conditions he expected to have the main body of air moving under viscous resistance; he measured the amplitude at the end of the tube, using a heated platinum grid. By using a constant amplitude of air-vibration at the beginning of the tube, and by altering the length of the latter, he was enabled to plot amplitude against distance from source; thus he obtained a measure of the absorption involved.

In the second paper the authors investigated the propagation of audible sound in tubes 0·2 mm. in radius. They used a wide pipe stopped at one end firstly with teak and secondly with a bundle of tubes of the diameter quoted, and they measured the amplitude of vibration of the air in each case. They thus obtained a value for the absorption coefficient of the sound in the narrow tubes. The results in both researches gave values for absorption in excess of the value calculated by theory.

The object of the present research is to examine the propagation of sound in tubes having diameters from 1 mm. downwards at high frequencies, so that we may compare the results obtained with those already mentioned. In such cases viscosity effects may be expected to play an important part, and pertinent theories have been evolved by Helmholtz, Kirchhoff, and the late Lord Rayleigh(3). Their work indicates that the damping of the sound waves increases with decrease in radius and increase in frequency. The viscosity effects tend to decrease the velocity of transmission of the sound.

§ 2. APPARATUS

The apparatus in principle consists of a magnetostrictive oscillator in a tube provided with a movable piston, the propagation and attenuation constants of the tube being derived from the reactions on the circuit maintaining the oscillator. This type of apparatus has already been used by Norton⁽⁴⁾ for measurement of the velocity of sound in wider tubes. Norton was able to use oscillators of the usual size, as developed by Vincent⁽⁵⁾ and Pierce⁽⁶⁾. In the present instance, needles had to be used owing to the narrow bore of the tubes, and after a number of materials had been tried, soft monel was finally adopted as giving the best oscillations.

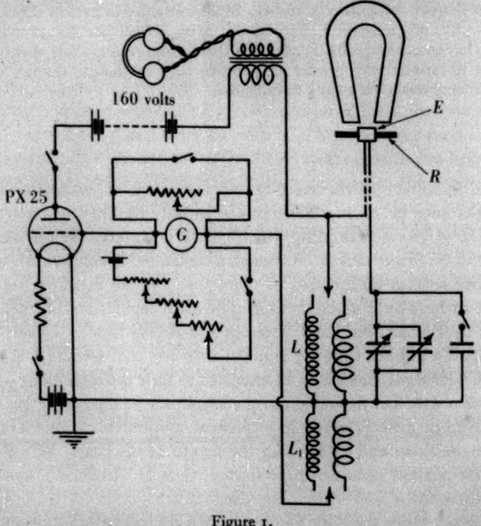

Figure 1.

Magnetostrictive rods having diameters from 0·5 to 3 mm. were experimented with. The oscillation of those less than 0·9 mm. in diameter was so slight and irregular that it was impossible to use them for the purpose in view. Both Vincent's and Pierce's circuits were tried, but Vincent's was found to be the more satisfactory. The circuit finally adopted is shown in figure 1.

The coils L and L_1 are coupled so that the valve oscillates without the rod R being in position, and the range of oscillation frequencies is made to include that of the rod under test. *E* is an exciting coil consisting of a few hundred turns of thin copper wire wound on a paper girdle round the tube. When the rod is replaced and the rotor of the variable condenser is turned round slowly, the grid current changes in the manner described by Vincent. As suggested by Pierce, telephone receivers were used to detect the production of rod vibrations. Both a permanent magnet and an electromagnet were used successfully to provide the polarizing field. By using tubes with walls of different thicknesses it was observed that maximum oscillation of the rod was produced with narrow-walled tubes. This would be expected, since in such a case a larger percentage of the available flux permeates the rod itself.

Since thin-walled capillary tubes were unobtainable, and very narrow rods are poor vibrators, composite glass tubes were used as shown in figure 2; the oscillator, shaded in the figure, was put in the thin-walled tube having a bore of 1·2 mm., and the reflector was moved along inside the thick-walled capillary. In this manner a single oscillator was made to serve for several capillaries of various diameters. To maintain a stable vibration the rod must be fixed at its centre. The readiest method of mounting was to glue a narrow tissue-paper girdle round the middle of the rod. By sliding the needle into the tube a fairly rigid clamping of this girdle was secured, and at the same time the efficiency of production of the sound-waves was not impaired by excessive clamping.

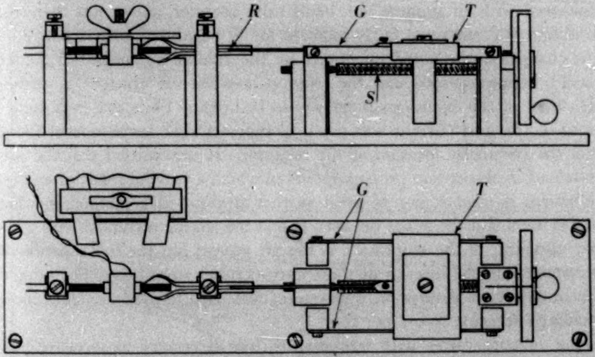

Figure 2. The interferometer.

The reflectors were made of soft metal (brass and copper), and satisfactory reflecting surfaces were obtained by filing on a fine grindstone. A scheme was devised whereby the reflector would not be rotated as it moved forward under the action of the turning handle; the reaction would be withstood by a rigid pillar. A diagram of the interferometer apparatus is shown in figure 2. The screw *S* is made to drive a table *T* along a pair of guides *GG*, the reflector *R* being attached to the table.

§ 3. METHODS OF MEASUREMENT

Although various ways of measuring the changes in the circuit currents with movement of the reflector were actually tried, the only reliable results were obtained when readings were taken with a galvanometer in the grid circuit. Connected across the galvanometer was a variable shunt for choosing the range of deflections desired, and a backing battery circuit to balance out the steady direct current.

In absorption measurements it is necessary to keep the power of the source constant when the supersonic intensity is measured with the reflector at various distances away. Klein and Hershberger(7) suggest that this condition is satisfied if the exciting e.m.f. is maintained constant irrespective of the reaction of the air column. To check this suggestion, the oscillating voltage across the exciting coil was measured with an anode e.m.f. bend valve rectifier, and it was then seen that the exciting e.m.f. remained fairly constant for all positions of the reflector. As the periodic changes in the e.m.f. produced by the gradual movement of the reflector were small, it was assumed that the relation between the changes of current and the variations of the exciting voltage would be linear. Thus the amplitude of the variations of the grid current was taken to represent the amplitude of the sound-waves at the particular location of the reflector. It is admitted that the precision to be attained in absorption measurements in which a moving reflector and reaction on the source is used is not as great as that attained in a method in which the reflector is fixed and the space between it and the source traversed with a hot wire or other measurer of the amplitude in the air waves; but the introduction of such an instrument into the interior of these narrow tubes would have been impossible. A Sullivan dynatron-absorption wave-meter was used to measure frequency. This gave readings accurate to 0·1 per cent.

As the velocity varies with temperature it is necessary to measure the latter accurately when the velocity of sound is to be measured. Neither a thermometer nor a thermojunction could be introduced into the air enclosure, so the only possible procedure was to place a thermometer or thermocouple near the interferometer, and to satisfy oneself that the temperature measured was actually equal to the temperature of the enclosure. The only methods of supplying heat to the air in the tube and thus altering the temperature would be (1) joule heating of the exciting coil, (2) eddy-current heating of the source, and (3) direct heating of the air by sound-waves. The fact that, within the limits of experimental error, the results of wave-length measurements did not vary as the reflector was moved seemed to indicate that heating of the air in the course of a set of measurements did not appreciably raise the temperature in the tube.

§ 4. RESULTS

The natural logarithms of the differences between successive extreme readings of the galvanometer as the reflector is moved are plotted against the number of half-wave-lengths. The slope of the resulting graph represents the absorption coefficient or attenuation per wave-length. Introducing the wave-length as determined from the locations of successive peaks gives us the amplitude-absorption coefficient per cm. The energy-absorption coefficient is twice as great. Each of the four graphs, figure 3, relates to a single tube at four frequencies. Actually the

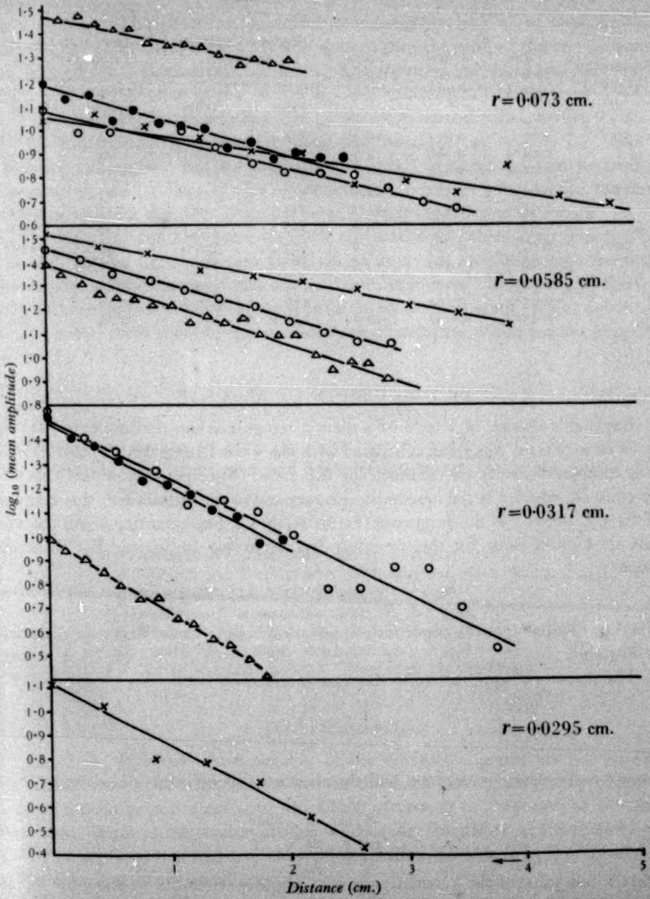

Figure 3. Variation of amplitude with distance. ×, 39·1 kc./sec.; ○, 58·0 kc./sec.; ●, 90·0 kc./sec.; △, 115·0 kc./sec.

logarithms plotted on the graphs are to the base 10, so that the amplitude-absorption coefficient is 2·3 times the slope. The velocity and absorption coefficients are grouped in the table, together with the corresponding values deduced from the Rayleigh theory, which are included for comparison.

Frequency (kc./sec.)	Tube radius (cm.)	Wave-length (cm.)	Tem-perature (° C.)	Reduced velocity (m./sec.)		Amplitude-absorption coefficient	
				Practical value	Theoretical value	Practical value	Theoretical value
39·1	0·073	0·871	16·7	330·4	329·3	0·18	0·053
	0·0585	0·868	14·7	329·2	328·7	0·22	0·061
	0·0295	0·843	17·2	319·8	325·8	0·52	0·121
58·0	0·073	0·582	14·5	329·4	329·7	0·27	0·071
	0·0585	0·576	14·7	325·5	329·3	0·33	0·082
	0·0317	0·576	14·4	325·5	327·7	0·55	0·151
90·0	0·073	0·384	19·8	333·1	330·0	0·32	0·090
	0·0317	0·380	19·6	333·0	328·1	0·60	0·191
115·0	0·073	0·297	18·3	329·6	330·4	0·25	0·100
	0·0585	0·294	18·1	326·1	330·0	0·38	0·115
	0·0317	0·293	18·0	325·1	328·4	0·73	0·212

§ 5. DISCUSSION OF RESULTS

Rayleigh's version of Kirchhoff's theory recognizes two distinct cases, (1) that in which a quantity h is small compared with the wave-length, and (2) that in which h is comparable with the radius r of the tube. The quantity h has the value $2\pi\sqrt{(2\nu/\omega)}$, where ν is the kinematic viscosity and ω the pulsatance; this simplifies to $1{\cdot}4/\sqrt{f}$, where f is the frequency, for air at 17° C. The quantity h will therefore have its highest value for the minimum frequency we are using. For these conditions

$$h_{\text{max.}} = 1{\cdot}4/\sqrt{40{,}000} = 0{\cdot}007 \text{ cm.}$$

It is thus obvious that the conditions in question belong to the first case considered by Rayleigh.

The velocity c' appropriate to this case is given by

$$c' = \left(1 - \frac{h}{4\pi r}\right) c,$$

where c is the open-air velocity, and the absorption coefficient α is given by

$$\alpha = \frac{h}{4\pi r}\frac{\omega}{c} = \frac{1}{rc}\sqrt{\frac{\omega\nu'}{2}},$$

where ν' is a value of the kinematic viscosity slightly enhanced to allow for thermal conduction. The theoretical values are given in the table for comparison with the experimental values.

§ 6. CONCLUSIONS

Velocity. The measurements indicate that at the frequencies used and with tubes having a bore of 1 mm. the velocity deviates very little from the normal velocity.

Absorption. The practical values for the absorption coefficient were much in excess of the theoretical values. It was noticed that the ratio of the two quantities was very constant throughout the series. The mean of this ratio was just over 3, which is about the same as that found at low frequencies.

To sum up: (1) the absorption of supersonics in narrow tubes, within the range of radii and frequencies considered, satisfies the theory as regards the effect of frequency and radius, but its magnitude is much in excess of that determined theoretically; and (2) the velocity of supersonics in narrow tubes within the range decreases with the radius in a similar manner to that predicted by theory.

The value for the kinematic viscosity obtained from tables is for a slow direct flow and may be quite different from the value which applies to high-frequency air vibrations. The viscosity may in fact be a function of the frequency, although within the range that we have covered little variation is apparent. If this conclusion is not correct, there must be some other form of damping which has not been considered by the theorists.

§ 7. ACKNOWLEDGEMENT

The author wishes to offer his best thanks to Dr E. G. Richardson for suggesting this piece of research and for helpful criticism during the course of it.

REFERENCES

(1) Richardson. *Proc. Roy. Soc.* A, **112**, 522 (1926).
(2) Penman and Richardson. *J. Acoust. Soc. Amer.* **4**, 322 (1933).
(3) Rayleigh. *Sound*, **2**, 348 (1896).
(4) Norton. *J. Acoust. Soc. Amer.* **7**, 16 (1935).
(5) Vincent. *Proc. Phys. Soc.* **41**, 477 (1929); **43**, 157 (1930).
(6) Pierce. *Proc. Amer. Acad. Sci.* **63**, 1 (1928).
(7) Klein and Hershberger. *Phys. Rev.* **37**, 760 (1931).

DISCUSSION

Mr H. L. Penman. In a number of the curves the points are not randomly distributed about the mean line, and in the third set, particularly for $v = 58$ kc./sec., there is a definite periodicity, the amplitude increasing as the length of air column increases. What is the source of this modulating frequency of about 20 kc./sec., which seems to have a negative absorption coefficient? Can it be due to reflection at the open end of the capillary tube?

The main point of interest arising out of the paper is the need for a reconsideration of the causes of absorption of sound in gases. The inadequacy of existing interpretations has been shown in tube measurements at audio-frequencies and supersonic frequencies, and for free propagation at supersonic frequencies. If there is such a thing as an oscillatory viscosity which is greater than the kinematic viscosity, it is somewhat disconcerting to find that its value appears to be independent of frequency, there being no appreciable change between 200 c./sec. and 115,000 c./sec. Would it be possible to measure this viscosity by measuring the flow through a vibrating nickel tube?

If this high-value oscillatory viscosity cannot be established, it would seem that an overhaul of the Rayleigh-Kirchhoff theory is needed, and it might be profitable to replace the conception of the medium as a structureless jelly obeying Boyle's law by taking into account the fact that the medium is a molecular aggregate whose parts are in rapid motion, that the gas is imperfect, and that, in addition to viscosity, thermal conductivity and diffusion will tend to annul the effects of an impressed adiabatic pressure wave. As the molecules are not without structure it may be necessary to consider also the changes in internal energy due to collisions, and the interactions of the components where the gas is not homogeneous. In this connexion it is interesting to recall the large increases in the absorption coefficient of air when small amounts (0·5 per cent) of water vapour are present.

AUTHOR'S REPLY. I do not attach any importance to the regular variations in the graphs which Mr Penman points out, since the circuit current fluctuated somewhat in consequence of the vibrations of the laboratory. This would account for the points being deflected a little from the mean straight line. I quite agree that practical results seem to indicate that the coefficient of viscosity is independent of the frequency, but I do not see how the high-frequency value could be measured by the flow of gas through a vibrating nickel tube.

ATTENUATION AND GROUP RETARDATION IN THE IONOSPHERE

By G. MILLINGTON, Marconi's Wireless Telegraph Co., Ltd.,
Research and Development Department

Received 14 *December* 1937. *Read in title* 13 *May* 1938

ABSTRACT. Expressions are derived from the Appleton-Hartree formula for the specific attenuation and group velocity at any given height, in a layer with a vertical electronic gradient, for a wave of any given frequency at vertical incidence in the presence of an oblique magnetic field. They are then used to study the overall attenuation and group retardation of a wave which either is reflected from the layer, or penetrates through it to be returned from a denser layer above. To do this in detail, a definite type of layer has to be assumed, and particular values have to be chosen for the frequency of the wave and the direction and magnitude of the earth's magnetic field, so that the results can be compared with typical experimental data obtained by the usual $P'f$ and $P't$ technique. The analysis shows that, as one would expect from general physical principles, the attenuation and group delay for a wave near to the critical escape frequency occur mainly in the region of maximum density in the layer, and also justifies the use of absorption and equivalent-height measurements to deduce an estimate of the collisional frequency of the electrons in this region. The problem is worked out in detail for one frequency for the extraordinary wave, for values of the earth's field and the angle of the dip corresponding roughly to the values for London, and for a parabolic and a sine-squared law of electronic density. The work falls into four main sections: (*a*) the derivation of the integrals from the Appleton-Hartree formula; (*b*) the effect of the type of the layer on the form of the integrals; (*c*) the application of a graphical method of integration, involving the initial transformation of the integrals to a form in which they can be accurately evaluated; (*d*) the detailed working out of a numerical example, with a discussion of the general conclusions to be drawn from it. It is hoped that the fundamental results for the specific attenuation and group velocity, on which the rest of the paper is based, may prove useful in other investigations.

§ 1. INTRODUCTION

It is well known from ionospheric observations made at vertical incidence by the usual $P'f$ technique, that the absorption of a wireless wave increases very rapidly when the frequency approaches the critical frequency corresponding to the maximum density in the layer. In general the increase in absorption occurs simultaneously with the rapid increase in the observed equivalent height of the layer at the end of the $P'f$ run. In a similar way when a $P't$ run is taken, the equivalent height of a layer may show a rapid increase in value, with an accompanying weakening of the echoes, due to the presence of an intermediate layer in which the density increases so that the critical frequency approaches the wave frequency. In this case, although the wave may still penetrate and be reflected at the upper layer, it will suffer heavy absorption, and the group retardation will cause an apparent increase in the equivalent height of the upper layer.

Eckersley(1) has suggested that when such conditions occur, the measurements of increased absorption and equivalent height may be used to estimate the collisional frequency of the electrons in the region of the intervening layer. Such a method assumes, however, that the attenuation and group retardation are largely independent of the type of layer involved, the major part occurring in the region of maximum density. Although this seems probable on general physical grounds, it was felt that it would be useful to confirm the conclusion by working out the overall attenuation and group retardation in a particular case, by using the Appleton-Hartree formula as a basis for the analysis. In the course of the analysis, explicit forms of the specific attenuation and group velocity are obtained which may be of interest in other connexions, and they are therefore given here in sufficient detail to enable them to be available for such use.

The Appleton-Hartree formula has already been discussed, notably by Ratcliffe(2) and Mary Taylor(3), and the general properties of the function for the refractive index have been studied for various values of the constants involved, including the absorption coefficient. In this paper it is assumed that the absorption coefficient is so small, that all powers higher than the first can be everywhere neglected. With this fundamental assumption, when the Lorentz term is taken to be zero, in conformity with the view now generally accepted, exact expressions for the specific attenuation and group velocity at any given electronic density in the layer can be derived by a long but straightforward process.. In order to integrate the effect over the length of the path in the layer, the relation between the density and the height in the layer has to be known, and the integrals so obtained have to be transformed before they can be applied to the accurate computation of attenuation and increase of equivalent height, for frequencies near to the critical escape frequency.

§ 2. GENERAL OUTLINE OF THE ANALYSIS

For convenience a list of the symbols to be used will first be given; it will serve to summarize the relations existing between them.

f is the wave frequency,
λ the wave-length in free space,
c the velocity in free space,
N the electronic density,
z the height, measured above the lower edge of the layer, at which the density N occurs,
e the electronic charge, and
m the electronic mass.
$f_0 = Ne^2c^2/\pi m$, the critical frequency corresponding to the density N;
z_0 is the height at which the maximum density in the layer occurs,
H the earth's magnetic field, and
θ the angle H makes with the vertical.
$f_H = eH/2\pi mc$, the gyromagnetic frequency;

$\tau = f_H/f$, and is a function of f;

$\zeta = f_0^2/f^2$, and is a function of f and N (i.e. of z).

f_c is the collisional frequency of the electrons at the height z,

β is a constant of the order of $\frac{3}{2}$, according to Burnett(4);

$\alpha = f_c/\beta\pi f$, and is the absorption coefficient;

$\zeta' = \zeta(1 - \iota\alpha)$, i.e. the complex form taken by ζ when α is not zero but very small,*

and

$\tau' = \tau(1 - \iota\alpha)$, the corresponding complex form of τ.

U is the group velocity at the height z,

μ the complex refractive index at the height z,

μ_R the real part of μ,

μ_I the imaginary part of μ, so that $\mu = \mu_R + \iota\mu_I$,

P' the equivalent path in the layer,

$h' = P'/2$, the equivalent height of the layer, and

T is the total group time in the layer, so that $P' = cT$.

In terms of this notation the Appleton-Hartree formula may be written

$$\mu^2 = \frac{(1-\zeta')(1-\tau'^2-\zeta') - \frac{1}{2}\zeta'\tau'^2\sin^2\theta \pm \zeta'\sqrt{\{\frac{1}{4}\tau'^4\sin^4\theta + \tau'^2\cos^2\theta\,(1-\zeta')^2\}}}{(1-\tau'^2) - \zeta'(1-\tau'^2\cos^2\theta)}.$$

In this form it is derived directly from a quadratic equation for μ^2, and it can be shown to be identical with the more familiar form of the Appleton-Hartree equation. Since we are neglecting all the terms involving α^2 etc., it follows at once that μ_R is obtained by merely replacing ζ' and τ' by ζ and τ respectively, while μ_I can be obtained as some function of ζ, multiplied by α, by expanding to the first power of α.

The specific attenuation at the height z is given by $\exp(-\mu_I . 2\pi/\lambda)$, and thus the overall attenuation may be written $\exp(-A)$, where

$$A = \int \frac{2\pi}{\lambda}\mu_I\,dz$$

taken between appropriate limits. The group velocity U is given by

$$\frac{c}{\mu_R + f\,d\mu_R/df}$$

so that the element of the group time T corresponding to dz is given by

$$dT = \frac{1}{c}\left[\mu_R + f\frac{d\mu_R}{df}\right]dz$$

$$= \frac{\mu_R}{c}\left[1 + \frac{f}{2\mu_R^2}\frac{d(\mu_R^2)}{df}\right]dz.$$

In evaluating $f.d(\mu_R^2)/df$ we notice that in μ_R^2 the various functions of ζ and τ involved are all proportional to $1/f^n$, so that any such function F will give

$$f\frac{dF}{df} = -nF,$$

for example

$$f\frac{d(\zeta\tau^2)}{df} = -4\zeta\tau^2.$$

---

* Strictly speaking, $\zeta' = \zeta/(1+\iota\alpha)$ and $\tau' = \tau/(1+\iota\alpha)$.

Thus the final result for $f.d(\mu_R^2)/df$ will not involve f explicitly. The overall equivalent path P' is given by $\int c\,dT$, so that

$$P' = \int \mu_R \left[1 + \frac{f}{2\mu_R^2}\frac{d(\mu_R^2)}{df}\right] dz$$

between the same limits.

The process of evaluating the integrands of our two integrals, though straightforward, involves a long reduction to express them as functions of ζ, and only the final results will be given here. These can be conveniently summarized in the form of a table for quick reference, and for comparison of the cases for the ordinary and extraordinary waves. First, however, we must give a set of polynomials in ζ which are derived in the reduction process, and which form the basis of all the computations. They may be written

$$\begin{aligned}
I_1 = {} & [(2-\tau^2+\tau^4)+3\tau^2\cos^2\theta-\tau^4\cos^2\theta] \\
& -2\zeta\,[2-\tau^2+3\tau^2\cos^2\theta]+2\zeta^2\,[1+\tau^2\cos^2\theta], \\
I_2 = {} & [3\tau^4\sin^4\theta-\tau^6\sin^4\theta+8\tau^2\cos^2\theta] \\
& -2\zeta\,[\tau^4\sin^4\theta+12\tau^2\cos^2\theta-2\tau^4\cos^2\theta\sin^2\theta] \\
& +4\zeta^2\tau^2\cos^2\theta\,[6-\tau^2\sin^2\theta]-8\zeta^3\tau^2\cos^2\theta, \\
I_3 = {} & 2(1-\tau^2)^2-\zeta\,[4(1+\tau^4\cos^2\theta)-5\tau^2(1+\cos^2\theta)] \\
& +\zeta^2\,[2(1-4\tau^2\cos^2\theta)+\tau^4\cos^2\theta\,(1+\cos^2\theta)]+2\zeta^3\tau^2\cos^2\theta, \\
I_4 = {} & [\tau^4\sin^4\theta+2\tau^2\cos^2\theta\,(1+\tau^2)]-\zeta\tau^2\cos^2\theta\,[\tau^4\sin^4\theta+6(1+\tau^2\cos^2\theta)] \\
& +\zeta^2\,.\,2\tau^2\cos^2\theta\,[3-\tau^2+4\tau^2\cos^2\theta]-\zeta^3\,.\,2\tau^2\cos^2\theta\,[1+\tau^2\cos^2\theta].
\end{aligned}$$

Table 1 introduces a number of new symbols which are functions of ζ, and serves both to define them and to explain their use. In the expressions for the extraordinary wave, the upper sign in terms such as $1 \mp \tau$ always refers to the condition $\tau < 1$, and the lower sign to $\tau > 1$.

The reflection point, where the group velocity is zero, is given by $\zeta = 1$ for the ordinary wave; and by $\zeta = 1 \mp \tau$ for the extraordinary wave; thus in both cases reflection occurs when $\delta = 0$. As $\delta \to 0$, Y, H and K remain finite, but X becomes proportional to δ. P and Q are defined to include the $\delta^{\frac{1}{2}}$ factor so as to make them finite at the limit when $\delta = 0$, and the integrands in A and P' have their infinities, for which $\delta = 0$, isolated in the factor $\delta^{\frac{1}{2}}$ in the denominator. The P and Q functions being finite over the whole range of ζ are very suitable for the further study of the integrals, and it is useful to know the end values, which are as follows:

Initially, when $\zeta = 0$, $P = 0$ and $Q = 1$ for both waves.

At the reflection point, $\delta = 0$. For the ordinary wave, $P = Q = \operatorname{cosec}\theta$.

For the extraordinary wave,

$$P = \frac{Q}{1 \mp \tau/2} = \frac{1}{(1 \mp \tau)}\left[\frac{8}{1+\cos^2\theta}\right]^{\frac{1}{2}}.$$

Table 1

<table>
<tr><th>Ordinary wave</th><th>Extraordinary wave</th></tr>
<tr><td colspan="2">$Y=(1-\tau^2)-\zeta(1-\tau^2\cos^2\theta)$,
$Z=\sqrt{(\frac{1}{4}\tau^4\sin^4\theta+\tau^2\cos^2\theta(1-\zeta)^2)}$,</td></tr>
<tr><td>$X=(1-\zeta)(1-\tau^2-\zeta)-\frac{1}{2}\zeta\tau^2\sin^2\theta+\zeta Z$,</td><td>$X=(1-\zeta)(1-\tau^2-\zeta)-\frac{1}{2}\zeta\tau^2\sin^2\theta-\zeta Z$,</td></tr>
<tr><td>$H=\zeta I_1-\frac{\zeta I_2}{2Z}$,</td><td>$H=\zeta I_1+\frac{\zeta I_2}{2Z}$,</td></tr>
<tr><td>$K=I_3-\frac{\zeta I_4}{2Z}$,</td><td>$K=I_3+\frac{\zeta I_4}{2Z}$,</td></tr>
<tr><td>$\delta=1-\zeta$,</td><td>$\delta=1-\frac{\zeta}{1\mp\tau}$,</td></tr>
<tr><td colspan="2">$P=\frac{\delta^{\frac{1}{2}}H}{2[XY^3]^{\frac{1}{2}}}$,
$Q=\frac{\delta^{\frac{1}{2}}K}{2[XY^3]^{\frac{1}{2}}}$.</td></tr>
<tr><td>For specific attenuation</td><td>$\mu_I=\frac{\alpha}{2}\frac{P}{\delta^{\frac{1}{2}}}$.</td></tr>
<tr><td>For group velocity</td><td>$\frac{U}{c}=\frac{\delta^{\frac{1}{2}}}{Q}$.</td></tr>
<tr><td>For overall attenuation</td><td>$A=\int\frac{\pi\alpha}{\lambda}\frac{P}{\delta^{\frac{1}{2}}}dz$.</td></tr>
<tr><td>For equivalent path</td><td>$P'=\int\frac{Q}{\delta^{\frac{1}{2}}}dz$.</td></tr>
</table>

As $\delta\to 0$, $P/Q\to 1$ for the ordinary wave, and $P/Q\to(1\pm\frac{1}{2}\tau)^{-1}$ for the extraordinary wave. Thus if the last part of the integrand near to the end value is predominant, measurements on the overall attenuation and group retardation will give a simple way of measuring α, and hence f_c the collisional frequency, in the region of maximum density.

In the computation of P and Q for the ordinary wave, a difficulty occurs at the value $\zeta_c=(1-\tau^2)/(1-\tau^2\cos^2\theta)$, where $Y=0$, since when $\tau<1$, this value occurs between $\zeta=0$ and 1, but it will be found that X, H, and K also are zero in such a way that the P and Q functions are continuous through the point. For the extraordinary wave $\zeta_c>1-\tau$ though it <1, and it therefore lies outside the range $\zeta=0$ to $1-\tau$; while when $\tau>\sec^2\theta$ and ζ_c is between $\sec^2\theta$ and $1+\tau$, i.e. within the range $\zeta=0$ to $1+\tau$, the P and Q functions are continuous through ζ_c for the extraordinary wave. By the usual methods the values of P and Q at ζ_c can be determined, but in practice it is only necessary to compute values a little way on either side of ζ_c, since we know that the functions are continuous through the point.

The integrands of our two integrals, though explicitly given in terms of ζ, are actually functions of z by virtue of the relation between ζ and z, and to consider the integrals further we must now investigate the nature of this relation.

3. THE CHOICE OF THE GRADIENT OF ELECTRONIC DENSITY

It would be possible to take any empirical relation which could be represented graphically, without assuming that it has any simple analytical form, and to plot our P and Q functions, which are expressed in terms of ζ, as functions of z by purely graphical means. This method of attack would, however, lead to a very unwieldy process for studying the effect of approaching near to the critical escape frequency for the layer assumed. Moreover, it would be almost impossible by such purely graphical means to obtain the accuracy required for deciding the point at issue.

It is therefore better to choose one or two typical kinds of layer which can be represented analytically as a function of ζ and z, and as P and Q are expressed explicitly in terms of ζ, it is more convenient to convert the integral so that the integration is performed with respect to ζ instead of z. This will also lead to simpler conditions for reflection and penetration, the wave being reflected or penetrating according as the maximum density in the layer is greater or less than that corresponding to $\zeta = 1$ or $1 \mp \tau$ for the ordinary and extraordinary waves respectively. Three types of layer will therefore be considered.

(*a*) A layer in which the initial density N is zero, the initial gradient dN/dz also is zero, and N increases indefinitely with z. Since for a given frequency ζ is proportional to N, a simple layer of this type is the square-law layer which can be represented by

$$\zeta = kz^2.$$

This gives

$$dz = \frac{d\zeta}{2k^{\frac{1}{2}}\zeta^{\frac{1}{2}}}.$$

For this type of layer the waves are always reflected, since we assume no upper limit to N.

(*b*) A layer in which the initial density is zero, but the initial gradient is finite and gradually decreases until a maximum density in the layer is obtained. A simple example is the parabolic layer for, which we may write

$$1 - \frac{\zeta}{\zeta_0} = \left(1 - \frac{z}{z_0}\right)^2,$$

where ζ_0 is the maximum value of ζ, i.e. of $(f_0)^2/f^2$, and occurs at a height z_0. z_0 is thus half the total thickness of the layer, which is symmetrical about the height $z = z_0$. This leads to

$$dz = \frac{z_0}{2\zeta_0^{\frac{1}{2}}} \frac{1}{(\zeta_0 - \zeta)^{\frac{1}{2}}} d\zeta.$$

For the ordinary wave there is reflection when $\zeta_0 > 1$, and the upper limit of the integrals is $\zeta = 1$. When $\zeta_0 < 1$ there is penetration, and the upper limit is $\zeta = \zeta_0$. For the extraordinary wave the condition is $\zeta >$ or $< 1 \mp \tau$.

(*c*) A layer similar to (*b*) in possessing a maximum density, but having also an initial zero gradient which increases, and then decreases again to zero at the point of maximum density. The simplest type is the sine-squared layer given by

$$\frac{\zeta}{\zeta_0} = \sin^2\left(\frac{\pi}{2}\frac{z}{z_0}\right).$$

Here ζ_0 and z_0 have meanings similar to those in (*b*), and the layer is again symmetrical about $z=z_0$. This leads to

$$dz=\frac{z_0}{\pi}\frac{1}{\zeta^{\frac{1}{2}}}\frac{1}{(\zeta_0-\zeta)^{\frac{1}{2}}}\,d\zeta,$$

and the conditions for reflection or penetration are the same as before.

We see that in case (*a*) the differential dz becomes infinite when $\zeta=0$, while in case (*b*) it does so when $\zeta=\zeta_0$. Case (*c*) combines both properties, dz being infinite when $\zeta=0$ and $\zeta=\zeta_0$. As we should expect, when $\zeta=0$, dz has the same form as for the square-law layer except for a constant, and when $\zeta=\zeta_0$, it has the same form as for the parabolic layer. When the layer is dense enough to reflect the waves, our integrands also become infinite at the upper limit, as we have seen, where $\delta=0$, but although the integrands can thus have three poles, the integrals themselves are finite, except when the two poles at $\zeta=\zeta_0$ and $\delta=0$ occur together, i.e. when the wave frequency is the critical escape frequency.

Thus considering, for instance, the ordinary wave, we have the scheme shown in table 2.

Table 2

$\zeta_0>1$	Reflection. Integral between the limits 0 and 1. $\zeta<\zeta_0$, $\delta=0$ when $\zeta=1$. Integral finite.
$\zeta_0<1$	Penetration. Integral between the limits 0 and ζ_0. At the upper limit $\zeta=\zeta_0$ but $\delta\neq 0$. Integral finite.
$\zeta_0=1$	Critical frequency. At the upper limit $\zeta=\zeta_0$ and $\delta=0$. Integral infinite.

As $\zeta\rightarrow\zeta_0$ when $\zeta_0=1$, the total attenuation and equivalent path both increase rapidly. The infinity in the integral should be rounded off, and its occurrence in the analysis is due to neglect of the higher powers of α, and to the fact that the conditions assumed in deriving the formula for the refractive index become invalid in this limiting case. But we can evaluate the integrals for values of ζ_0 closer and closer to the values 1 or $1\mp\tau$, and compare the calculated rapid increase in total attenuation and equivalent path with the results obtained experimentally in the region of the critical frequency.

In order to study this critical region more carefully, it is convenient to replace ζ_0 by $1+l$ and $(1\mp\tau)(1+l)$ for the ordinary and extraordinary waves respectively for the case of reflection, so that $l=0$ at the critical frequency, and l can have any positive value; and to replace ζ_0 by $1-l$ and $(1\mp\tau)(1-l)$ for penetration, where $l<1$. Thus l may be regarded as a parameter defining the nearness of approach to the critical condition.

We are now in a position to rewrite our integrals to include the effect of the type of layer chosen, by writing the relation between dz and $d\zeta$ as

$$dz=\phi(\zeta)\,d\zeta,$$

where the form of the function $\phi(\zeta)$ is determined by the choice of layer as above. In the case of reflection we will consider the total path to include the reflected wave, and similarly in the case of penetration we will include the path of the transmitted wave as it goes out through the upper half of the layer. By virtue of the symmetry in the layer about the height $z=z_0$—we need not consider further here the square-law layer of case (*a*)—this merely involves multiplying the integrals by 2, so that they become

$$2\int_0^{1 \text{ or } 1\mp\tau} \frac{\pi\alpha}{\lambda}\frac{P}{\delta^{\frac{1}{2}}}\phi(\zeta)\,d\zeta \quad \text{and} \quad 2\int_0^{1 \text{ or } 1\mp\tau} \frac{Q}{\delta^{\frac{1}{2}}}\phi(\zeta)\,d\zeta$$

for reflection, and

$$2\int_0^{(1-l) \text{ or } (1\mp\tau)(1-l)} \frac{\pi\alpha}{\lambda}\frac{P}{\delta^{\frac{1}{2}}}\phi(\zeta)\,d\zeta \quad \text{and} \quad 2\int_0^{(1-l) \text{ or } (1\mp\tau)(1-l)} \frac{Q}{\delta^{\frac{1}{2}}}\phi(\zeta)\,d\zeta$$

for penetration.

In dealing with the attenuation integrals, we must remember that the absorption coefficient α is really a function of the height z, since the collisional frequency f_c in which we are interested is known to be so, and if we know the law of its variation with height, we can embody this in the integral. But if we assume that the variation is small over the range of height with which we are concerned, we may take α outside the integral; in any case we may interpret the final value of α so obtained as an average value. To avoid further complications we will make this approximation here, pointing out that as in the sequel it will appear that most of the attenuation does take place in the region of maximum density, the assumed value of α is appropriate to that region.

§4. THE TRANSFORMATION OF THE INTEGRALS

In general, the integrals have to be solved by graphical means, although in some cases it may be found possible to represent the P and Q functions, to a fair degree of accuracy, by simple expressions that will lead to integrals which can be solved analytically. When we adopt the graphical method, however, we find that it is a difficult matter to estimate the areas under our curves because of the presence of the infinite values discussed above. As we shall need to measure the areas with the greatest accuracy in the cases in which the greater part of the area lies in the region of the pole at $\delta=0$, we must find some method of removing the poles from the integrands.

The necessary transformations involved are rather more difficult in the case of the sine-squared layer owing to the extra pole at $\zeta=0$, but actually in practice they can be quite quickly applied, and for the purpose of estimating the area under the curve, by counting squares or by using a planimeter, it is more satisfactory to work with a curve which is finite over the whole range. In giving these transformations we shall only state the initial integral, the substitutions used, and the resulting transformed integral. For purposes of comparison we shall give the results for both the parabolic layer and the sine-squared layer; in the latter case the process is a modification of the former case. The results are given for reflection and penetration, but we need to write out in detail only the cases of attenuation. We have therefore four cases to consider.

Case A: parabolic layer; reflection.

$$A = 2\frac{\pi\alpha}{\lambda}\int_0^{1 \text{ or } 1\mp\tau} \frac{P}{\delta^{\frac{1}{2}}}\frac{z_0}{2\zeta_0^{\frac{1}{2}}}\frac{1}{(\zeta_0-\zeta)^{\frac{1}{2}}}\,d\zeta.$$

Now put $\zeta = 1-\gamma^2 \quad \text{or} \quad (1\mp\tau)(1-\gamma^2),$

and then

$$\xi = \frac{\log_e[1+\gamma/\sqrt{l}]}{\log_e[1+1/\sqrt{l}]},$$

and we get

$$A = 2\frac{\pi\alpha}{\lambda}z_0\frac{\log_e[1+1/\sqrt{l}]}{\sqrt{(1+l)}}\int_0^1 P\frac{\sqrt{l}+\gamma}{\sqrt{(l+\gamma^2)}}\,d\xi.$$

Case B: parabolic layer; penetration.

$$A = 2\frac{\pi\alpha}{\lambda}\int_0^{(1-l) \text{ or } (1\mp\tau)(1-l)} \frac{P}{\delta^{\frac{1}{2}}}\frac{z_0}{2\zeta_0^{\frac{1}{2}}}\frac{1}{(\zeta_0-\zeta)^{\frac{1}{2}}}\,d\zeta.$$

Now put $\zeta = (1-l)(1-\gamma^2) \quad \text{or} \quad (1\mp\tau)(1-l)(1-\gamma^2),$

and then

$$\xi = \frac{\log_e[1+\gamma\sqrt{\{(1-l)/l\}}]}{\log_e[1+\sqrt{\{(1-l)/l\}}]},$$

and we get

$$A = 2\frac{\pi\alpha}{\lambda}z_0\frac{\log_e[1+\sqrt{\{(1-l)/l\}}]}{\sqrt{(1-l)}}\int_0^1 P\frac{\sqrt{l}+\gamma\sqrt{(1-l)}}{\sqrt{\{l+(1-l)\gamma^2\}}}\,d\xi.$$

Case C: sine-squared layer; reflection.

$$A = 2\frac{\pi\alpha}{\lambda}\int_0^{1 \text{ or } 1\mp\tau} \frac{P}{\delta^{\frac{1}{2}}}\frac{z_0}{\pi}\frac{1}{\zeta^{\frac{1}{2}}}\frac{1}{(\zeta_0-\zeta)^{\frac{1}{2}}}\,d\zeta.$$

Now put $\zeta = 1-\gamma^2 \quad \text{or} \quad (1\mp\tau)(1-\gamma^2),$

then $\gamma = 1-\chi^2$

and $\chi = 1-\phi,$

and lastly

$$\xi = \frac{\log_e[1+\phi/\sqrt{l}]}{\log_e[1+1/\sqrt{l}]},$$

and we get

$$A = 2\frac{\pi\alpha}{\lambda}\cdot\frac{4z_0}{\pi}\log_e\left[1+\frac{1}{\sqrt{l}}\right]\int_0^1\frac{P}{\sqrt{(2-\chi^2)}}\frac{\sqrt{l}+\phi}{\sqrt{(l+\gamma^2)}}\,d\xi.$$

Case D: sine-squared layer; penetration.

$$A = 2\frac{\pi\alpha}{\lambda}\int_0^{(1-l) \text{ or } (1\mp\tau)(1-l)} \frac{P}{\delta^{\frac{1}{2}}}\frac{z_0}{\pi}\frac{1}{\zeta^{\frac{1}{2}}}\frac{1}{(\zeta_0-\zeta)^{\frac{1}{2}}}\,d\zeta.$$

Now put
$$\zeta=(1-l)(1-\gamma^2) \quad \text{or} \quad (1\mp\tau)(1-l)(1-\gamma^2),$$
then
$$\gamma=1-\chi^2$$
and
$$\chi=1-\phi,$$
and lastly
$$\xi=\frac{\log_e[1+\phi\sqrt{\{(1-l)/l\}}]}{\log_e[1+\sqrt{\{(1-l)/l\}}]},$$
and we get
$$A=2\frac{\pi\alpha}{\lambda}\cdot\frac{4z_0}{\pi}\frac{\log_e[1+\sqrt{\{(1-l)/l\}}]}{\sqrt{(1-l)}}\int_0^1\frac{P}{\sqrt{(2-\chi^2)}}\frac{\sqrt{l}+\phi\sqrt{(1-l)}}{\sqrt{\{l+(1-l)\gamma^2\}}}d\xi.$$

To get the corresponding values for the equivalent path P', we have only to omit the factor $\pi\alpha/\lambda$ and to replace P by Q.

In every case the transformed integral is between the limits 0 and 1, and it can be shown that the integrand is finite over the whole range, even when $l=0$. The pole in the critical case in which $l=0$ has been shifted outside the integral in the logarithmic term. For the cases of reflection, the term $\log_e[1+1/\sqrt{l}]$ approaches zero as l becomes large, and the substitutions reduce to $\xi=\gamma$ and $\xi=\phi$ respectively. The values of the integrals approach zero, in correspondence with the fact that with a very dense layer the wave is reflected with very little penetration into the layer. For the cases of penetration, the term $\log_e[1+\sqrt{\{(1-l)/l\}}]/\sqrt{(1-l)}$ approaches 1 as l approaches 1, i.e. for an infinitely sparse layer. The substitutions again reduce to $\xi=\gamma$ and $\xi=\phi$ respectively, and the total attenuation becomes zero, since the P function becomes zero over the whole range from $\xi=0$ to 1, while if ζ is equated to 0 in the value of Q the equivalent path reduces to $2z_0$ (going right through the layer without retardation).

Of course, well away from the critical frequency the substitutions in terms of ξ are hardly necessary in practice, and in the case of penetration as $l\to 0$ the substitutions for ξ reduce to those used in the case of reflection, but it seems better to express them formally as above, and then to use any convenient approximations in practice.

The general procedure for the case of the parabolic layer is to evaluate P or Q as a function of ζ and hence of γ. A set of values of ξ is then chosen, say 0, 0·1, 0·2 up to 1·0, and for each given value of l the corresponding values of γ are worked out. For these values of γ, the values of the functions of the type $P(\sqrt{l}+\gamma)/\sqrt{(l+\gamma^2)}$ are tabulated, so that they can be plotted as ordinates with ξ as abscissae over the range 0 to 1. The area under the curve can then be measured with a planimeter.

For the sine-squared layer the process is slightly longer but equally straightforward. The values 0, 0·1 etc. of ξ having been chosen as before, ϕ is now the same as the corresponding γ in the parabolic case. We have then to tabulate χ and γ, and to work out the values of
$$\frac{P}{\sqrt{(2-\chi^2)}}\frac{\sqrt{l}+\phi}{\sqrt{(l+\gamma^2)}}$$
etc. from which to plot the final curves for the estimation of the areas as before. The detailed significance of these transformations, as regards the relation of the final variable ξ to the original variable z, will be considered when we discuss the practical

example which is to follow. We can however see from the form of our integrals the general conditions which must hold, if the assumption made by Eckersley in deriving the value for the collisional frequency is to be justified.

§ 5. DISCUSSION OF THE INTEGRALS

We have seen that for the extraordinary wave the end value of the Q function in the equivalent path integral is $(1 \mp \tau/2)$ times the end value of the P function in the attenuation integral. It is found convenient, therefore, in this case, in considering the integrals with respect to ξ, to include a factor $(1 \mp \tau/2)$ under the integral sign for the attenuation integral, so that we can more conveniently compare the areas when determining the values of the integrals graphically. We then call the areas under the curves in the two cases R and S respectively, for example in case A of a parabolic layer and reflection we write

$$\int_0^1 \left(1 \mp \frac{\tau}{2}\right) P \frac{\sqrt{l+\gamma}}{\sqrt{(l+\gamma^2)}}\, d\xi = R$$

and

$$\int_0^1 Q \frac{\sqrt{l+\gamma}}{\sqrt{(l+\gamma^2)}}\, d\xi = S.$$

Then as $l \rightarrow 0$, the two areas R and S, which remain finite, should approach one another in value. In the particular case we have chosen we now have

$$A = 2\frac{\pi\alpha}{\lambda} z_0 \frac{\log_e [1 + 1/\sqrt{l}]}{\sqrt{(1+l)}} \frac{R}{(1 \mp \tau/2)}$$

and

$$P' = 2z_0 \frac{\log_e [1 + 1/\sqrt{l}]}{\sqrt{(1+l)}} S.$$

We must now relate A and P' to the experimentally observed change in the strength of the echo, due to the attenuation, and the equivalent height h' respectively. If the strength of the echo is represented in decibels by D with respect to zero attenuation as datum, we have from the expression of the overall attenuation as $\exp(-A)$ that

$$D = 20 \log_{10} [\exp(-A)] = -20 [\log_{10} e] A.$$

Thus

$$D = -20 (\log_{10} e) \frac{2\pi\alpha}{\lambda} z_0 \frac{\log_e [1 + 1/\sqrt{l}]}{\sqrt{(1+l)}} \frac{R}{(1 \mp \tau/2)}.$$

The equivalent height h' is simply $P'/2$, so that

$$h' = z_0 \frac{\log_e [1 + 1/\sqrt{l}]}{\sqrt{(1+l)}} S.$$

Suppose now that we write

$$\frac{D}{20 (\log_{10} e)\, 2\pi\alpha z_0/\lambda} = y$$

and

$$\frac{h'}{z_0} = x,$$

so that

$$y = -\frac{\log_e [1 + 1/\sqrt{l}]}{\sqrt{(1+l)}} \frac{R}{(1 \mp \tau/2)}$$

and

$$x = \frac{\log_e [1 + 1/\sqrt{l}]}{\sqrt{(1+l)}} S.$$

As $l \to 0$ and R and S get very nearly equal,

$$\frac{y}{x} \to -\frac{1}{1 \mp \tau/2},$$

so that

$$\frac{D}{h'}\frac{\lambda}{40\,(\log_{10} e)\,\pi\alpha} \to -\frac{1}{1 \mp \tau/2}.$$

If we put

$$\lambda = \frac{c}{f} \quad \text{and} \quad \alpha = \frac{f_c}{\beta\pi f},$$

this gives

$$f_c = -\frac{D}{h'}\frac{\beta c\,(1 \mp \tau/2)}{40 \log_{10} e}.$$

This is the relation which Eckersley used, where D/h' is simply the slope of the $\{D, h'\}$ curve, which he found experimentally to be a straight line. It is obvious that the same relation follows if we take any of the other cases A to D of § 4, except, of course, that for the ordinary wave the factor $(1 \mp \tau/2)$ is replaced by 1.

The validity of the method therefore depends upon the assumption that the $\{y, x\}$ curve is a straight line whose slope is $-1/(1 \mp \tau/2)$. Now we can show that the $\{y, x\}$ curve does eventually become asymptotic to a line whose slope is $-1/(1 \mp \tau/2)$. In the example given above, the relation between y and x can be put in the form

$$y = -\frac{x}{1 \mp \tau/2} + C,$$

in which

$$C = \frac{\log_e [1 + 1/\sqrt{l}]}{(1 \mp \tau/2)\sqrt{(1+l)}}[S - R],$$

and from case A in § 4, it will be found that R and S can be expressed in terms of integrals with respect to γ, giving

$$\log_e\left[1 + \frac{1}{\sqrt{l}}\right][S - R] = \int_0^1 \frac{Q - (1 \mp \tau/2)\,P}{\sqrt{(l+\gamma^2)}}\,d\gamma.$$

Now if we assume that $Q - (1 \mp \tau/2)\,P$ can be represented as a polynomial of the form $a_1\gamma + a_2\gamma^2 + a_3\gamma^3 + \ldots$ (since it is zero when $\gamma = 0$), the integral becomes tractable by the substitution $\gamma = \sqrt{l}\tan\theta$. It is then found that as $l \to 0$

$$C \to \frac{\Sigma\,(a_n/n)}{1 \mp \tau/2},$$

which is independent of l.

For the sine-squared layer the corresponding integral is

$$\int_0^1 \frac{Q - (1 \mp \tau/2)\,P}{\sqrt{(1-\gamma^2)}\sqrt{(l+\gamma^2)}}\,d\gamma,$$

and this with the substitution

$$\gamma^2 = \frac{1-l}{2} + \left(\frac{1+l}{2}\right)\sin\theta$$

gives

$$\underset{l \to 0}{C} = \frac{1}{(1 \mp \tau/2)}\left[a_1 + \frac{2}{\pi}a_2 + \tfrac{1}{2}a_3 + \ldots\right],$$

which also is independent of l.

The validity of the analysis will be borne out by the practical example in § 6, the point of which is to show that actually the $\{y, x\}$ curve does approach closely to the asymptote, well within the range of values which we can observe experimentally. The asymptote itself does not go through the origin, for it is found that the intercept C is quite appreciable on the scale on which the $\{y, x\}$ curves are drawn, but this will not affect results that are based on measurements of points which are effectively on the straight line. We proceed therefore to a typical practical example to illustrate the use of the analysis, and to justify the general conclusions we have drawn from it.

§ 6. A PRACTICAL EXAMPLE

The evaluation of the P and Q functions depends upon the computation, in any particular case, of the polynomials in ζ which we have called I_1 to I_4, and as some of the terms in these expressions are positive and others are negative, the values of I_1 to I_4 can in special cases be much less than any of the individual terms. In these cases this implies that we must determine the coefficients in I_1 to I_4 to a considerable degree of accuracy. It therefore helps to choose values of τ and θ which will make this a relatively simple task, and as those coefficients involve τ and θ as functions of τ^2, $\cos^2\theta$ and $\sin^2\theta$, we will choose $\tau^2 = 0{\cdot}1$ and $\tan\theta = \frac{1}{3}$. This value of θ corresponds to an angle of dip of 71° 34′, which is of the order of the value of the dip at London. The value $\tau = 0{\cdot}3162$ corresponds, for the value of the earth's magnetic field at London, to a wave-length of 70 m., which is in the region in which experimental observations have been made. With these values of τ and θ we have the following end values at the reflection point:

For the ordinary wave $\zeta = 1$, $P = Q = 3{\cdot}162$.
For the extraordinary wave $\zeta = 0{\cdot}684$, $P = 1{\cdot}500$, $Q = 1{\cdot}263$.

P and Q are plotted as functions of ζ for the ordinary and extraordinary waves in figure 1. It will be seen that the functions for the ordinary wave are more difficult to handle than those for the extraordinary wave, owing to the rapid rise of the P and Q curves near to the reflection point. The significance of this rise will be considered in the general discussion in the next section, and here we will content ourselves with the detailed working out of the case of the extraordinary wave; this was the case cited by Eckersley. We need only to consider the case of reflection.

In cases A and C in § 4, the first substitution is $\zeta = (1-\tau)(1-\gamma^2)$, so we take a set of values of γ, namely 0, 0·1, up to 1, and work out the corresponding values of ζ. We can then read off values from the curves in figure 1, and draw out new curves of P and Q plotted against γ. These are given in figure 2. Now taking case A for the parabolic layer first, we choose a series of values of l, say 0·1, 0·01, 0·001, and taking each in turn, we work out, for a series of values 0, 0·1 up to 1 of ξ, the corresponding values of γ. For these values of γ we compute $(\sqrt{l}+\gamma)/\sqrt{(l+\gamma^2)}$, and multiply each value by the corresponding values of P and Q read off figure 2, and finally we get a series of graphs of $(1-\tau/2)\, P\, (\sqrt{l}+\gamma)/\sqrt{(l+\gamma^2)}$ and $Q\, (\sqrt{l}+\gamma)/\sqrt{(l+\gamma^2)}$ against ξ for each value of l. A set of such curves is shown in figure 3, and the areas under these curves are measured with a planimeter, and give the values of R and S.

For the sine-squared layer the calculations are similar, but slightly more involved owing to the extra χ and ϕ substitutions. In this case it is useful to draw graphs of $P/\sqrt{(2-\chi^2)}$ and $Q/\sqrt{(2-\chi^2)}$ as functions of ϕ, and these are given in figure 4. The set of curves for $\left(1-\frac{\tau}{2}\right)\frac{P}{\sqrt{(2-\chi^2)}}\frac{\sqrt{l+\phi}}{\sqrt{(l+\gamma^2)}}$ and $\frac{Q}{\sqrt{(2-\chi^2)}}\frac{\sqrt{l+\phi}}{\sqrt{(l+\gamma^2)}}$ for the determination of R and S is given in figure 5.

We can see from figures 3 and 5 that as l gets smaller, the area R approaches the value of S, although even for the smallest values shown, the difference in the areas is quite a large percentage of either area alone. But when we plot y against x, as in figures 6 and 7, we see that the points lie on a straight line to a close approximation, even the point for $l=0{\cdot}1$ being only a small distance away from the line. Since, even at the smallest values of l, R is markedly different from S, the straight line does not go through the origin, but shows an appreciable value of the intercept C.

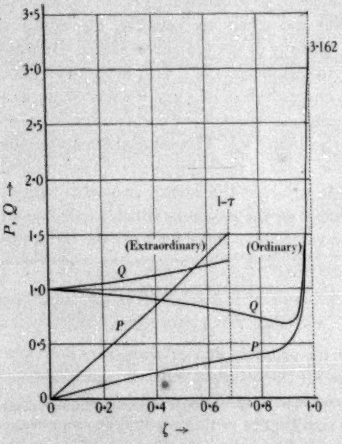

Figure 1. P and Q as functions of ζ for ordinary and extraordinary waves. $\tau=0{\cdot}3162$, $\tan\theta=\frac{1}{3}$.

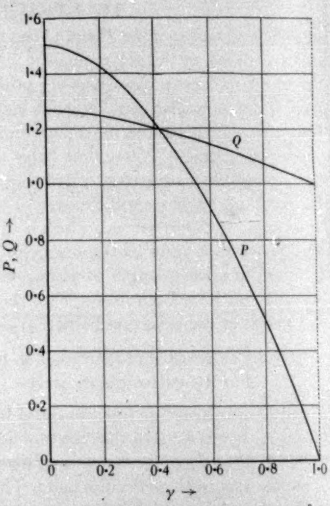

Figure 2. P and Q as functions of γ for extraordinary wave. $\tau=0{\cdot}3162$, $\tan\theta=\frac{1}{3}$.

It is found from figure 2 that in our case P and Q can be represented closely by parabolic curves, so that $Q-(1-\tau/2)\,P$ can be expressed as $a_1\gamma+a_2\gamma^2$. By determining from the curves the values of a_1 and a_2, we can estimate the value of C by the analysis given in § 5, i.e.

$$C=\frac{a_1+a_2/2}{1-\tau/2} \quad \text{and} \quad \frac{a_1+(2/\pi)\,a_2}{1-\tau/2}$$

respectively, and actually the straight lines drawn in figures 6 and 7 are lines of slope

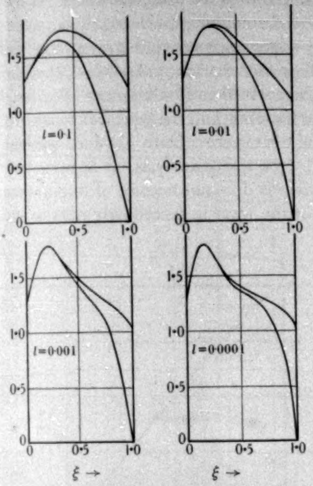

Figure 3. Curves for estimating R and S for parabolic layer for various values of l. Upper curves, $Q\,(\sqrt{l}+\gamma)/\sqrt{(l+\gamma^2)}$; lower curves, $(1-\tau/2)\,P\,(\sqrt{l}+\gamma)/\sqrt{(l+\gamma^2)}$.

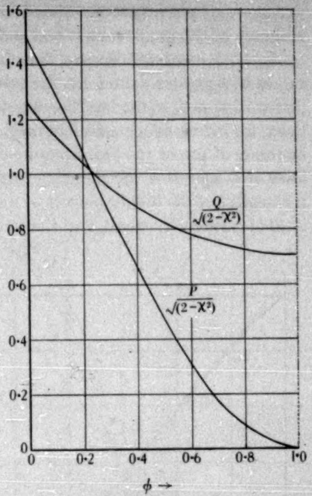

Figure 4. $P/\sqrt{(2-\chi^2)}$ and $Q/\sqrt{(2-\chi^2)}$ as functions of ϕ for extraordinary wave. $\tau=0{\cdot}3162$, $\tan\theta=\frac{1}{3}$.

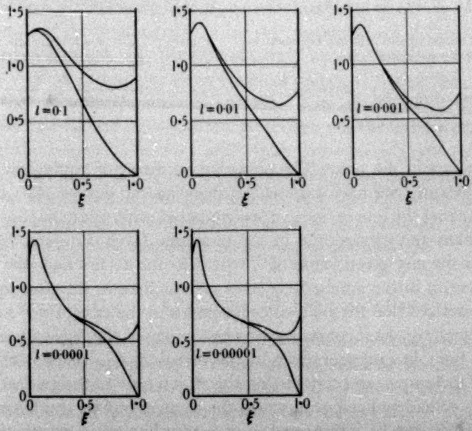

Figure 5. Curves for estimating R and S for sine-squared layer for various values of l.

$$\text{Upper curves, } \frac{Q}{\sqrt{(2-\chi^2)}}\,\frac{\sqrt{l}+\phi}{\sqrt{(l+\gamma^2)}}; \qquad \text{Lower curves, } \frac{(1-\tau/2)\,P}{\sqrt{(2-\chi^2)}}\,\frac{\sqrt{l}+\phi}{\sqrt{(l+\gamma^2)}}.$$

$-1/(1-\tau/2)$ with these computed intercepts. We thus have a good check on the accuracy of the graphical method and the general soundness of the analysis.

In both cases we can say that the $\{y, x\}$ curve approaches the asymptote for values of x greater than 2, i.e. for values of h' greater than $2z_0$. Assuming that the half-thickness z_0 of the layer is, say, 50 km., the curve therefore becomes effectively linear for increases of equivalent height greater than 100 km. In typical experiments increases of 400 or 500 km. are quite usual, and the experimentally obtained straight lines of D against h' are therefore explicable by the above analysis. It appears that the neglect of the higher powers of α in the analysis does not become of importance until l is made very small, and the frequency of the wave is exceedingly near to the critical frequency in the layer. The observed increases of equivalent height imply the small values of l we have assumed in deriving the curves. The closer spacing of the points along the line in figure 7, as compared with figure 6, shows the greater total attenuation and group time in the parabolic layer compared with the sine-squared layer for any given value of l, which is due to the fact that at any given height the density in the parabolic layer is greater than in the sine-squared layer.

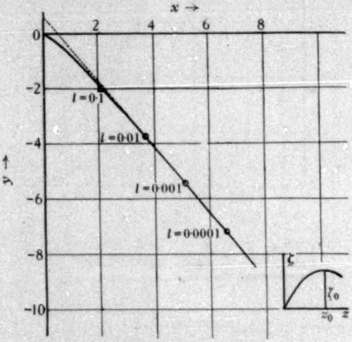

Figure 6. Curve showing the relation between y and x for parabolic layer.

$$y=\frac{D}{20\,(\log_{10}e)\,2\pi\alpha z_0/\lambda},\qquad x=h/z_0,$$

$$(1-\zeta/\zeta_0)=(1-z/z_0)^2.$$

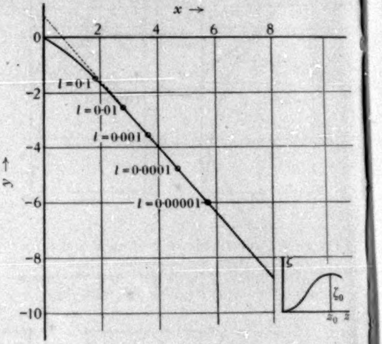

Figure 7. Curve showing the relation between y and z for sine-squared layer.

$$y=\frac{D}{20\,(\log_{10}e)\,2\pi\alpha z_0/\lambda},\qquad x=h/z_0,$$

$$\zeta/\zeta_0=\sin^2(\tfrac{1}{2}\pi z/z_0).$$

It will be noticed that the analysis corresponds to the case of a $P't$ run, in which the wave-frequency is kept constant, and the density of the layer alters gradually in the course of time, in a manner given by the variation of l. But it is obvious that by using the $P'f$ technique, and considering the region near to the critical frequency of the layer, now considered constant, where the changes of f are small compared with f itself, the analysis can be interpreted to give the changes in attenuation and equivalent height near to the critical frequency in a $P'f$ run.

The fact that most of the attenuation and retardation near to the critical frequency takes place in the region of the maximum density, can be seen from figures 6 and 7 by considering, say, the points for $l=0{\cdot}01$ and $l=0{\cdot}001$. The extra attenuation in the case of $l=0{\cdot}001$ must occur mainly in the small extra distance travelled in the layer very near to the level of the maximum density. Thus the straight line can be interpreted as giving a value of the collisional frequency in the region of the maximum density.

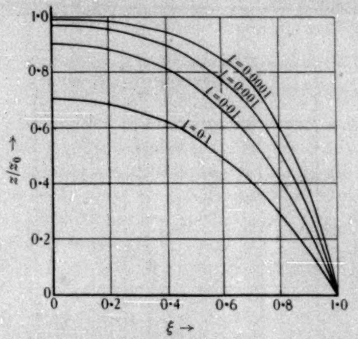

Figure 8. Curve showing the relation between ξ and z/z_0 for parabolic layer.

This point can be further seen by considering the significance of the transformations used in § 4. By taking case *A*, we can draw a set of curves of the original variable z in terms of the final variable ξ, for the various values of l we have chosen, and this is given in figure 8. By using these curves we can then see what part of the areas *R* and *S* originate from any given range of values of z, and it is obvious that most of the range of ξ corresponds to values of z in the region of the maximum density. In the case of the sine-squared layer this will be even more so, as the $\{z, \xi\}$ curve in the region $z=0$, $\xi=1$ will climb more steeply, on account of the initial zero gradient in the layer, involving the extra χ and ϕ substitutions in the transformations. We thus conclude from the analysis that the method suggested by Eckersley for determining the collisional frequency f_c is justified, and it remains only to consider some of the more general aspects of the analysis.

§ 7. GENERAL RESULTS OF THE ANALYSIS

The analysis gives explicit forms both for the specific attenuation and the group velocity at any height z, corresponding to any given ζ value in the layer. It is useful therefore to draw graphs of these, as functions of ζ, for the particular example we have considered above. For the specific attenuation we can take $P/\delta^{\frac{1}{2}}$, for the comparison of the ordinary and extraordinary waves, and for the group velocity we can take $\delta^{\frac{1}{2}}/Q$, which is equal to U/c.

From the curves for P and Q in figure 1 we therefore derive the curves given in figure 9. These curves show that up to any given height the ordinary wave travels faster than the extraordinary wave, the fact that the ordinary echo normally appears beyond the extraordinary echo in $P'f$ and $P't$ observations arising from the greater height to which the ordinary wave must go to be reflected. This also explains why in the presence of an intermediate layer not dense enough to reflect either wave, the order of the echoes reflected from an upper layer may be reversed, as a result of the greater delay suffered by the extraordinary wave in traversing the intermediate layer.

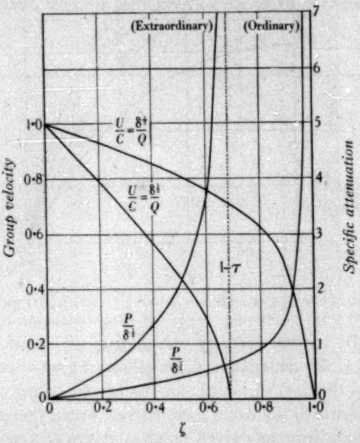

Figure 9. Group velocity and specific attenuation as functions of ζ. $\tau=0{\cdot}3162$, $\tan\theta=\frac{1}{3}$.

The specific attenuation at a given height is considerably greater for the extraordinary wave than for the ordinary wave, so that in general on such wave-lengths the ordinary echo is the stronger of the two. It is difficult however to determine the relation of the overall attenuation and group retardation for the two waves in any given case, without a closer examination of the kind given in the practical example above. The shapes of the P and Q curves vary considerably for different values of τ and θ, and in particular for small values of θ, for the ordinary wave, they show the rapid rise to a large end value as seen in figure 1. This end value is cosec θ, and tends to ∞ as θ tends to zero and the field approaches the vertical, and the computation of the curve in this region needs special care. This rapid rise is associated with the value of ζ_c when $\gamma=0$.

In our practical example $\zeta_c=0{\cdot}989$, and is very close to $\zeta=1$. The curve in the region of $\zeta=1$ is best computed by converting the polynomials I_1 to I_4 into functions of δ, equal to $(1-\zeta)$, and as it may be of considerable interest to compute curves for other values of τ and θ, these expansions are given here. Thus for the ordinary wave for which $\delta = 1 - \zeta$,

$$I_1 = [\tau^2 \sin^2\theta\,(1+\tau^2)] - \delta\,[2\tau^2 \sin^2\theta] + \delta^2\,[2\,(1+\tau^2\cos^2\theta)],$$

$$\begin{aligned} I_2 = {} & [\tau^4 \sin^4\theta\,(1-\tau^2)] + \delta\,[2\tau^4 \sin^2\theta\,(1+\cos^2\theta)] \\ & - \delta^2\,[4\tau^4 \cos^2\theta \sin^2\theta] + \delta^3\,[8\tau^2\cos^2\theta], \end{aligned}$$

$$\begin{aligned} I_3 = {} & [\tau^2 \sin^2\theta\,(1+\tau^2+\tau^2\sin^2\theta)] - \delta\,[\tau^2 \sin^2\theta\,(5-2\tau^2\cos^2\theta)] \\ & + \delta^2\,[2\,(1-\tau^2\cos^2\theta) + \tau^4\cos^2\theta\,(1+\cos^2\theta)] - \delta^3\,[2\tau^2\cos^2\theta], \end{aligned}$$

$$\begin{aligned} I_4 = {} & [\tau^4 \sin^4\theta\,(1-\tau^2\cos^2\theta)] + \delta\,[\tau^4 \cos^2\theta \sin^2\theta\,(4+\tau^2\sin^2\theta)] \\ & - \delta^2\,[2\tau^4\cos^2\theta \sin^2\theta] + \delta^3\,[2\tau^2\cos^2\theta\,(1+\tau^2\cos^2\theta)]. \end{aligned}$$

By means of these relations it was found possible to compute P and Q to an accuracy of 1 in 1000 for a value 0·990 of ζ, i.e. within 0·001 of ζ_c.

If τ is made smaller, so that it approaches zero, the end value of P and Q remains at cosec θ, but in the limit the curve for Q approaches the horizontal line $Q = 1$, and the final rise is delayed until it becomes the line $\zeta = 1$. Our equations then reduce to the simple case of zero magnetic field;

$$\frac{U}{c} = \frac{\delta^{\frac{1}{2}}}{Q}$$

becomes

$$\frac{U}{c} = \delta^{\frac{1}{2}},$$

and since we then have

$$\mu_R{}^2 = 1 - \zeta = \delta,$$

$$U = c\mu_R$$

as it should.

If θ is made to approach zero while τ remains constant, the end value of P and Q for the ordinary wave approaches infinity, and it appears that in this case also the rise is delayed towards $\zeta = 1$; but in this case we approach the discontinuity at $\theta = 0$, i.e. vertical field, when the reflection at $\zeta = 1$ no longer occurs, and we go over to the longitudinal case with reflections at $\zeta = 1 - \tau$ and $1 + \tau$.

In a similar way we can check up for other special values of τ and θ. The general expressions we have developed also embrace values of ζ beyond the reflection point, and hold for the isolated real branches of the wave function which are known to occur. Thus the group-velocity analysis is strictly equivalent to that given by Goubau(5) and by Rai(6), and curves of the type given by Bajpai and Mathur(7) can be derived from it.*

The method we have adopted of obtaining the fundamental ζ polynomials whose coefficients are functions only of τ and θ, and of defining the P and Q functions in terms of them, should be found helpful and instructive in following out the changes which occur as τ and θ are altered. Although this aspect of the problem has not yet been attacked in detail, it is obvious that such a set of curves would be very useful for studying generally the nature of propagation in the presence of a magnetic field.

---

[*] Actually Goubau, by using approximations, includes the Lorentz term in his analysis.

§ 8. ACKNOWLEDGEMENTS

I am indebted to Mr T. L. Eckersley for suggesting the specific problem which entailed the general analysis presented here, and for the helpful advice he has given during the course of the work. I also wish to thank Dr F. T. Farmer for much stimulating criticism and advice on the method of presentation.

REFERENCES

(1) Eckersley, T. L. *Nature, Lond.*, **135**, 435 (1935); **136**, 953 (1935).
(2) Ratcliffe, J. A. *Wireless Engr*, **10**, 354 (1933).
(3) Taylor, Mary. *Proc. Phys. Soc.* **45**, 245–65 (1933); **46**, 408–18 (1934).
(4) Burnett, D. *Proc. Camb. Phil. Soc.* **27**, 578 (1931).
(5) Goubau, G. *Hochfrequenztech. u. Elektroakust.* **44**, 17 (1934).
(6) Rai, R. N. *Proc. Nat. Inst. Sci.* (*India*), **3**, 307–17 (1937).
(7) Bajpai, R. R. and Mathur, K. B. *Indian J. Phys.* **11**, 165 (1937).

EMISSION BANDS OF $SiCl_2$ AND $SnCl_2$

By R. K. ASUNDI, M. KARIM and R. SAMUEL
The Muslim University, Aligarh (India) and The Hebrew
Technical Institute, Haifa (Palestine)

Received 12 *November* 1937. *Read in title* 25 *February* 1938

ABSTRACT. The discharge through flowing vapour of $SiCl_4$, $SnCl_4$, and $SnCl_2$ shows a number of regions of selective continuous emission, and, intimately connected with them, several sets of new bands. These appear under conditions unfavourable for the production of the known bands of SiCl and SnCl respectively. They are broad and diffuse, and have not the appearance of bands due to a diatomic emitter of low molecular weight. They are quite different from the known SiCl and SnCl bands as far as the anharmonic factor of the ground level of the molecule is concerned. They are therefore attributed to the triatomic molecules $SiCl_2$ and $SnCl_2$ respectively.

An analysis carried out on this assumption reveals two excited electronic levels of $SiCl_2$ ($\nu\nu = 28295$ and 29952), and one of $SnCl_2$ ($\nu = 22237$). The presence of the deforming (breathing) vibration ω_1, and of the symmetrical valence vibration ω_2 are indicated both in the ground state and in the various excited states. The antisymmetric valence vibration is absent, in agreement with Herzberg-Teller's selection rules. For certain reasons ω_2' is smaller than ω_2'', despite ω' being larger than ω'' in the corresponding excited terms of SiCl and SnCl. The energies of excitation and the values of ω_2'' of $SiCl_2$ and $SnCl_2$ show a close similarity to the corresponding constants of SiCl and SnCl respectively, and also the bond energies appear to be rather unaffected by the transition from the diatomic to the triatomic molecule. The later ones appear to be triangular.

§ 1. INTRODUCTION

In this paper are described the spectra of the flowing vapours of $SiCl_4$, $SnCl_4$, and $SnCl_2$. The spectra of $SnCl_4$ and $SnCl_2$ have been studied only with uncondensed discharge and with a constant pressure of the flowing vapour, while the spectrum of $SiCl_4$ has been taken under varying conditions of pressure and with condensed and uncondensed discharge. Previous work of this nature has been done by Jevons(1) in the case of CCl_4, $SiCl_4$, $TiCl_4$, and BCl_3 and more recently for $SiBr_4$(2). This work, however, does not deal with variations in spectra brought about by different conditions of excitation and pressure. It is shown in the experiments described below that the nature of the spectra, in most of these substances, undergoes certain radical changes under varying conditions of the pressure of the flowing vapour.

§ 2. EXPERIMENTAL

For each substance a separate discharge tube of the H pattern fitted with a quartz window has been used. These had the usual side bulbs containing phosphorus pentoxide and crushed sodium hydroxide. The substance was contained in another side bulb with a stop cock for the regulation of the flow of the vapour. All substances investigated, except $SnCl_2$, are liquids at ordinary temperatures. We have used $SnCl_2 . 2H_2O$ which melts at about 38° C. It was found that in vacuum the solid itself gave sufficient vapour pressure and it was not found necessary to heat it. Only in the case of $SiCl_4$, since the use of aluminium electrodes gave rise to the well known AlCl bands(3), nickel electrodes have been used. The discharge tube was connected to the high-vacuum apparatus, operated by a mercury diffusion pump which was backed by a rotary oil pump. The flow of the vapour was adjusted to give the desired pressure by having two stop-cocks on either side of the discharge tube. Pressures were measured on a MacLeod gauge. The tubes were run on a 0·25-kw. transformer delivering 15,000 v. For the condensed discharge a set of three ordinary Leyden jars arranged in parallel were used with a spark gap of about 2 mm. in series with the tube. The spectrum of $SnCl_2$ has been studied only in the uncondensed discharge. In all the cases the medium Hilger quartz spectrograph has been used to investigate the ultra-violet region of the spectrum, while for the visible region the Hilger constant deviation glass spectrograph has been employed. In the case of $SiCl_4$ attempts were made to photograph the spectrum on a three-prism quartz spectrograph with a Littrow mounting. This necessitated long exposures, during which it was found difficult to maintain the constancy of pressure. The plates have been measured on an Abbé comparator, using copper arc lines as standards. The wave-lengths of the beginning, maximum, and end of continuous emission bands have been determined from microphotometer records, which were obtained on a Zeiss recording microphotometer.

§ 3. THE EMISSION SPECTRUM OF $SiCl_4$

The spectrum of the discharge through flowing $SiCl_4$ vapour has been studied under different conditions of pressure and in each case with condensed and uncondensed discharge. With a pressure of about 0·5 mm. of mercury, the uncondensed discharge shows four maxima of continuous emission at $\lambda\lambda$4022, 3250, 2560, and 2450, and the set of bands of SiCl due to the transition B → X(4). Jevons(1) records two regions of continuous emission between $\lambda\lambda$6300 to 5300 and 4850 to 3100. The first region of continuous emission starts at about λ5200. We have, however, regarded this as a continuation towards longer waves of the maximum at λ4022, on the basis that the region in which the gap appears is such that here the plates that we have used are not sensitive and most of the molecules studied exhibit the same gap. The second region of the continuum between $\lambda\lambda$4850 and 3100 recorded by Jevons, really consists of two continuous regions with a maximum at λ4022, to which Jevons's first region of continuous emission belongs, and λ3250, which, however, merge into one continuous whole at pressures higher than about 0·5 mm. of mercury. With pressures of 0·2, 0·1, and 0·05 mm. of mercury and with condensed and uncondensed discharge the continuous maxima at $\lambda\lambda$2560 and 2450 disappeared and the SiCl bands(4) due to the transitions C → X and D → X were observed. The two maxima on the longer wave-length side, i.e. $\lambda\lambda$4022 and 3250, became weaker in intensity as the pressure was reduced and were accompanied each by a set of narrow bands. Figure 1 is a reproduction of the plate showing these bands. In the condensed discharge they were further enhanced in intensity at the expense of the continua. A pressure of 0·05 mm. of mercury was found to be the most favourable for the production of these bands. The bands in the body of the maximum at λ4022 are broad and diffuse, which fact makes it difficult to locate the heads. The bands in the maximum at λ3025, on the other hand, are narrow and they also do not show any structure, but their heads in most cases could be more accurately located. In any case, on account of the low dispersion used, the possibility of the overlap of the heads due to different transitions is great. In both these sets the direction of degradation is difficult to ascertain with certainty. The measurements, however, have been made on the assumption that they are degraded towards longer waves. The data on the continuous regions are given in table 1.

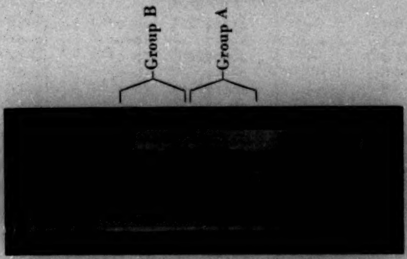

Figure 1. Spectrogram of $SiCl_2$ bands.

Table 1

Long-wave-length limit			Maxima			Short-wave-length limit A.
A.	Kcal.	Electron-volts	A.	Kcal.	Electron-volts	
6500	44·0	1·9	4022	70·5	3·0	3550
3550	80·0	3·5	3260	86·7	3·8	3160
2620	108·0	4·7	2570	110·5	4·8	2535
2500	113·7	4·9	2450	116·0	5·0	2400

Table 2 contains the list of the bands observed in the first two continua. They represent the mean of three independent measurements. In the first set of bands the agreement between the three values is not so good, the discrepancy amounting in some cases to 2 A. For the other set, however, it amounts to about 0·8 A., so that the measurements are accurate to within 0·7 A. in the first case and to 0·3 A. in the second case. Exposures ranging from 15 min. to 1½ hr. were tried, but measurable plates were obtained with an exposure of 30 min. on the medium Hilger quartz spectrograph. An attempt was made to photograph the bands on a three-prism

Table 2

	λ_{air} (A.)	Intensity	$\nu_{\text{vac.}}$ (cm.$^{-1}$)	Classification		$\nu_{\text{obs.}}-\nu_{\text{calc.}}$
				$(\omega_a\,\omega_b)'$	$(\omega_a\,\omega_b)''$	
			Group A			
e	3916·7	—	25524	(0–0)′	(5–1)″	+ 6
n	3881·3	—	25757	(0–0)′	(5–0)″	− 9
d	3844·0	—	26007	(0–0)′	(4–1)″	− 1
m	3807·8	—	26254	(0–0)′	(4–0)″	− 2
c	3770·6	—	26513	(0–0)′	(3–1)″	+ 1
l	3734·3	—	26771	(0–0)′	(3–0)″	+ 11
b	3702·0	—	27005	(0–0)′	(2–1)″	− 1
k	3667·3	—	27260	(0–0)′	(2–0)″	+ 6
a	3633·8	—	27512	(0–0)′	(1–1)″	+ 6
j	3602·6	—	27750	(0–0)′	(1–0)″	− 4
h	3564·1	—	28050	(0–0)′	(0–1)″	− 6
i	3533·2	—	28295	(0–0)′	(0–0)″	− 9
			Group B			
L	3482·1	(1)	28710	(2–1)′	(4–1)″	− 1
x	3476·1	(2)	28760	(2–0)′	(4–0)″	+ 1
	†3471·9?	(2)	28795			
s′	3464·4*	(2)	28857	(1–0)′ (3–0)′	(3–0)″ (4–1)″	− 7 − 9
B	3451·2	(2)	28967	(2–1)′	(4–0)″	+ 7
T	3446·5	(2)	29009	(2–0)′	(3–1)″	− 6
C	3440·2*	(3)	29069	(1–1)′ (3–1)′	(3–0)″ (4–1)″	− 5 − 4
P	3435·2*	(1)	29102	(1–0)′ (3–0)′	(2–1)″ (4–0)″	− 7 − 9
H	3428·6	(1)	29158	(0–0)′	(1–1)″	− 6
K	3422·3	(1)	29212	(2–1)′	(3–1)″	− 4
w	3417·7	(1)	29251	(2–0)′	(3–0)″	− 12
J	3410·3	(1½)	29315	(1–1)′	(2–1)″	+ 5
s	3406·3*	?	29349	(1–0)′ (0–1)′	(2–0)″ (1–1)″	− 8 − 16
p	3399·0	(3)	29412	(0–0)′	(1–0)″	0
S	3388·7	(2)	29501	(2–0)′	(2–1)″	− 8
D	3383·2	(2)	29549	(1–1)′	(2–0)″	− 9
O	3377·1*	(1½)	29603	(1–0)′ (0–1)′	(1–1)″ (1–0)″	− 6 − 10
A	3370·7	(1)	29659	(4–1)′	(4–0)″	+ 6
g	3366·2*	(3)	29699	(0–0)′ (2–1)′	(0–1)″ (2–1)″	− 5 − 11
v	3359·7	—	29756	(2–0)′	(2–0)″	− 1
I	3355·4	—	29794	(1–1)′	(1–1)″	− 16
r	3347·9*	(3)	29861	(1–0)′ (3–0)′	(1–0)″ (2–1)″	+ 4 0
f	3343·3	(3)	29902	(0–1)′	(0–1)″	− 3
R	3331·7	(4)	30006	(2–0)′	(1–1)″	− 2
E	3326·2*	(3)	30056	(1–1)′ (3–1)′	(1–0)″ (2–1)″	− 2 − 6
z	3320·5	(4)	30107	(3–0)′	(2–0)″	− 2
N	3316·7*	?	30142	(1–0)′ (0–1)′	(0–1)″ (0–0)″	− 7 − 11
X	3309·6*	—	30205	(4–0)′ (2–1)′	(2–1)″ (1–1)″	+ 3 − 5
u	3304·1	(4)	30257	(2–0)′	(1–0)″	0
V	3293·3*	(4)	30356	(3–0)′ (1–1)′	(1–1)″ (0–1)″	− 5 + 6

Table 2 (*cont.*)

	λ_{air} (A.)	Intensity	$\nu_{vac.}$ (cm.$^{-1}$)	Classification $(\omega_a\,\omega_b)'$	Classification $(\omega_a\,\omega_b)''$	$\nu_{obs.}-\nu_{calc.}$
			Group B (*cont.*)			
q	3288·6*	(1)	30399	(1–0)′	(0–0)″	+ 2
				(4–1)′	(2–1)″	− 7
c′	3283·2*	(2)	30449	(4–0)′	(2–0)″	− 1
				(2–1)′	(1–0)″	− 9
	†3279·7	?	30482		Cu?	
Q	3272·8*	—	30546	(2–1)′	(0–1)″	− 3
				(3–1)′	(1–1)″	−16
y	3265·4*	(2)	30615	(3–0)′	(1–0)″	+ 6
				(1–1)′	(0–0)″	+17
W	3255·9	(4)	30705	(4–0)′	(1–1)″	+ 3
G	3250·7*	—	30754	(2–1)′	(0–1)″	+ 4
				(5–0)′	(2–0)″	− 4
t	3246·4	—	30795	(2–0)′	(0–0)″	− 2
U	3235·0*	(3)	30903	(3–0)′	(0–1)″	+ 2
				(4–1)′	(1–1)″	0
b′	3229·7*	(2)	30954	(4–0)′	(1–0)″	+ 4
				(5–1)′	(2–0)″	− 5
Y	3223·3*	(2)	31016	(5–0)′	(1–1)″	+ 6
				(2–1)′	(0–0)″	+18
F	3214·5	(2)	31100	(3–1)′	(0–1)″	− 2
M	3204·2	(8)	31200	(5–1)′	(1–1)″	−11
a′	3174·9	(6)	31488	(4–0)′	(0–0)″	− 2
	†3158·1	(5)	31656			

† These bands have been measured only once and on one plate only and are, therefore, doubtful. Capital and lower-case letters indicate the transitions in figures 3 and 4. Figures in brackets in second column indicate visually estimated intensities.

quartz spectrograph giving higher dispersion, but this involved a much longer time of exposure during which it was not possible to maintain the optimum pressure of the flowing vapour. The spectra obtained on these plates were not sufficiently intense for measurements, but they enabled us to find that the bands did not show any resolution in their structure even at this higher dispersion of about 6 A. per mm. in the region λλ3275 to 3200. The twelve bands of group A can be arranged as shown in the table 3.

Table 3

$(v_a v_b)''$ / $(v_a v_b)'$	(0–0)	(0–1)	(1–0)	(1–1)	(2–0)	(2–1)	(3–0)	(3–1)	(4–0)	(4–1)	(5–0)	(5–1)
		(538)		(507)		(492)		(506)		(483)		
(0–0)	28050		27512		27005		26513		26007		25524	
	(245)		(238)		(255)		(258)		(247)		(233)	
		28295		27750		27260		26771		26254		25757
			(545)		(490)		(489)		(517)		(497)	

The bands can thus be regarded as forming a single *v′* progression and as having a mean doublet separation of 246 cm.$^{-1}$ The $\Delta G''(v_a)$ values are irregular, but $\omega_{\frac{1}{2}}''$ 540 cm.$^{-1}$ indicates a rough correspondence with $\omega_{\frac{1}{2}}''$ 530 cm.$^{-1}$ of the ground state of the diatomic molecule SiCl[(4)]. The doublet separation of the ground state of SiCl is 208 cm.$^{-1}$ and this again suggests the possibility that the bands observed here might be due to a transition from an excited $^2\Pi$ inverted level with a separation of about 38 cm.$^{-1}$ to the ground $^2\Pi$ state of SiCl. This interpretation, however, has to be discounted for the following reasons:

(1) Although the $\Delta G''v_a$ values are not very regular and $\omega_{\frac{1}{2}}''$ has a value which in view of the errors of observations may be assumed to agree quite well with the corresponding value in the ground state of SiCl, the second differences $\omega''x''$ which are of the order of 4·5 cm.$^{-1}$ in the latter case do not appear to present themselves in these bands.

(2) The analysis of the second set of the bands, as is shown later, also yields $\Delta G''$ (v_a) values similar to those of the first set of bands, and therefore suggests that both these two sets of bands have a common final state which is certainly different from the ground state of the SiCl molecule, but which has a close correspondence with it, so far as the frequency of vibration of the molecule is concerned.

(3) The bands are broad, those of group A particularly so, and they do not show any structure, at least with the instruments used, which is rather uncommon for a diatomic molecule of low molecular weight.

(4) These bands as well as those of group B are not excited under conditions which produce SiCl bands, but require particularly low pressures, and are more intense in the condensed discharge under which the SiCl bands get weaker in intensity. At relatively high pressures the bands disappear and merge into the continuous bands which they accompany.

In the bands of group B, doublets with a mean interval of 201·1 cm.$^{-1}$ as well as of 504 cm.$^{-1}$ can be picked out. The first doublet separation reminds us of the doublet separation in the ground state of SiCl, viz. 207·9 cm.$^{-1}$, while the second is without doubt the same vibrational difference as we observe in the group A bands. As said above, the bands can be arranged in v' progressions which give first differences that can be identified with those of group A. It has not been possible, however, to arrange the bands in v' progressions having first differences comparable with the v' progressions of the B → X system[(4)] of SiCl.

These peculiarities suggest that both groups of bands have a common emitter and arguments 3 and 4 given above indicate that this emitter in all probability is a multi-atomic one. Furthermore, the argument given under 2 suggests that the emitter is very probably the $SiCl_2$ molecule. It has been shown [(5,6)] that the symmetric valence vibration in the ground state of many triatomic molecules has an order of magnitude comparable with the ground frequency of the corresponding diatomic molecule. For example, the ground frequencies of SO and SeO are 1118 and 910 cm.$^{-1}$ respectively, while those of the symmetric valence vibration of SO_2 and SeO_2 are 1128 and 901 cm.$^{-1}$ respectively[(5,6)]. From a comparison with data on Raman spectra similar relations have been shown to exist for H_2O and OH, CH_4 and CH, $SnCl_4$ and SnCl, $BiCl_3$ and BiCl, and many other pairs[(5)].

Hence an attempt was made to analyse these bands, attributing them to a triatomic molecule. The analysis of the bands is displayed in table 4. The analysis

Table 4

$(v_a v_b)''$ $(v_a v_b)'$	(0, 0)	(0, 1)	(1, 0)	(1, 1)	(2, 0)	(2, 1)	(3, 0)	(3, 1)	(4, 0)	(4, 1)
(0, 1)		29902		29349*						
		(203)		(190)						
		29699		29159						
(0, 0)			(253)							
			29412							
			(191)							
(0, 1)	30142*		29603*							
	—	454	396	445						
	473	443	453	444						
(1, 1)		30356*		29794		29315				
		(214)		(191)		(213)				
		30142		29603		29102				
(1, 0)	(257)		(258)		(247)					
	30399		29861		29349		28857			
	(216)		(195)		(200)		(203)			
(1, 1)	30615*		30056		29549		29060			
	396	398	396	411	407	384	394			
	401	404	393	403	—	399	—			
(2, 1)		30754		30205*		29699*		29212		28710
		(208)		(199)		(198)		(203)		
		30546		30006		29501		29009		—
(2, 0)	(249)		(251)		(255)		(242)			
	30795		30257		29756		29251		28760	
	(221)		(192)						(207)	
(2, 1)	31016*		30449*		—		—		28967	
	—	346	358	341	351	357	—	—	342	350
	—	357	—	350	—	360	—	—	—	—
(3, 1)		31100		30546*		30056*		—		29060*
		(197)		(190)		(195)				(203)
		30903		30356		29861*		—		28857*
(3, 0)			(259)		(246)				(245)	
	—		30615		30107		—		29102*	
(3, 1)	—		—		—		—		—	
	—	—	339	357	342	343	—	—	—	—
	—	—	—	349	—	344	—	—	—	—
(4, 1)		—		30903*		30399*		—		—
				(198)		(194)				
		—		30705		30205		—		—
(4, 0)			(249)		(244)					
	31488		30954		30449		—		—	
(4, 1)	—		—		—		—		29659	
	—	—	—	297	255	—	—	—		
	—	—	—	311	—	—	—	—		
(5, 1)		—		31200		—		—		
				(184)						
		—		31016		—		—		
(5, 0)										
	—		—		30754*		—			
					(200)					
(5, 1)	—		—		30954*		—			

indicates that two modes of vibration are exhibited in the ground state of the molecule. We shall denote by ω_a'' and ω_b'' the frequencies connected with these two modes of vibrations and by $\Delta G''$ (v_a) and $\Delta G''$ (v_b) the vibrational term differences. In tables 5 and 6 we compare the vibrational term differences for the two sets of lands observed. The agreement between these term values for the two sets of bands

Table 5. $\Delta G''$ (v_a) values for ω_a mode of vibration

Band group	0–1	1–2	2–3	3–4	4–5
A	538 545	507 490	492 491	506 517	483 497
	Mean 541·5	498·5	491·5	510·5	490·0
B	540 509 538 540 538 547 528	479 501 512 507 505 508 500 505	492 492 505	502 491	
	Mean 538·6	502·1	496·3	496·5	
Accepted	Mean 540·0	500·3	493·9	503·5	490·0

Table 6. $\Delta G''$ (v_b) values for ω_b mode of vibration

Group A	Group B
245 238 255 258 247 233	253 257 258 247 249 251 255 242 249 249 244
Mean 246·0	Mean 250·4
Accepted Mean 248·2	

is satisfactory and the slight discrepancies are within the experimental error. It has not been possible to arrange both sets of bands into one system. This, coupled with the fact that the two sets of bands differ in appearance, as has already been stated above, inclines us to regard them as two systems, both having the same final state, but having different excited states. The excited electronic level to which the bands of group B are due, again exhibits the same two modes of vibration as are found in the final state. If we denote, as before, by ω_a' and ω_b' the excited frequencies with the two modes of vibrations and by $\Delta G'(v_a)$ and $\Delta G'(v_b)$ the excited vibrational term differences, we collect the data in tables 7 and 8.

Table 7. $\Delta G'(v_a)$ values for ω_a mode of vibration. Bands group B

0–1	1–2	2–3	3–4	4–5
443	394	346	339	311
444	407	357	342	305
449	399	350		
	404	358		
	396	351		
	403			
	396			
Mean 445·3	399·9	352·4	340·5	308

Table 8. $\Delta G'(v_b)$ values for ω_b mode of vibration. Bands group B

0–1	203, 191, 213, 195, 200, 203, 208, 211, 203, 207, 197, 184, 200 Mean 201·1

The excited electronic level associated with the bands of group A does not exhibit any vibrational levels. It is difficult to say whether this is due to instability of the molecule in this state. This possibility is discussed later. The other possibility is the following. The vibration frequencies associated with this level are of an order of magnitude such that the differences between these and the frequencies of the ground state result in bands which differ very slightly in wave-lengths. The breadth of the bands suggests this possibility. If, for example, ω_a' and ω_b' were about 500 and 200 cm.$^{-1}$ respectively, and these values are possible on comparison with frequencies associated with the electronic level A, then a little calculation will show that the successive bands of a sequence will lie close together. The reproduced microphotometer curve given in figure 2 actually shows at least two or three maxima which are close together in each band.

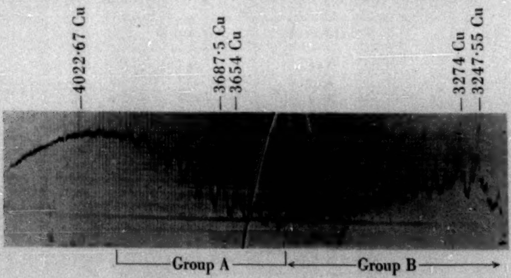

Figure 2. Microphotometer record of $SiCl_3$ bands.

Some of the bands of group B can be classified in two ways, as shown in table 2. Such bands are marked with an asterisk. In most cases they appear to fit equally well with one classification as with the other. For purposes of calculating the vibrational differences both these classifications have been taken into account, while only the classifications not marked with an asterisk are represented in the diagrams of figures 3 and 4, which give a graphical representation of the transitions involved.

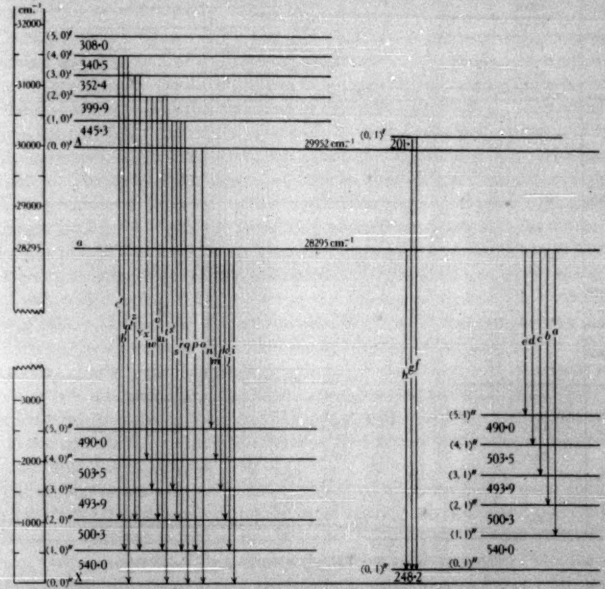
cm.⁻¹
32000
31000
30000
29000
28295
3000
2000
1000
(5, 0)′
308·0
(4, 0)′
340·5
(3, 0)′
352·4
(2, 0)′
399·9
(1, 0)′
445·3
(0, 0)′ A
29952 cm.⁻¹
(0, 1)′
201·1
a
28295 cm.⁻¹
z y x w v u t s r q p o n m l k j i
h g f
e d c b a
(5, 0)″
490·0
(4, 0)″
503·5
(3, 0)″
493·9
(2, 0)″
500·3
(1, 0)″
540·0
(0, 0)″ X
(0, 1)″
248·2
(5, 1)″
490·0
(4, 1)″
503·5
(3, 1)″
493·9
(2, 1)″
500·3
(1, 1)″
540·0
(0, 1)″

Figure 3. Simple transitions of $SiCl_2$ bands.

The analysis proposed here, shows that the two band systems observed are, in all probability, due to $SiCl_2$, and that they involve three electronic levels, namely, X, *a* (28,034 cm.⁻¹ above X), and A (29952 cm.⁻¹ above X). With level X are associated five vibrational levels belonging to one mode of vibration ω_a'' and one vibrational level belonging to ω_b''. The level A is similarly associated with five vibrational levels belonging to the excited state of frequency ω_a' and one vibrational level belonging to the second mode of vibration ω_b' of the excited state. The spacings of the vibrational levels of the ω_a'' frequency are irregular, so that a correct evaluation of the anharmonic factor is not possible. Roughly $2\omega_a''x'' \simeq 12$ and $2\omega_a'x' \simeq 40$, indicating a large increase in the anharmonicity factor in the excited *a* state. Evidently no information is obtained for the anharmonicity factor for the frequency ω_b.

A non-linear triatomic molecule possesses three fundamental modes of vibration, viz. the total symmetric or deformation or breathing vibration ω_1, the symmetric valence vibration ω_2, and the antisymmetric valence vibration ω_3. In table 9 we give some examples of the actual values of these vibrational frequencies for the

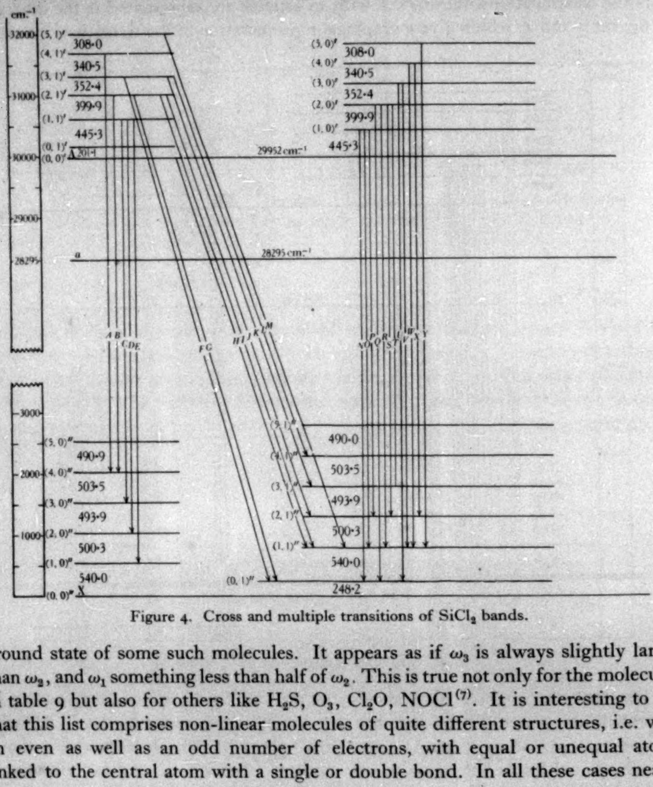
cm.⁻¹
32000
31000
30000
29000
28295
3000
2000
1000
(5, 1)′
(4, 1)′
(3, 1)′
(2, 1)′
(1, 1)′
(0, 1)′
(0, 0)′
308·0
340·5
352·4
399·9
445·3
201·1
(5, 0)′
(4, 0)′
(3, 0)′
(2, 0)′
(1, 0)′
29952 cm.⁻¹
a
28295 cm.⁻¹
A B C D E
F G
H I J K L M
N O P Q R S T U V W X Y
(5, 0)″
(4, 0)″
(3, 0)″
(2, 0)″
(1, 0)″
(0, 0)″
X
490·9
503·5
493·9
500·3
540·0
(5, 1)″
(4, 1)″
(3, 1)″
(2, 1)″
(1, 1)″
(0, 1)″
490·0
248·2

Figure 4. Cross and multiple transitions of $SiCl_2$ bands.

ground state of some such molecules. It appears as if ω_3 is always slightly larger than ω_2, and ω_1 something less than half of ω_2. This is true not only for the molecules in table 9 but also for others like H_2S, O_3, Cl_2O, NOCl⁽⁷⁾. It is interesting to see that this list comprises non-linear molecules of quite different structures, i.e. with an even as well as an odd number of electrons, with equal or unequal atoms linked to the central atom with a single or double bond. In all these cases nearly

Table 9

Molecule	ω_1	ω_2	ω_3
H_2O	1595·4	3600	3756
SO_2	524·0	1152	1361
NO_2	640·0	1370	1615
ClO_2	529·0	946	1109

the same ratio for ω_1, ω_2 and ω_3 persists. As discussed elsewhere(6), the reason for this uniformity may be that ω itself is more sensitive to the mass than to the forces or to the energy of the bond.

At the same time we know that in the transition from a diatomic radical like SO or SeO to a triatomic molecule like SO_2 or SeO_2 the symmetric valence vibration of the latter has almost the same value as the vibrational frequencies of the radical. For SO and SO_2 the values are respectively $\omega''=1150$, $\omega_2''=1128$, and $\omega'=623$, $\omega_2'=662$.

Considering the figures $\omega_a''=540$, $\omega_b''=248$, $\omega_a'=445$, $\omega_b'=201$, we find ω_b'' something less than half of ω_a''. At the same time $\omega_a''=540$ is in close agreement with $\omega''=531$ of SiCl. Doubtless ω_a has to be identified with the symmetric valence vibration ω_2, whereas ω_b is the breathing or deforming vibration ω_1. This correlation receives support from the values of 425 of the total symmetric vibration of $SiCl_4$, which corresponds to the symmetric valence vibration of a tetrahedron-like molecule(7). The above values therefore indicate that $SiCl_2$ is a *non-linear* molecule.

A new feature is, however, added by the fact that ω_2' of $SiCl_2$ does not agree any longer with $\omega_a'=660$ to 700 (according to the excited term considered) of SiCl. Molecules like SO and SO_2 both have an even number of electrons; in both the bond energies are weakened by excitation and hence $\omega_2'<\omega_2''$ and $\omega'<\omega''$. In $SiCl_2$ both *p* electrons of Si take part in the linkage, while in SiCl, however, one remains as an odd electron. For SiF it could be shown(8) that this electron disturbs the linkage, in agreement with the theory developed earlier(9). For SiCl the uncertainty of $\omega'x'$ still prevents a correlation of the atomic and molecular terms, but doubtless the same conditions hold good for this molecule as for SiF. It is therefore by no means surprising, but in good agreement with theoretical conceptions, that in the odd numbered molecule SiCl we find $\omega'>\omega''$ but in the even numbered molecule $SiCl_2$, as in SO_2, $\omega_2'<\omega_2''$.

The similarity between ω'' of SiCl and ω_2'' of $SiCl_2$ is again in good agreement with the Heitler-London pair-bond theory of valency. In this conception the bonds are strongly localized in molecules possessing a pronounced central atom. This receives confirmation from considerations of bond energies. For SiCl the extrapolation of the vibrational levels give a rough value of about 4 e.v. for *D* (SiCl) which will be an upper limit. Parti and Samuel(10) have shown that *D* ($SiCl_2$) may be roughly estimated as 3/5 of *D* ($SiCl_4$). The energy of formation of gaseous $SiCl_4$ from the elements is given as 151 kcal./mol.(11), the sublimation energy(12) of Si, is 47, $D(Cl_2)=57{\cdot}9$, and the heat of sublimation of $SiCl_4$ is 7·2 kcal./mol.(13). By means of Born's cycle, 308 kcal./mol. is obtained for the energy of formation of $SiCl_4$ by combination of unexcited atoms. The value of the heat of sublimation of Si, however, appears to be rather inaccurate and too high. According to the above ratio, *D* ($SiCl_2$) is 185 and the energy of a single Si^{II}—Cl bond 92·5 kcal./mol. or 4 e.v. in good agreement with *D* (SiCl). The similarity of ω'' (SiCl) and ω_2'' ($SiCl_2$) may be considered as a consequence of this. The bond energy of $SiCl_4$ of course is not one-quarter of *D* ($SiCl_4$). Exactly as in CCl_4, the ground level of the molecule involves a Si atom in the excited configuration sp^3. The value of the corresponding

^{5}S term is not known for Si, but has been calculated(14) as about 4 e.v. for *C*. The value of the *D* states belonging to the same configuration sp^3, as well as the ionization potential of Si is about 33 per cent less than that of *C*(15). Hence the excitation energy of the ^{5}S term will be about 2·7 e.v. *D* ($SiCl_4$) being 13·4 e.v., $\frac{1}{4}$ (13·4 + 2·7) or about 4·0 e.v. obtains for the bond energy of the Si^{IV}—Cl link. As always in such cases, involving the splitting of the s^2 group, the bond energy should increase slightly for the state of maximal valency, and hence our figures appear to be slightly incorrect, probably on account of too high a value of the heat of sublimation of silicon.

The determination of the dissociation energy of a polyatomic molecule by vibrational extrapolation is yet problematic. Still, as a first approximation it should be possible to obtain a rough estimate of the single bond energy from the extrapolation of the vibrational levels of the symmetric valence vibration alone, for which a number of levels are measured, neglecting at first the other modes. The thermochemical value of D_B (Si—Cl) being in agreement with D'' (SiCl), such an extrapolation again should give a value of about 3 to 4 e.v. On account of the similarity of the two frequencies ω'' (SiCl) and ω_2'' ($SiCl_2$), $\omega_2''x_2''$ therefore should again have a value of the order of $\omega''x''$ of SiCl, i.e. about 2·2. The vibrational levels of the ground state obtained for ω_2 mode of vibration are rather irregular and perturbed. The accepted means of $\Delta G''(v_a)$ values have been listed in table 5 and the first value of $2\omega_2''x_2''$ of about 12 cm.$^{-1}$ which appears in the analysis as well of the A group as of the B group bands, may be due to real perturbations, and not only to overlapping of bands involving other vibrational levels of either electronic state. Also the remaining values are too few in number to permit an extrapolation with any degree of accuracy. From the experience of the band spectra of diatomic molecules it is known that even a far larger number of observations, more often than not, yields an absolute value of *D* which is incorrect by 25 to 50 per cent, just on account of the inaccuracy of ωx. It is, however, worthy of note that the remaining second differences of the B-group bands which appear to be the least perturbed, give a mean value of 5·1 or $\omega_2''x_2'' = 2{\cdot}55$, rather near to the expected one. But it goes without saying, that no conclusion can be drawn from this fact at present.

One more conclusion can, however, be drawn. The value of 4 e.v. has been determined thermochemically for the bond energy. The excitation energy of the two levels *a* and A is 3·5 and 3·7 e.v. respectively. The dissociation energy of both the excited levels appears to be very small. For level *a*, this follows from the fact, that the excited vibrational levels do not appear, and for level A, from the large value of $\omega_2'x_2'$. Actually an extrapolation with the values $\omega_2' = 445$ and $\omega_2'x_2' = 34{\cdot}2$ would yield a value of D' (A) = 0·3 e.v., which we may consider as the upper limit. It is therefore probable that both excited states involve unexcited dissociation products or at the most Cl in its $^2P_{\frac{1}{2}}$ term, about 0·1 e.v. above $^2P_{\frac{3}{2}}$, its ground state.

Contrary to the spectra of SO_2 and SeO_2 recently investigated, the antisymmetric valence vibration is not involved in the bands of $SiCl_2$. This is in agreement with Herzberg and Teller's(16) theory, according to which transitions involving an antisymmetric frequency should occur if at all, with low intensity, and only if $\Delta\nu_{\text{antisym.}}$

is even. This latter postulate indeed holds good in SeO_2. Incidentally the fact that odd and even combinations of the two frequencies are involved in the bands of $SiCl_2$ also shows that none of them is ω_3. Herzberg and Teller's selection rule(16) is the more valid the smaller the change in the internuclear distance on excitation. The appearance of ω_1 in the spectrum of $SiCl_2$ and its absence in those of SO_2 and SeO_2 may well be due to the fact that this distance changes much less in the present case. This possibility receives confirmation from the fact that ω_2' is comparatively less smaller than ω_2''. For $SiCl_2$, ω_2' is about 25 per cent of ω_2'', for SO_2 and SeO_2 about 45 per cent. In the present state of knowledge it would be premature to do more than just to point out this possibility. It may well be that the difference in the modes of vibration involved in the spectra is due to quite other reasons, e.g. to the fact that SO_2 and SeO_2 are investigated in absorption and $SiCl_2$ in emission.

A few new bands of SiCl have been observed on some heavily exposed plates, which fit into the existing scheme. These are given in table 10. Except on one heavily exposed plate which shows three or four very faint bands probably due to SiO (not checked by measurements) no SiO bands have been registered on any of the plates of $SiCl_4$ vapour.

Table 10

λ_{air} (A.)	Intensity	$\nu_{vac.}$ (cm.$^{-1}$)	Classification $v'-v''$	$\nu_{obs.}-\nu_{calc.}$*
3240·3	(3)	30853	P_1 0–6	− 5·0
3219·0	(2)	31057	P_2 0–6	− 8·9
3188·4	(6)	31355	P_1 0–5	− 12·1
3134·5	(1)	31894	P_1 0–4	+ 13·5
3115·4	(1)	32089	P_2 0–4	+ 0·6
2896·6	(1)	34513	P_2 2–2?	− 10·0
2852·2	(1)	35050	P_2 2–1?	+ 0·4

* Calculated values are from the following equation(4):

$$\nu = \underset{33894\cdot 8}{34102\cdot 7} + \{(701\cdot 5x' - 1\cdot 40x'^2) - (535x'' - 2\cdot 20x''^2)\}, \quad \text{where } x' = (v' + \tfrac{1}{2}) \text{ and } x'' = (v'' + \tfrac{1}{2}).$$

§4. THE EMISSION BANDS OF $SnCl_2$

The discharge through the vapours of $SnCl_4$ and $SnCl_2$ has been studied for a pressure of slightly less than 1 mm. of mercury, in each case with uncondensed discharge. Each discharge tube had a quartz window attached to one side of the end-on tube while the other side was fitted with a glass window. Simultaneous exposures were taken on the medium Hilger quartz spectrograph and a Hilger constant deviation glass spectrograph. In the case of both substances the two known band systems of SnCl were observed. In addition to these bands(17) the spectrum of $SnCl_2$ vapour showed a set of narrow bands in the region λλ4500 to 4900. These were absent in the spectrum of $SnCl_4$ vapour. We shall discuss these bands below. The regions of continuous emission given by $SnCl_4$ have their maxima at λλ4245, 3260, 2580, and (2365?), while those of $SnCl_2$ are at λλ4500 and 3100. The detailed data on these continua are given in tables 11 and 12. The set of narrow bands observed in $SnCl_2$ have been measured on plates taken on Hilger constant deviation glass spectrograph giving an average dispersion of about 28 A. per mm. in the region

Table 11. $SnCl_4$

Long-wave-length limit			Maxima			Short-wave-length limit
A.	Kcal./mol.	Electron-volts	A.	Kcal.	Electron-volts	A.
5100	55·5	2·5	4525	62·5	2·7	3910
3470	82·0	3·5	3260	87·0	3·6	3210
2620	108·0	4·7	2580	110·0	4·8	2520
2520	112·5	4·9	2365?	120·0	5·1	2400

Table 12. $SnCl_2$

Long-wave-length limit			Maxima			Short-wave-length limit
A.	Kcal.	Electron-volts	A.	Kcal.	Electron-volts	A.
5200	55·2	2·4	4500	62·5	2·7	4000
3400	82·8	3·6	3100	92·0	4·0	3000

λλ4500 to 4900. The bands are very faint and lie in the body of the first region of continuous emission. The bands are similar in appearance to those of group A bands of $SiCl_2$ system. They are rather broad and the direction of their degradation is not quite certain. Figure 5 is a reproduction of the plate. Table 13 gives the wave-lengths of the bands measured, together with the classification proposed.

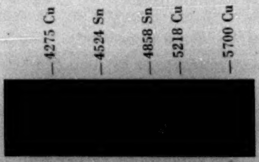

Figure 5. Spectrogram of $SnCl_2$ bands.

These are the mean of two values obtained from two independent plates which are measured on the assumption that the bands are degraded towards longer waves. The average discrepancy between the two measurements is of the order of 1 A. which introduces an error of about 3 $cm.^{-1}$. A few bands below λ4549 were visible on the plate to the naked eye, but could not be measured on the comparator.

The frequency of vibration connected with the ground state of the diatomic molecule SnCl is of the order of 351·4 $cm.^{-1}$. Differences of this order of magnitude can be easily recognized in the present bands. The progressions in which the bands can be thus arranged give vibrational differences which, however, show marked

Table 13

Transitions, figure 7	λ_{air} (A.)	$\nu_{vac.}$ (cm.$^{-1}$)	Classification		$\nu_{obs.}-\nu_{calc.}$
			$(\omega_a\,\omega_b)'$	$(\omega_a\,\omega_b)''$	
D	4796·4	20843	(0–0)′	(4–0)″	−5
J	4770·5	20956	(0–0)′	(3–2)″	+2
G	4744·5	21071	(0–0)′	(3–1)″	+4
C	4719·9	21181	(0–0)′	(3–0)″	−5
I	4691·2	21311	(0–0)′	(2–2)″	−2
F	4666·2	21425	(0–0)′	(2–1)″	−1
B	4639·6	21548	(0–0)′	(2–0)″	+3
H	4617·7	21650	(0–0)′	(1–2)″	0
E	4594·4	21760	(0–0)′	(1–1)″	−3
A	4568·1	21885	(0–0)′	(1–0)″	+3
K	4543·1	22005	(0–0)′	(0–2)″	0

discrepancy with those of the ground state of SnCl. This correspondence, without a close agreement, again indicates that the final level involved in these bands is probably the ground state of the triatomic molecule $SnCl_2$. Furthermore, the ground level of SnCl is a $^2\Pi$ level with an electronic separation of 2360 cm.$^{-1}$. If the final level of the bands under discussion were identical with the ground level of SnCl we should obtain a similar set of bands at about the same distance either on the long or short wave-length side of the bands. No such bands have been observed though looked for.

The analysis of the bands on the assumption that they are due to a triatomic molecule $SnCl_2$, is displayed in table 14. In conformity with the analysis given for the group A bands of $SiCl_2$, we again obtain frequencies ω_a and ω_b associated with two modes of vibration. We obtain three vibrational levels associated with one mode of vibration and two levels with the other in the ground state of the molecule. The excited state does not exhibit any vibrational levels, exactly as in the group A bands of $SiCl_2$. The breadth of the bands again indicates the possibility that the vibrational frequencies associated with this excited level are of an order of magnitude such that the differences between these and the frequencies in the ground state result in bands which differ very slightly in wave-lengths, as in the case of group A

Table 14*

—		—		22005
				(355)
21885	(125)	21760	(110)	21650
(337)		(335)		(339)
21548	(123)	21425	(114)	21311
(367)		(354)		(355)
21181	(110)	21071	(115)	20956
(338)				
20843		—		—

---

* The actual vibrational quantum numbers of the transitions giving these bands are given in table 13.

bands of $SiCl_2$. Figure 6 shows a reproduced microphotometer curve showing at least three components in each band. The (0–0)′–(0–0)″ band is too faint to be measured, being on the shorter wave side of the last band measured on the comparator. Figure 7 is a diagrammatic representation of the transitions observed.

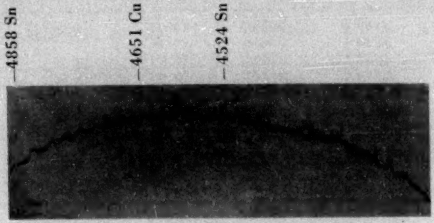

Figure 6. Microphotometer record of $SnCl_2$ bands.

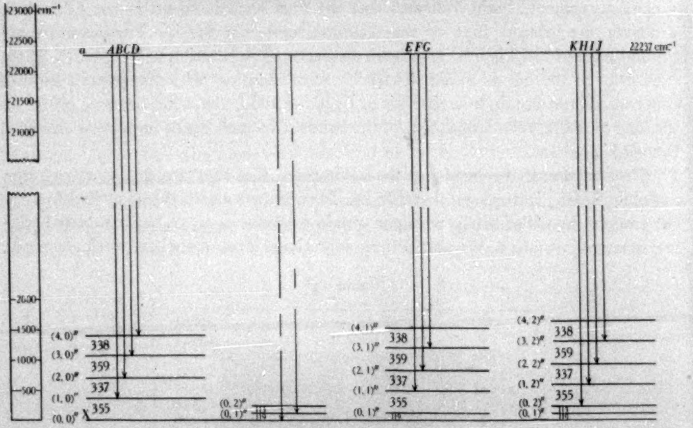
23000 cm⁻¹
22500
22000
21500
21000
2000
1500
1000
500
a
ABCD
EFG
KHIJ
22237 cm⁻¹
(4, 0)″
(3, 0)″
(2, 0)″
(1, 0)″
(0, 0)″
338
359
337
355
(0, 2)″
(0, 1)″
118
(4, 1)″
(3, 1)″
(2, 1)″
(1, 1)″
(0, 1)″
338
359
337
355
118
(4, 2)″
(3, 2)″
(2, 2)″
(1, 2)″
(0, 2)″
(0, 1)″
338
359
337
355
118

Figure 7. Simple and multiple transitions of $SnCl_2$ bands.

With the same notation as is used before for $SiCl_2$, the $\Delta G''(v_a)$ and $\Delta G''(v_b)$ values are given in tables 15 and 16.

Table 15. $\Delta G''(v_a)$ values for ω_a mode of vibration

0–1	1–2	2–3	3–4
355	337 335 339	367 354 355	338
Mean 355	337	359	338

Table 16. $\Delta G''\ (v_b)$ values for ω_b mode of vibration

0–1	1–2
125 123 110	110 114 115
Mean 119·3	113·0

The $\Delta G''\ (v_a)$ values are irregular and an evaluation of the anharmonic factor is not possible. For $\Delta G''\ (v_b)$ we have only two values which decrease regularly and which give $\omega x = 3$. ω_a is therefore $=355$ cm.$^{-1}$ and $\omega_b = 122$ cm.$^{-1}$.

Exactly as in $SiCl_2$, we identify ω_a'' as the symmetric valence vibration, the value of 355 being near to $\omega'' = 351{\cdot}4$ of SnCl and the valence vibration of $SnCl_4$(7) of 366 cm.$^{-1}$. The frequency $\omega_b'' = 122$ becomes the deforming vibration, being smaller than half of ω_a''. Applying the same remarks that we have offered for $SiCl_2$, we are led to the conclusion that this level of $SnCl_2$ is also the ground state of the molecule, and that the molecule is non-linear. The close proximity of $\omega_b'' = 122$ with the two deforming frequencies $^3\delta$ and $^2\delta$ of $SnCl_4$, which are 134 cm.$^{-1}$ and 104 cm.$^{-1}$ respectively, further indicates that ω_b'' represents the frequencies connected with the deforming mode of vibration. The antisymmetric valence vibration has not been observed for $SnCl_2$. In this respect also the behaviour of the molecule is completely analogous to that of $SiCl_2$ and is in agreement with Herzberg and Teller's theory(16).

An extrapolation of the bond energy of $SnCl_2$ from the band spectroscopical data is out of question, but the atomic heat of formation has been calculated recently(10) as $D\ (SnCl_2) = 180{\cdot}8$ and $D\ (SnCl_4) = 300{\cdot}5$ kcal./mol. This gives 3·8 e.v. for the bond energy $D_B\ (Sn^{II}—Cl)$ and for $D_B\ (Sn^{IV}—Cl) = 3{\cdot}9$ e.v. obtains if the excitation energy of the ^5S term of Sn is estimated to about 2·4 e.v.

The main results of these investigations are displayed in table 17. Some of the figures are not very accurate, both of spectroscopic as well as of thermochemical origin. But the table shows certain regularities which appear to be real. The excitation energy of the triatomic molecule with an even number of electrons is less than that of the odd numbered corresponding diatomic one. The symmetric valence vibration of both are almost identical, those of the corresponding higher polyatomic chlorides are not far off. Similarly the bond energies of both the former ones appear to be very nearly related. For the higher chloride we expect a higher bond energy because the electronic configuration undergoes a sudden change by the s^2 group being fissured, probably the internuclear distance becomes smaller and the molecular refractivities in such cases show a smaller polarizability. A tendency in this direction is certainly present among the tin chlorides but is less marked among those of silicon. One feature, however, cannot be understood at present, i.e. the valence vibration of $SiCl_4$ is smaller than those of SiCl and $SiCl_2$, whereas among the tin chlorides just the opposite happens. Summarizing, we might say that these spectra again indicate a close relation between the bonds of these corresponding molecules and therefore a rather strong localization of the bonds.

Table 17

	$SiCl$	$SiCl_2$	$SiCl_4$	$SnCl$	$SnCl_2$	$SnCl_4$
Excitation energy (cm^{-1})	34136 41235 45006	28295 29952 —	— — —	28939 33622 —	22237 — —	— — —
Symmetric valence vibration. Ground state (cm^{-1})	531	540	425	351	355	366
Deforming vibration. Ground state (cm^{-1})	—	248	221,151	—	122	134,104
Bond energy (e.v.)	4·0*	4·0†	4·0†	3·5*	3·8†	3·9†

* Band spectra. † Thermochemical value.

REFERENCES

(1) Jevons, W. *Proc. Roy. Soc.* A, **89**, 187 (1913); **106**, 174 (1924).
(2) Miescher, E. *Helv. phys. Acta*, **8**, 587 (1935).
Jevons, W. and Bashford, L. A. *Proc. Phys. Soc.* **49**, 554 (1937).
(3) Bhaduri, B. N. and Fowler, A. *Proc. Roy. Soc.* A, **145**, 312 (1934).
(4) Jevons, W. *Proc. Phys. Soc.* **48**, 563 (1936).
(5) Asundi, R. K. and Samuel, R. *Proc. Ind. Acad. Sci.* **2**, 30 (1935).
(6) Asundi, R. K., Jan Khan, M. and Samuel, R. *Proc. Roy. Soc.* A, **157**, 28 (1936).
(7) Sponer, H. *Molekülspektren*, **1** (1935).
(8) Asundi, R. K. and Samuel, R. *Proc. Ind. Acad. Sci.* **3**, 346 (1936).
(9) Lessheim, H. and Samuel, R. *Phil. Mag.* **21**, 41 (1936); *Proc. Ind. Acad. Sci.* **1**, 623 (1935); *Proc. Phys. Soc.* **46**, 523 (1934); *Z. Phys.* **84**, 637 (1933).
(10) Parti, Y. P. and Samuel, R. *Proc. Phys. Soc.* **49**, 568 (1937).
(11) *Landolt and Boernstein Tables.*
(12) *International Critical Tables.*
(13) Kelley, K. K. *Contributions to the Data on Metallurgy* (Washington, 1935).
(14) Van Vleck, J. H. *J. Chem. Phys.* **2**, 297 (1934).
(15) Bacher, R. F. and Goudsmit, S. *Atomic Energy States* (McGraw-Hill, 1932).
(16) Herzberg, G. and Teller, E. *Z. phys. Chem.* **21**, 410 (1933).
(17) Jevons, W. *Proc. Roy. Soc.* A, **110**, 365 (1926).
Ferguson, W. F. C. *Phys. Rev.* **32**, 607 (1928).

THE ACOUSTICAL CONDUCTIVITY OF ORIFICES

By N. W. ROBINSON, A.R.C.S., B.Sc., Ph.D.

Received 14 *December*, 1937. *Read in title* 11 *March*, 1938

ABSTRACT. Measurements made on the acoustical conductivities of the following orifices are described: (1) At the junctions between two tubes in series and two tubes in parallel; (2) Multiple thin orifices in parallel; (3) Long orifices forming constrictions in a tube and long orifices terminating a tube. Equations are given for calculating the conductivities of orifices associated with various acoustical structures. A method is described, of determining the shapes of acoustical wave-fronts near any constriction in a cylindrical tube, and results are given for thin circular orifices.

§ 1. INTRODUCTION

The conductivity of an orifice is defined as the constant of proportionality between the difference in velocity-potential on each side of the orifice and the resulting volume velocity. It is called conductivity because of its analogue in electricity, the reciprocal of resistance. The acoustical impedance of an orifice can be shown to be almost a pure reactance $i\rho\omega/K$, where ρ is the density of the medium, ω is the pulsatance, and K is the conductivity. When the orifice is of very small diameter, viscous effects may introduce a resistance term into the impedance, but in all the orifices to be considered here the reactance term predominates and hence the resistance may be neglected.

The method of experiment has been described previously⁽¹⁾ but the theory may be briefly recapitulated without any of the practical details. The impedance Z_1 at any point in a cylindrical tube is given by

$$Z_1=\frac{i\cos kl_1Z_2-R\sin kl_1}{-R^{-1}\sin kl_1Z_2-i\cos kl_1} \qquad \text{......(1)},$$

where Z_2 represents the terminating impedance, $i_2=-1$, $k=\omega/c=2\pi/\lambda$, where c and λ are the velocity and wave-length of the sound respectively, $R=\rho c/S$, S is the area of cross-section of the tube, and l_1 is the distance from the point P to the terminating impedance Z_2.

If, now, Z'_2 is the terminating impedance at the other end of the tube, distant l'_1 from P, an expression similar to (1) may be written down for the impedance at P. The two expressions are identical, but a distinction is made in the nomenclature in order to distinguish between the impedance at the point due to one end of the tube and that due to the other. The loudspeaker, which drives the system, forms part of the impedance Z'_2, the other part being a branch tube with which the impedance can be varied. Z_1 is made zero by making Z_2 a rigid end and l_1 equal to $\frac{1}{4}n\lambda$, where n is an odd integer. A microphone placed at P will record minimum sound but not necessarily silence. Silence can be obtained, however, by adjusting Z'_2. The impedance at P and hence the acoustic pressure must be zero. Putting $Z_1=0$ in expression (1) we have

$$0=i\cos kl_1Z_2-R\sin kl_1$$

or

$$Z_2=-i\rho c/S_1\tan 2\pi l_1/\lambda \qquad \ldots\ldots(2).$$

Hence Z_2 is given in terms of l_1.

By applying this method, the conductivities of thin orifices forming constrictions in a tube were found to be represented by the formula

$$C=\frac{0{\cdot}787\,d}{\left(1-\frac{d}{D}\right)^{1{\cdot}895}} \qquad \ldots\ldots(3),$$

where d and D are the diameters of the orifice and tube respectively and C is the conductivity in an infinitely thin sheet. When the orifices formed terminations to the tube the conductivity was given by

$$C=d\left(1+\frac{d}{D}\right)^{1{\cdot}19} \qquad \ldots\ldots(4).$$

§ 2. WAVE-SHAPES NEAR AN ORIFICE IN A TUBE

One of the effects noticed in the first set of experiments on constrictions in a tube was that the measured value of the conductivities depended upon the nearness of the pressure tube to the orifice. When the tube was remote from any particular orifice a constant value of conductivity was obtained for that orifice, but when the tube was within 1 or 2 cm. of the orifice abnormally high values were obtained. The effect is shown in figure 5 of the paper quoted. It was thought to be due to the distortion of the wave-fronts in the tube as a result of the presence of the orifice.

The actual shapes of the waves were determined as follows: with the opening of the pressure tube on the axis of the main tube, distance pieces were inserted in the tube whereby the orifice was moved in steps of 0·159 cm. away from the pressure tube, i.e. l_1 was increased in steps of 0·159 cm. For each setting of l_1 the length of tube l_2 behind the orifice was adjusted by means of a piston until silence was obtained. The pressure tube was then displaced from the axis, and again measurements of l_2 were made while l_1 was varied. The experiments were performed for radial displacements of the pressure tube of 0·25, 0·5, 1·0, 1·5, 2·0 and 2·3 cm. from the axis. Curves were drawn, figure 1 (a, b, c, d), showing the relationship between l_2 and the radial displacement r, for the various values of l_1 shown alongside the curves.

The decrease in l_2 shown where the pressure tube is actually in the orifice, so that the radial displacement is zero and $l_1=0$, is due to effective reduction in area causing decreased conductivity at the orifice. It will be seen that this effect is greatest in the smallest orifice, where the pressure tube occupies a relatively large proportion of the opening. The dotted lines show the probable value of l_2.

Consider a line on figure 1 (*b*) corresponding to a constant value of l_2 of 7·3 cm. It intersects lines of constant l_1 at points *u*, *v*, *w*. This may be interpreted by

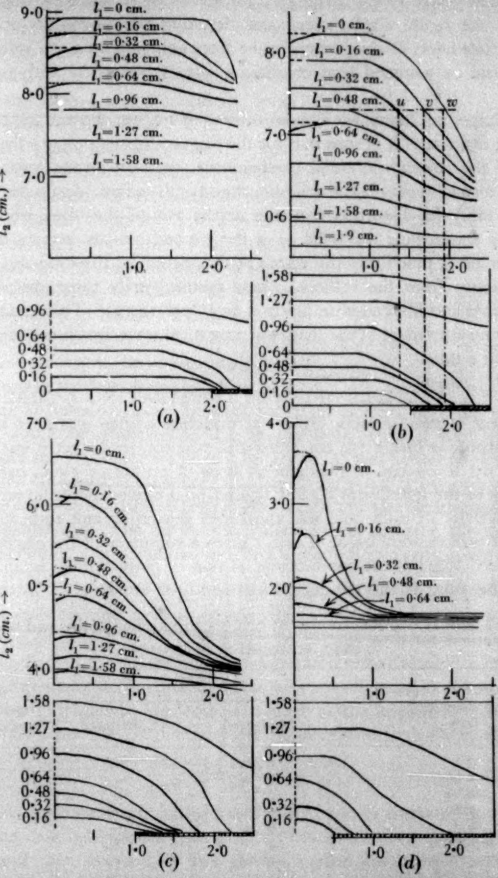

Figure 1. Relation between l_2 (cm.) and the radial displacement *r* (cm.). Diameter of orifice: (*a*) 4·0 cm.; (*b*) 3·0 cm.; (*c*) 2·0 cm.; (*d*) 1·0 cm.

assuming that the experiment had been performed by keeping the length of tube behind the orifice constant at 7·3 cm. and obtaining silence in the microphone by adjusting the length of tube in front of the microphone. Silence would have been obtained at the values of l_1 and r given by the points u, v, and w on the graph. Now if l_1 and r are plotted the contours of the equipressure or equipotential surfaces are obtained. The lower graph of figure 1 (*b*) shows these surfaces, the accentuated portion of the radial displacement axis denoting the surrounds of the orifice. Radial displacements of the pressure tube were only made on one side of the axis, since it could be assumed that conditions were symmetrical with regard to the latter.

Wave shapes are shown for circular orifices of 1·0, 2·0, 3·0 and 4·0 cm. in a tube 5·08 cm. in diameter. It is seen that for the largest orifice (4·0 cm.) the plane components of the velocity-potential predominate, the non-planar wave-front being confined to a small region in the neighbourhood of the edges. Again, for the smallest orifice (1·0 cm.) the disturbed region is at the axis of the tube, while the plane components persist near the walls. For the 3·0 and 2·0-cm. orifices the distorted wave-fronts affect practically the whole of the section of the tube and persist to a greater distance from the orifices. These results verify those described in the previous paper and illustrated in figure 5 on p. 778 thereof. This method is applicable to the measurement of the shapes of acoustical wave-fronts near any apparatus connected in a tube.

§ 3. MULTIPLE ORIFICES TERMINATING A TUBE

The effect of two or more orifices terminating a tube was next investigated. For this purpose, a disk 0·159 cm. thick and 7·62 cm. in diameter was bored with holes from 0·1 to 0·9 cm. in diameter in steps of 0·1 cm., 0·5 cm. being omitted. The centres of the holes were equally spaced on a circle round the largest orifice. The conductivity of each hole was measured separately and then various combinations of orifices were used. Table 1 gives a summary of the results obtained. The measured value of the conductivity of two or more orifices is, in every case, less than the sum of the conductivities measured separately. By reference to

Table 1. Conductivities of orifices in parallel at the end of a tube, arranged as in figure 2

Arrangement of orifices, and diameters (cm.)	K		Ratio of measured K to calculated K
	Measured	Calculated	
0·4	0·40	—	—
0·60	0·62	—	—
0·70	0·76	—	—
0·80	0·86	—	—
0·9	0·94	—	—
0·80, 0·9	1·56	1·80	0·87
0·7, 0·8, 0·9	1·86	2·56	0·72
0·6, 0·7, 0·8, 0·9	2·31	3·28	0·73
0·4, 0·6, 0·7, 0·8, 0·9	2·50	3·58	0·70
0·9, 0·7	1·49	1·70	0·88
0·9, 0·6	1·36	1·56	0·87
0·8, 0·6	1·33	1·48	0·90
0·8, 0·70	1·35	1·62	0·83
0·7, 0·6	1·14	1·38	0·83

figure 2, which shows the relative positions of the orifices, it is noticeable that the orifices 0·8 and 0·6 cm. in diameter show the greatest percentage ratio between the measured and additive values. They are also the farthest apart. The 0·9 and 0·7, the 0·9 and 0·6, and the 0·9 and 0·8-cm. orifices have the same spacing and show a ratio of 87 per cent, while the combinations of the 0·8 and 0·7 and the 0·7 and 0·6 orifices, being less distant, show a lower ratio.

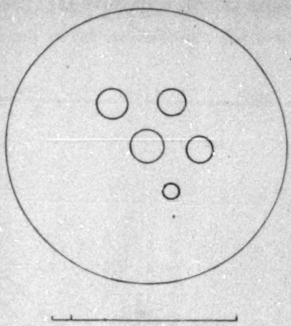

Figure 2.

The results show, therefore, that the proximity of the orifices has the effect of reducing the ratio of the measured conductivity to the sum of the separate conductivities. The ratio also decreases with the number of orifices arranged in parallel. It was impossible, in a tube 5·08 cm. in diameter, to space the orifices sufficiently far apart to enable a numerical relation between the spacing of two similar orifices and their conductivity to be determined. Nor was it convenient to determine the effect of a large number of holes of equal diameter, for if the orifices were too near to the walls there would be interference due to the wall, while if the orifices were made too small the resistance would not be negligible and hence the results would not be reliable. It appears, therefore, that the actual conductivity of a set of holes forming a constriction in a tube or terminating a tube must be determined separately in each individual case. The results given do indicate, however, the order of the reduction in conductivity which is produced when multiple orifices are used.

§ 4. ORIFICES IN PARALLEL WITH THE MAIN TUBE

Experiments were now performed on orifices bored in the walls of the main tube. The orifices were therefore effectively in parallel with the main tube, since a wave propagated in the tube could be transmitted either along it or through an orifice. The impedance Z_2 in equation (1) is now the effective impedance of a pipe and the orifice in parallel. The case is treated in the appendix, equation (3*a*), where it is shown that the conductivity can be calculated from the relation

$$\frac{\lambda K}{2\pi S} = \tan\frac{2\pi l_2}{\lambda} - \cot\frac{2\pi l_1}{\lambda} \qquad \text{......(3a).}$$

Measurements were made on six orifices 0·6–2·52 cm. in diameter at a frequency corresponding to a half-wave-length of 15·73 cm. at 21·2° C. Several values of l_1 were used and then $\tan(2\pi l_2/\lambda)$ was plotted against $\cot(2\pi l_1/\lambda)$, figure 3. The intercepts of the resulting straight lines on the axes were given by $\lambda K/2\pi S_1$, from which K was calculated for each orifice. The measured value was reduced to the conductance of a similar orifice in a thin sheet by the relation

$$\frac{1}{K} = \frac{1}{C} + \frac{L}{A} \qquad \text{......(5).}$$

Experimental points are indicated in figure 4, which also shows the conductivities of orifices forming constrictions, curve (1), and of orifices terminating a tube, curve (2), reproduced from the previous paper. It is seen that the points agree closely with curve (2). The agreement is not so good for the larger orifices, and this may be due to the fact that the orifices were not plane in section but were bored directly out of the walls of the tube. Another difference in the conditions is that instead of the wave arriving in the same phase all over the orifice, as it does in a terminating impedance, there is a slight difference in phase from one end to the other. This is small except in the larger orifices. Lower values for the conductivities may be expected, too, because the orifice is practically free on each side and hence approaches the Rayleigh condition.

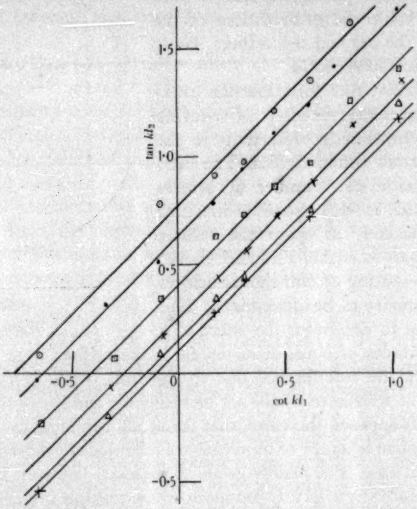

Figure 3. Orifices in parallel in a tube; $k=2\pi/\lambda$. Diameter of orifice (cm.): ⊙, 2·52; ●, 2·06; ⊡, 1·50; ×, 1·06; △, 0·80; +, 0·60.

§5. CONDUCTIVITIES AT THE JUNCTION OF TWO TUBES OF DIFFERENT DIAMETERS

The problem of the impedance at the junction of two tubes was next investigated, with the tubes first in series and then in parallel with the main tube. The tubes to be measured were fitted with massive pistons similar to that in the main tube, and each subsidiary tube was soldered to a flange which could be easily attached to the connecting piece and so form an extension to the main tube. The structure thus consisted of an orifice in series with a closed tube and its impedance was therefore given by

$$\frac{i\rho\omega}{K}-\frac{i\rho c}{S_2}\cot\frac{2\pi l_2}{\lambda},$$

where S_2 is the area of cross-section of the small tube and l_2 is the distance from the piston to the orifice. When silence was obtained in the headphones, the conductivity could be calculated from the relation

$$\frac{2\pi S_1}{\lambda K}=\frac{S_1}{S_2}\cot\frac{2\pi l_2}{\lambda}-\tan\frac{2\pi l_1}{\lambda} \qquad \text{......(1}a\text{)},$$

see equation (1*a*) of the appendix.

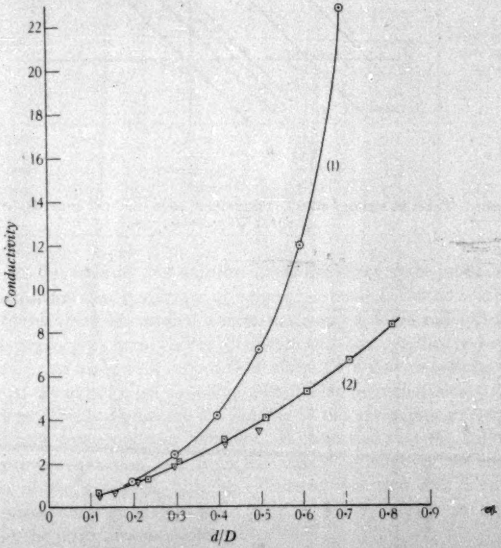

Figure 4. ⊙, orifices forming constrictions in a tube; ⊡, orifices terminating a tube; ▽, orifices in the tube walls.

The small tube was placed about half a wave-length from the pressure tube, in order to avoid the region of nonplanar wave-shapes and also to avoid large values of $\cot(2\pi l_2/\lambda)$ and $\tan(2\pi l_1/\lambda)$ which would be obtained if the junction were in the neighbourhood of a node. In this case $(S_1/S_2)\cot(2\pi l_2/\lambda)$ was plotted against $\tan(2\pi l_1/\lambda)$ as shown in figure 5. K was calculated from the intercepts. The results are also plotted against the ratio of the diameter of the smaller tube to that of the larger in figure 6. The curve is found to be represented by the formula

$$C=\frac{2{\cdot}0d}{(1-d/D)^{1{\cdot}446}} \qquad \text{......(6)}.$$

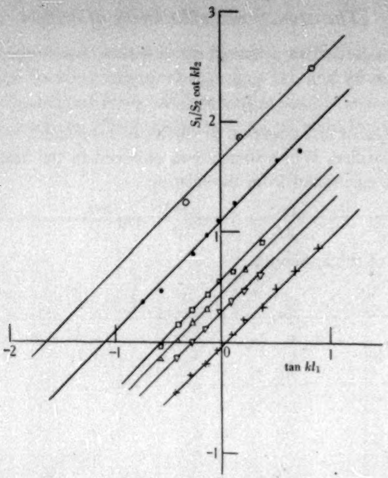

Figure 5. Tubes in series; $k=2\pi/\lambda$. Diameter of tube (cm.): ○ 0·91; ●, 1·24; □, 1·86; △, 2·17; ▽, 2·48; +, 5·98.

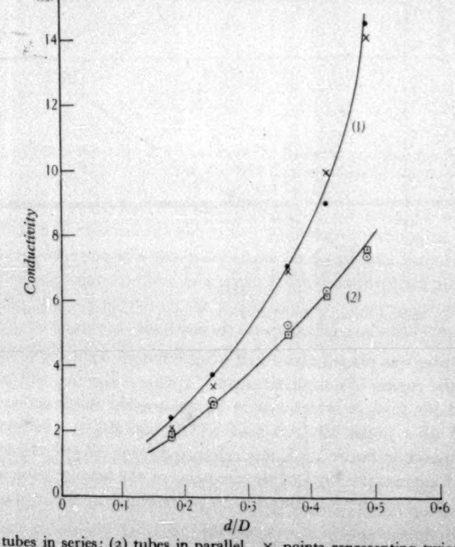

Figure 6. (1) tubes in series; (2) tubes in parallel. × points representing twice the conductivity of thin orifices in series; ⊡ points representing twice the conductivity of thin orifices in parallel.

Values calculated from the above expression are placed in column 5, table 2, and in the same table are shown the conductivities of thin constrictive orifices of the same diameter as the various tubes taken from curve (3), figure 4. The ratio of the conductivity at the junction to that for a thin constriction is about 2·1. This confirms a result previously obtained by A. E. Bate(2) that the conductivity of a single face should be twice that of an orifice having two sides.

Table 2. Conductivities at the junction between two tubes.
D, 5·08 cm.; $\lambda/2$, 15·84 cm.; temperature, 21° C.

Diameter d of tube (cm.)	d/D	Intercepts from figure 5	Conductivities			Ratio of K for tube to K for orifice
			Measured	Calculated from equation (6)	For orifice from curve (3) of figure 4	
2·48	0·488	0·285	14·0	13·1	7·1	1·98
2·17	0·427	0·435	9·2	9·7	5·0	1·85
1·86	0·366	0·555	7·24	7·20	3·5	2·07
1·24	0·244	1·09	3·70	3·72	1·7	2·18
0·91	0·179	1·65	2·43	2·42	1·05	2·43
5·98	1·17	0·03	134	158	—	—

A. E. Bate has also investigated experimentally the effect at the junction of two tubes. His experiments were performed on organ pipes having extensions of different diameters, and with these he verified a relation given by Aldis and stated in the appendix. The organ pipe was 5·4 cm. diameter and had attached a large tube 7·6 cm. in diameter which gave a ratio d/D of 1/0·71. He determined the position of an antinode in the organ pipe, sounding a particular frequency alone, and then attached the large tube and adjusted the lengths of the organ pipe and extension pipe until the same frequency was obtained. He assumed that the antinode remained at its previous position, and from the remaining length of the main pipe and the length of the extension pipe he calculated the ratio d/D from Aldis's formula. His results show good agreement (0·75, 0·78, 0·73, 0·71, 0·70, 0·71, 0·73) but the effect at the junction was neglected.

There is no reason to suppose that the conductivity at the junction between two tubes of different area should be greater in one direction than another, so that equation (6) should be applicable when d and D are interchanged; the junction may be regarded as composed of a tube 7·6 cm. forming the main tube and an end tube 5·4 cm. in diameter. Therefore $d/D = 0{\cdot}71$. With this assumption $K = 65$ and the term $2\pi S_1/\lambda K$, by which equation (1a) differs from the Aldis equation (2a), amounts to only 0·048. The two expressions therefore differ from each other only slightly when d/D is large. Where d/D is small, however, there may be considerable differences. The Aldis equation assumes that the corrected lengths of the respective tubes are used.

The meaning of end correction in such a case is very vague because when the diameters of the tubes are not too dissimilar each may be considered an approximately open pipe and hence each would require an end correction. The total end correction can be determined easily by experiment, but the proportion of end correction to be applied to each tube would be very difficult to assess.

It seems preferable therefore to consider the junction as a separate entity having a conductivity from which the impedance can be calculated, and to use the geometrical lengths of the two associated tubes for calculating the impedance of the structure embodying the junction.

§ 6. TUBES IN PARALLEL WITH THE MAIN TUBE

In order to attach tubes in parallel with the main tube a short length of brass tube 5·08 cm. in diameter was fitted with flanges by means of which it could be connected in the main tube. It had a platform screwed to it so that the branch tubes could be attached. A hole was bored right through the centre of the platform and the wall of the main tube towards the axis. Owing to the thickness of the platform and the curvature of the main tube there was a region which had to be filled with plasticene to form the junction to the branch. The actual opening of the branch tube into the main tube thus conformed to the curvature of the main tube. In equation (4*a*) of the appendix it is shown that the conductivity of the orifice at the junction of the two tubes is given by

$$\frac{2\pi S_1}{\lambda K}=\frac{S_1}{S_3}\cot\frac{2\pi l_3}{\lambda}-\frac{1}{\tan(2\pi l_2/\lambda)-\cot(2\pi l_1/\lambda)} \qquad \ldots\ldots(4a),$$

where S_1 and S_3 are the areas of cross-section of the main tube and branch respectively, l_1 is the length in the main tube from the pressure tube to the centre of the branch, l_2 the length in the main tube from the centre of the branch to the rigid piston, and l_3 is the length of the branch tube. The procedure was to keep l_1 constant and increase l_2 in steps of 1·0 cm., l_3 being adjusted at each step to give silence in the headphones. An alternative method was to vary l_3 in steps of 1·0 cm. and adjust l_2 to give a minimum. Both methods were tried but it was found that a more definite minimum was given by the first method. Figure 7 shows the result of plotting $(S_1/S_3)\cot(2\pi l_3/\lambda)$ against $(\tan 2\pi l_2/\lambda-\cot 2\pi l_1/\lambda)^{-1}$, from which the intercepts $2\pi KS_1/\lambda$ were obtained.

There was some doubt as to the length to be measured for l_3, for the length measured along the axis of the branch tube to the wall of the main tube was shorter than that measured along the wall of the branch tube to the wall of the main tube on a section perpendicular to the main tube axis and lying along the branch tube axis. The results were calculated for both methods of measurement and it was found that the latter gave better agreement with twice the conductivity of orifices of the same diameter in parallel, since this relationship was found to hold between these orifices and tubes in series with the main tube. The conductances are plotted in curve (2) of figure 6, the measured points being marked with a dot and circle while points marked with a square represent twice the conductivity of corresponding thin orifices in parallel as obtained from curve (2) of figure 4. W. P.

Mason(3) in his treatment of acoustical wave filters specifies that the length of a branch tube should be measured from the centre of the main tube, but this view is not borne out by the above results. The subject requires further investigation.

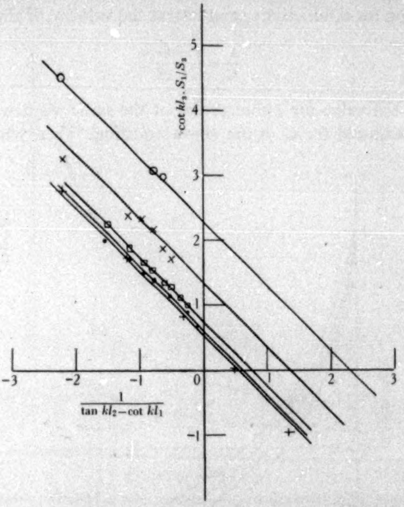

Figure 7. Tubes in parallel; $k = 2\pi/\lambda$. Diameter of tube in parallel (cm.): ○, 0·91; ×, 1·24; □, 1·86; ●, 2·17; +, 2·48.

It should be possible to obtain the shape of the wave-fronts in the neighbourhood of the junction by the method described in § 2. It would probably be found that in the case of ratios of d/D greater than about 0·5 the disturbance of the wave-fronts extends right across the main conduit, in which case it would be very difficult to predict an end correction. It seems preferable therefore to calculate the conductivity from the geometrical lengths of the tubes used.

§ 7. LONG ORIFICES AS CONSTRICTIONS IN A TUBE

The same method of experiment was used to measure the conductivities of long orifices or short tubes placed as constrictions in or at the end of a tube. A set of disks of thickness 0·3175, 0·635, 0·953 and 1·25 cm. was used, and all were bored at the centre with a hole of the same diameter. By using each disk separately and then in various combinations the length of the orifice could be increased to 3·175 cm. in steps of 0·3175 cm. The conductivity could be calculated from equation (8*a*). In order to prevent inaccurate results due to non-planar wave-fronts, the orifice was removed to distances in the neighbourhood of $\lambda/2$ from the pressure tube.

Orifices of 1·24, 1·89 and 2·52 cm. were measured at a frequency corresponding to a wave-length of 36·26 cm. at a temperature of 23° C., and the results are plotted in figure 8, each point on the graph being the mean of from six to ten separate measurements. It is evident from the graph that the length of the orifice has a profound effect on its conductivity, and to test the validity of the equation

$$\frac{1}{K}=\frac{1}{C}+\frac{L}{A}$$

for long orifices the value for a thin orifice of the same diameter was taken from figure 4 and substituted for C in the above equation. Then when A, the area of cross-section, and K, the measured conductivity, were known, a length L could be calculated which would be the effective length of the orifice. The ratio of the effective length to the measured length of the largest orifice is given in table 3. The experiments on the largest orifice were repeated at several different frequencies, and the results are shown in figure 9. As at the lowest frequency, the ratio of the effective length to the measured length was calculated, and this also is shown in table 3. There it is shown that the ratio is unity for an orifice whose length is equal to the diameter up to a frequency of about 1200 c./sec. when the diameter of the orifice is half the diameter of the tube. If the length is increased further, or the frequency raised, then the effective length is much larger than the actual length.

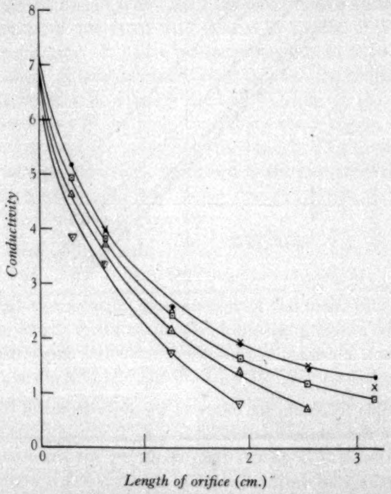

Figure 8. Orifices in tubes; variation of conductivity with length and frequency. Half-wave-length (cm.): ●, 18·13; ×, 13·35; □, 10·56; △, 7·98; ▽, 6·15.

On theoretical grounds one would expect that, at any particular frequency, as the length increased the medium inside the orifice would cease to move bodily, as the idea of conductivity implies, but begin to take up part of the wave-motion.

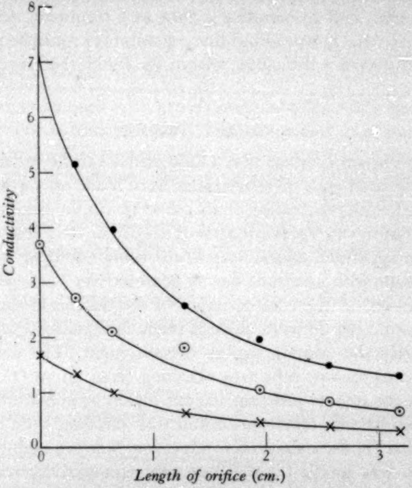

Figure 9. Orifice in tube; variation of conductivity with length. Diameter of orifice (cm.): ●, 2·54; ⊙, 1·89; ×, 1·24.

The orifice would then need to be considered as a short length of open tube with a separate orifice at each end. This case has been examined mathematically in the appendix, and a rather complicated expression, equation (7*a*), results. For the short lengths of tube under consideration it is sufficiently accurate to consider their lengths to be increased in the ratios given in table 3.

Table 3

Half-wave-length (cm.)	18·13	13·85	10·56	7·98	6·15
Length of orifice (cm.)	Ratio of effective length to measured length				
0·32	1·01	1·01	0·98	1·14	1·37
0·635	1·01	1·01	1·00	1·20	1·47
1·27	1·00	1·00	1·11	1·28	1·82
1·91	1·00	1·00	1·21	1·53	2·81
2·54	1·00	1·04	1·31	1·88	—
3·18	1·00	1·13	1·43	—	—

Diameter of orifice, 2·52 cm.; diameter of tube, 5·08 cm.

A tube which could be considered short at one wave-length would need to be considered long at a shorter wave-length. The limiting frequency at which the orifice may be considered short enough for equation (5) to apply without modification is rather indefinite, but these results indicate that a ratio (length of orifice)/(wave-length) of about 0·07 represents the upper limit.

Similar measurements were made on an orifice 2·5 cm. in diameter, of a length increasing to 2·54 cm., and terminating a tube at a frequency corresponding to a wave-length of 36·26 cm. It was found that equation (5) could be used for reducing the conductance to that of a thin sheet within the limits that are applicable for the orifices in a tube.

§ 8. SHORT TUBES

In order to test the supposition that a long orifice can be considered as an open tube with orifices at each end, measurements were made on constrictions 2·66 cm. in diameter and of lengths increasing from 1·0 to 16 cm. in steps of 1 cm., and at a frequency corresponding to a wave-length of 16·51 cm. at a temperature of 24° C. As is shown in the appendix, equation (7*a*), the tubes could be considered as consisting of a single tube with junctions having conductivity K at each end. Since the structure was symmetrical the conductivities of the orifices at each end should be the same, but a distinction between them is made in equation (7*a*) so that it might be possible to verify the assumption by measurement. The conductivity at the junction nearest the pressure tube was obtained from curve (1) of figure 6, and the conductivity at the remote junction was calculated by substituting the measured lengths of the tubes when a minimum sound was obtained from the microphone.

It was found that (1) the measured conductivity was unreliable when the length of the constriction was small; (2) the measured conductivity was also unreliable when the length of the constriction was approximately one quarter wave-length, and (3) a mean of conductivities measured on six constrictions of lengths 10 to 16 cm. resulted in a figure 12 being obtained instead of 15 from curve (1) of figure 6.

The agreement in finding (3) may be considered to be as satisfactory as the method will allow, as equation (7*a*) involves the tangents of three angles one of which $2\pi l_2/\lambda$ could be only approximate as the position of minimum sound intensity was not so clearly defined as in the previous experiments. The method of calculation was not strictly applicable to finding (1), for then the constriction could be treated as a short orifice and a correction applied for length as given by equation (5). In the second finding, however, the method of measurement was inaccurate because the length of the constriction gave rise to angles $2\pi l_1/\lambda$ and $2\pi l_3/\lambda$ in which the tangents were varying very rapidly.

The same tubes were then made to terminate the main tube. As for the long constrictions, the orifice was treated as a length of tube having an orifice at each end, the nearer orifice being at the junction between the main tube and the smaller tube while that at the remote end was the open end of the tube fitted with a baffle 5 ft. square. The case is treated mathematically in the appendix, and the result is given in equation (10*a*). Again the minimum was not so sharp as with the shorter orifices and hence the results are not so consistent. The measured conductivity at the remote end of the orifice tube was found to be 5·5 for the mean of seven lengths of tube from 10 to 16 cm., instead of 6·0 calculated from equation (4). For lengths of tube about one-quarter of a wave-length long the measurements were inaccurate. For shorter lengths of tube they could be considered as having been made on a single orifice and the usual correction could be applied.

APPENDIX. EVALUATION OF EQUATION (2)

The structures to be dealt with can be considered as made up of orifices together with open and closed cylindrical tubes. The impedances of these basic structures can be readily obtained from equation (1). Thus the impedance of an orifice is given by $i\rho\omega/K$, that of a closed tube by $-(i\rho c/S)\cot(2\pi l/\lambda)$, and that of an open tube by $(i\rho c/S)\tan(2\pi l/\lambda)$, where ρ is the density of the medium and c and λ are respectively the velocity of sound and wave-length in the medium, while K is the conductivity, ω the pulsatance, l the length of tube considered, and S the area of cross-section.

Let P, figure 10 (*a*), represent a point in the experimental acoustical system. Then the condition for zero acoustical pressure at P is given by

$$Z_2 = -(i\rho c/S_1)\tan 2\pi l_1/\lambda \qquad \text{......(2)},$$

where Z_2 is the terminating impedance.

The first structure considered consists of a closed tube concentric with a larger tube, figure 10 (*b*). In this case

$$Z_2 = i\rho\omega/K - (i\rho c/S_2)\cot(2\pi l_2/\lambda),$$

where K is the conductivity at the junction. Substituting in equation (2) we have

$$i\rho\omega/K - (i\rho c/S_2)\cot(2\pi l_2/\lambda) = -(i\rho c/S_1)\tan(2\pi l_1/\lambda),$$

from which

$$2\pi S_1/\lambda K = (S_1/S_2)\cot(2\pi l_2/\lambda) - \tan(2\pi l_1/\lambda) \qquad \text{......(1}a\text{)}.$$

If the impedance at the junction is neglected, then equation (1*a*) becomes

$$S_1/S_2 = \tan(2\pi l_1/\lambda)\tan(2\pi l_2/\lambda) \qquad \text{......(2}a\text{)}.$$

Here l_1 and l_2 are supposed to contain the end corrections. This equation was given by Aldis (4).

Orifice in parallel with the tube, figure 10 (*c*). In this case Z_2 must be considered as the effective impedance of the orifice and a closed tube in parallel. For zero acoustic pressure at P we have

$$\frac{1}{Z_2} = \frac{1}{i\rho\omega/K} - \frac{1}{(\rho c/S_1)\cot(2\pi l_2/\lambda)}$$

from which we have

$$\lambda K/2\pi S_1 = \tan(2\pi l_2/\lambda) - \cot(2\pi l_1/\lambda) \qquad \text{......(3}a\text{)}.$$

Closed tube as a side branch, figure 10 (*d*). The side branch consists of an orifice at the junction of the tubes and the length l_3 of closed tube in series. The effective impedance is that of the side branch and the stopped portion of the main tube in parallel.

$$\frac{1}{Z_2}=\frac{1}{i\rho\omega/K-(i\rho c/S_3)\cot(2\pi l_3/\lambda)}-\frac{1}{(i\rho c/S_1)\cot(2\pi l_2/\lambda)}$$

$$=-\frac{1}{(i\rho c/S_1)\tan(2\pi l_1/\lambda)}.$$

Therefore $$\frac{2\pi S_1}{\lambda K}=\frac{S_1}{S_3}\cot(2\pi l_3/\lambda)-\frac{1}{\tan(2\pi l_2/\lambda)-\cot(2\pi l_1/\lambda)} \qquad \text{......(4a).}$$

Narrower tube of any length forming a constriction. Referring to figure 10 (*e*) and using the notation of the diagram, we write

$$Z_q=i\rho\omega/K'-(i\rho c/S_1)\cot(2\pi l_2/\lambda) \qquad \text{......(5a),}$$

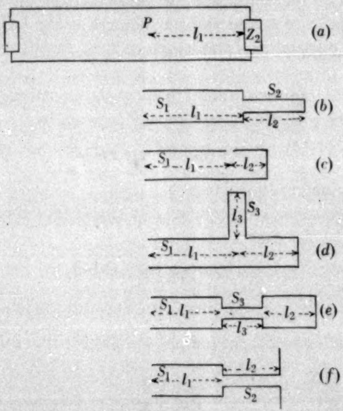

Figure 10.

where Z_q is the impedance facing the junction between tubes of areas S_3 and S_1, and K' is the conductivity at the junction. This should be the same as the conductivity at the junction S_1 and S_3 but is here kept distinct to enable the equation to be verified.

$$Z_2=\frac{i\rho\omega}{K}-\frac{iZ_q-(\rho c/S_3)\tan(2\pi l_3/\lambda)}{Z_q\tan(2\pi l_3/\lambda)\,S_3/\rho c+i}$$

$$=-(i\rho c/S_1)\tan(2\pi l_1/\lambda) \qquad \text{......(6a)}$$

for zero pressure at the pressure tube. Substituting for Z_q from (5*a*) and reducing we find

$$\frac{1}{K'}=\frac{\lambda}{2\pi S_1}\cot(2\pi l_2/\lambda)$$

$$+\frac{(\lambda/2\pi S_3)\tan(2\pi l_3/\lambda)+(\lambda/2\pi S_1)\tan(2\pi l_1/\lambda)+1/K}{(2\pi S_3/\lambda)\tan(2\pi l_3/\lambda)-1+(S_3/S_1)\tan(2\pi l_1/\lambda)\tan(2\pi l_3/\lambda)} \qquad \text{......(7a).}$$

It will be seen that if l_3 is considered small and K identical with K' then equation (7*a*) reduces to

$$2\pi S_1/\lambda K = \cot(2\pi l_2/\lambda) - \tan(2\pi l_1/\lambda), \qquad \ldots\ldots(8a).$$

which is the expression for an orifice in series with a stopped tube.

Length of open tube forming a termination. Referring to figure 10 (*f*), we write

$$Z_q = i\rho\omega/K'.$$

Hence, on substitution in equation (6*a*),

$$Z_2 = \frac{i\rho\omega}{K} + \frac{\rho\omega/K' + (\rho c/S_2)\tan(2\pi l_2/\lambda)}{(i\rho\omega/K')(S_2/\rho c)\tan(2\pi l_2/\lambda) + i}$$

$$= -(i\rho c/S_1)\tan(2\pi l_1/\lambda) \qquad \ldots\ldots(9a).$$

Which reduces to

$$\frac{1}{K'} = \frac{(\lambda/2\pi S_2)\tan(2\pi l_2/\lambda) + (\lambda/2\pi S_1)\tan(2\pi l_1/\lambda) + 1/K}{(S_2/S_1)\tan(2\pi l_1/\lambda)\tan(2\pi l_2/\lambda) - 1 + (2\pi S_2/\lambda K)\tan(2\pi l_2/\lambda)} \ldots\ldots(10a).$$

As will be seen if l_2 is made very small K and K' become inseparable and the equation reduces to

$$\lambda K/2\pi S_1 = -\cot(2\pi l_1/\lambda),$$

which is the relation for a single orifice terminating a tube.

REFERENCES

(1) Robinson, N. W. *Proc. Phys. Soc.* **46**, 772 (1934).
(2) Bate, A. E. Ph.D. Thesis, London (1932).
(3) Mason, W. P. *Phys. Rev.* **31**, 283 (1928).
(4) Aldis. *Nature, Lond.*, No. 309 (30 Aug. 1924).

DEMONSTRATION

A NEW DEMONSTRATION OF THE PHENOMENON OF BEATS *given* 25 *March* 1938 *by* D. A. RICHARDS, A.R.C.S., M.Sc., D.I.C., University College of Wales, Aberystwyth

THE apparatus used in this demonstration is shown diagrammatically in figure 1. Two brass cylinders *A* and *B* of equal mass are supported by two identical vertical steel spiral springs *C* and *D*. *A* and *B* are connected by a light flexible string *E* which passes under a light pulley *F*, the diameter of which is equal to the horizontal separation of the axes of the springs. A large needle *G* through the centre of the pulley serves as an axle. Suspended from this is a light rod *J*, the attachment being effected with thin brass wire. To the lower end of *J* is fixed a vertical card *K* which serves as a damping vane to prevent oscillations of *J* in a vertical plane perpendicular to the axle and also to lower the centre of gravity of the system supported by the string *E*. Fixed to the axle *G* is a light pointer *H*. Details of these attachments can be seen in figure 2.

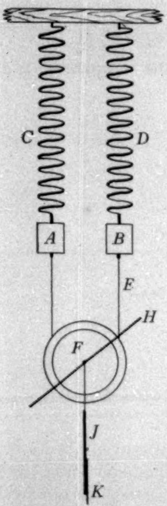

Figure 1.

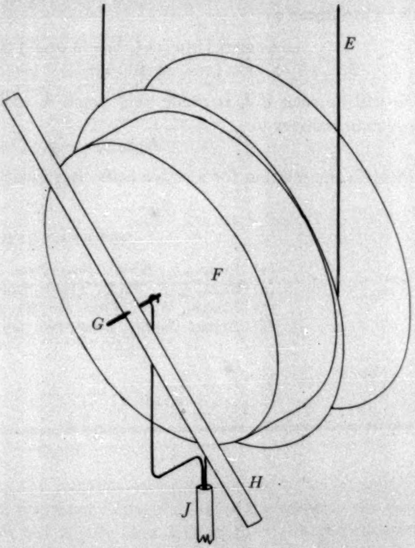

Figure 2.

If *A* is at rest and *B* is set oscillating in a vertical line, *G* will oscillate in a vertical line with half the displacement of *B* at any instant. Similarly *B* may be considered at rest and *A* displaced. If both *A* and *B* are displaced vertically the linear vertical displacement of *G* will be one-half the algebraic sum of the displacements of *A* and *B*. The difference in frequency between the two oscillating systems can be varied at will by the addition of a rider to the cylinder *B*. When this difference of frequency exists *G* will oscillate with a periodic change of amplitude.

Moreover, if *A* and *B* oscillate with the same amplitude, then when the oscillations are in phase, there will be no angular oscillation of the pointer *H* about *G*. Conversely when the two oscillations are out of phase there will be an angular oscillation of *H* about *G*. A difference of frequency between the two systems results in a continuous change in their phase difference. Hence the amplitude of the angular oscillation of *H* will vary periodically.

If the two springs are of equal strength, the two systems can be made to oscillate with the same amplitude by depressing *J* in a vertical line and then releasing.

Strictly speaking the two vibrating systems are not independent but are coupled, the degree of coupling being a function of the tension in the string *E*. The coupling can however be reduced to a small value by making the mass of the pulley small in comparison with that of *A* and *B*. The pulley was constructed by fitting a cardboard **V** groove to a large pill-box. *H* and *J* were light drinking straws. The mass of the system supported by the string is 13 g.

The apparatus is capable of giving good quantitative results. The individual vibrations were timed to an accuracy of about one part in 500, and the results are tabulated below. N_A and N_B are the frequencies of *A* and *B* respectively in cycles per second; N_F is the beat frequency.

N_A	N_B	$N_A - N_B$	N_F
1·072	0·862	0·210	0·2101
1·072	0·946	0·126	0·1266
1·072	1·010	0·062	0·0624

In the demonstration, a shadow of the apparatus was cast upon a white screen, the source of illumination being a bare arc. A considerable magnification could thus be obtained. The change in amplitude of the vertical oscillation of *G* can be more easily followed if the position of the centre of the shadow of the pulley on the screen is first marked when both *A* and *B* are at rest.

REVIEWS OF BOOKS

A Philosophy for a Modern Man, by Prof. H. LEVY. Pp. 287. (London: Victor Gollancz, Ltd., 1938.) 7*s*. 6*d*. net.

Prof. Levy evidently considers that the "modern man" for whom this philosophy is written is clever enough to study this difficult book, in which he not only expounds some of the fundamental concepts of physical science and mathematics but also attempts to apply these to socialism. The author, it will be remembered, is a professor of mathematics, a socialist, and a writer of works interpreting modern scientific conceptions for the non-specialist. It is not unnatural therefore that his methodical mind should encourage him to attempt to arrange this array of interests into some logical order—that is what he tries to do in this book. We have heard a good deal in recent years about the application of science to industry, but it is less usual to find science applied to the support of a political doctrine. Whether Prof. Levy is justified in the deductions which he draws from this application must be a matter for each reader to judge for himself and in any case this journal is hardly the place to discuss such matters. Some idea of the angle from which the book is written can perhaps be gleaned from the following quotation (p. 187): "It (the Darwinian theory) appears little more than the bald application of certain economic theories concerning the society of man, prevalent at the time of Darwin, to the animal world."

In the last chapters of the book will be found many of the well-known diatribes on socialism, which are not always in keeping with the more measured terms of the scientist adopted in the earlier part of the book. The author's conclusion appears to be that "the next age will be the classless society" and that no matter what else happens this stage is bound to come; therefore, he argues, we might just as well make deliberate plans to arrive at this stage by peaceful paths, rather than submit to world upheavals in trying to resist it.

The book contains some rather crude sketches and illustrations; and the print is small, making it a little trying to read.

For those scientists who interest themselves in political creeds and philosophies—and there are many who consider that it is the scientist's duty to do so—this book will be of considerable interest, whatever their own beliefs. The dust cover tells us that the book "may well have a profound effect on the thought of our generation". Perhaps it may.

H. R. L.

The Evolution of Physics, by A. EINSTEIN and L. INFELD. Pp. x + 320. (Cambridge: The University Press, 1938.) 8*s*. 6*d*. net.

Once again we have original workers of the highest rank attempting to explain physics to the layman. Unlike some of their predecessors, the authors do not stress the numerical or sensational aspects of recent work, and there is no description of the results of experiments on atom-splitting. Their task is harder, for they wish to make clear what is the nature of the change which has come over physics in the last 35 years, that is, since the advent of the relativity and quantum theories. To this end they trace in very brief outline the history, not of physics, but of physical thought, taking their origin with Galileo's realization of the law of inertia, without reference for example to Roger Bacon or any of the earlier thinkers on the matter.

The first change which they regard as significant was the introduction, or perhaps the stressing, of the concept of the "field" in place of particles and charges, and this step they describe very clearly. It is a question for experiment to decide whether even the clearest description can bring out the significance to laymen, though there is no question that physicists who read the book will gain some insight which is not provided by a more detailed treatment, where the equations perhaps obscure the ideas. As we should expect, the philosophy of relativity is explained very clearly indeed. The last section deals with quantum theory (real quantum theory, not quantum additions to classical theory) and quite satisfactorily leads to an account of the difficulties which still confront us. In particular, there is the difficulty that nobody has yet succeeded in formulating the equations of quantum mechanics in a form invariant to the Lorentz transformation.

As far as externals go, the book is certainly made as easy as possible for the layman. There really is not an equation in it, even in disguise, and the illustrations show a delightful freshness. An author in search of flatland, in order to explain by analogy what a fourth dimension in space would be, has it ready to hand on the cinema screen, but Drs Einstein and Infeld are, I imagine, the first to realize this. They admit in their preface that they have given considerable thought to the properties of their ideal reader. They find that his great virtues are patience and perseverance, and they say that he is not to proceed to a fresh page till he has mastered the current one. Thus the book is not intended to while away an idle hour, but the greater effort required is compensated by the truer and clearer grasp of the subject which should result.

J. H. A.

Modern Physics, by G. E. M. JAUNCEY. Second Edition; pp. xviii + 602. (London: Chapman and Hall, 1937.) 22*s*. net.

It is never very difficult, and rarely quite fair, to criticize an elementary "Modern Physics" on the ground of its author's selection of material. Prof. Jauncey, for example, says nothing about the Zeeman effect, though he gives the theories of the reversible pendulum and the parallel-plate condenser, which are appreciably less "modern" in any sense of the term. Although the Zeeman effect has played a most important part in the development of electrical theories of matter and quantum theories of spectra, its omission here is clearly deliberate, as it had several pages in the first edition of 1933. On the whole, it must be said that Prof. Jauncey has made an excellent choice of topics—ranging from geophysics to nuclear physics—and has handled them in the manner of an experienced teacher and active physicist, without unduly stressing the portions which happen to be cognate with his own special subjects of research.

He starts from two very sound premises—viz., that some instruction in "modern" physics is desirable at a quite early stage in undergraduate courses, and that "it is necessary to know something of the history of physics in order to understand fully the meaning of modern physics". The book therefore begins with a short (34-page) historical introduction, and more attention than is usual in books of similar scope is given to both the historical and the numerical aspects of the topics under consideration. There are well-chosen numerical examples, with solutions, and the book is very suitable for use by first-year honours students of physics and other science students.

H. R. R.

A Text-Book on Crystal Physics, by W. A. WOOSTER, M.A., Ph.D. Pp. xxii + 295. (Cambridge: The University Press, 1938.) 15*s*. net.

No book devoted entirely to crystal physics has previously been published in English, and this in itself should be a sufficient excuse for the appearance of the present volume. The book is intended to be a textbook for students at universities and has been written with two objects—to present the classical treatment of the physical properties of crystals in terms of tensor notation, and to indicate the lines of development of modern theoretical and experimental researches. With these objects in mind the mechanical, thermal, electrical, magnetic and optical properties of crystals are discussed and related where possible to the crystal structure or the nature of the constituent atoms or ions.

Certain subjects—ferromagnetic crystals, the mechanics of crystal lattices and much of crystal optics for example—are deliberately omitted, but a considerable amount of information is nevertheless packed into a relatively small space. One of the most desirable features of the book is, in fact, its conciseness and freedom from wasteful repetition, but as a result there is a tendency in places towards a certain amount of obscurity. Parts too will be difficult for the student who, with no previous knowledge of tensor notation, is equipped only with the knowledge of the "elements of physics, mathematics and crystallography" demanded of him.

The book as a whole, however, is one that will thoroughly repay study, and may be recommended to student and research worker alike.

J. T.

A Text-book of Physics, by L. B. SPINNEY. 5th edition. Pp. xii+720. (The Macmillan Co.) 16*s*. net.

All who have recommended earlier editions of this textbook for junior students will welcome the new edition. Among other changes there is a new chapter on electron tubes and some brief reference is made to recent experimental work in nuclear physics. Much of the text has been revised and many new diagrams and problems have been added.

J. H. B.

Grimsehls Lehrbuch der Physik, revised by R. TOMASCHEK. Vol. II, Pt. 2. Matter and Ether. Pp. viii+456. (Leipzig: B. G. Teubner.) RM. 14.

The number of the editions of Grimsehl's textbook of physics (vol. I is in its ninth, vol. II in its eighth edition) speaks for the popularity of the work in Germany. This popularity can only be enhanced by the present volume. Prof. Tomaschek deals here with those properties of matter and radiation which directly involve atoms, electrons, protons, quanta, and the like. The treatment of this subject-matter is as comprehensive and up-to-date as could be required of a textbook. For example, the discussion of spectral lines embraces Landé's formula for the splitting factor g, Russell-Saunders coupling, superfine structure, the Raman effect and the isotope effect in band spectra. There is an excellent chapter on nuclear transformations (new in this edition) and short accounts are given of many special lines of work such as the scattering of X rays by liquids, Heitler and London's theory of the hydrogen molecule, ortho- and para-hydrogen, the inner photoelectric effect in crystals, the mode of origin of the northern lights, and axiality of light-emission. The more fundamental topics—the Rutherford-Bohr atom, the wave properties of the electron and so on—receive adequate treatment. A chapter on the electrodynamics of moving media finds a place, although it stands apart from the rest of the subject-matter.

The book is written in a clear, terse style. This is not unconnected with the fact that Prof. Tomaschek has been at pains to keep the experimental facts in the forefront. Where mathematical treatment is necessary the symbols are carefully defined, and space is devoted to the interpretation of the final result rather than to details of the proof. The text is embellished with 44 tables and 339 figures, included in the latter being a good selection of cloud-chamber photographs. There can be no doubt that this book reaches a very high standard, and the student who makes his acquaintance with the elements of atomic physics in its pages may count himself fortunate.

W. S. S.

The Flow of Homogeneous Fluids, by M. Muskat, Ph.D. Pp. xix + 763. (London: The McGraw-Hill Publishing Co. Ltd.) 45*s.* 0*d.*

The full title of this monograph, which is one of the International Series in Physics, is "The flow of homogeneous fluids through porous media". It is to be regretted that an abbreviated title should have been used on the cover, since it hardly conveys a precise indication of the scope of the volume.

The book deals in a thorough and comprehensive manner with the flow of liquid in porous media, a subject which is of considerable interest to the oil and gas industries. As the author points out, no attempt is made to solve what is really the fundamental physical problem in most actual cases of oil production, namely, the nature of the flow of gas-oil mixtures through porous media. This problem is one in the flow of heterogeneous fluids through porous media whilst the work is limited to the flow of homogeneous fluids. There is nevertheless a considerable number of problems of oil-production which can be solved by means of analytical results derived from a homogeneous-fluid theory, and there is a possibility that these problems will find still wider application in the future when more efficient use comes to be made of the possibilities of natural water drives.

This book has not been written simply as a college textbook. A thorough knowledge of the calculus and some familiarity with the elements of differential equations are assumed. The treatments of the problems have been given with such detail as to illustrate clearly the method of solution as well as the physical significance of the problem.

The treatment of the subject is divided into four parts. In the first the foundations are laid for the subsequent analytical treatment. The technique for determining the permeability of the medium is described. The empirical laws are formulated generally in three partial differential equations which form the starting-points for the analysis of the other three parts. The second part treats of problems of fluid flow in the steady state, the compressibility being formally neglected in the sense that the fundamental dependent variable satisfying Laplace's equation is taken as the pressure rather than the density. Potential-theory methods are then applied successively for the solution of two-dimensional and three-dimensional problems, gravity-flow systems, systems in which the porous medium is of non-uniform permeability, systems involving two homogeneous fluids, and finally multiple-well systems. In several cases experiments with sand and electrical models are described as means for obtaining results in cases in which the analysis becomes impracticable. Part 3 gives the treatment of typical cases of the non-steady-state flow of liquids, as based upon the Fourier heat-conduction equation with the fluid density as dependent variable. Part 4 in a single chapter gives the solutions for typical cases of gas flow, though here the analysis for the unsteady state is only approximate owing to the difficulty of obtaining exact solutions of the basic differential equation.

The methods employed are developments of potential theory and the theory of heat-conduction. A large part of the analysis is taken from papers and reports written by the author and his colleagues for the Gulf Research and Development Co. The volume impresses one with the vast amount of labour which has been expended on a highly specialized subject.

E. G.

An Introduction to Laboratory Technique, by A. J. Ansley. Pp. xiii + 313. (London: Macmillan and Co. Ltd.) 12*s.* 6*d.*

This book has been written primarily at the request of persons engaged in teaching physics, but it will also be of some use for laboratory assistants. It contains a résumé of several of the processes and certain of the techniques normally required in laboratories. The chapter headings are: Care of laboratory equipment; Cements, lutes and solvents; Electrical measuring and indicating instruments; Electric motors; Electro-plating; Glassblowing and glass-working; Graduation of apparatus; Insulators and their working; Mercury and its purification; Optical projection of lantern slides; Production of mirror surfaces; Soldering of metals; Storage cells; Miscellaneous; First aid treatment for laboratory workers; and Tables.

The author does not claim the book to be more than "an introduction" and it is written in a style which may be taken to assume that the reader has little or no previous knowledge of the subject. As the author himself points out, "no mere book-work, however, can completely fulfil the purpose for which this volume is designed; this can only be realised in its highest degree by patient and constant practice. Some of the recipes given are perhaps controversial; but on the other hand every experienced laboratory technician has his own favourite way of achieving an end which may be reached by several alternative methods." The occasional use of such unscientific expressions as "high degree of heat" or "in the best glasses the prolonged action of cold water merely attracts a minute trace of alkali," is unfortunate; and the continuous use of adjectives such as "carefully" "good" and "best-quality" detracts from the greater emphasis they would give if used more sparingly. The book contains some information which must be well known even to those for whom it is primarily intended. In table XX the units of specific heat are omitted and we are not told whether the coefficient of linear expansion is per °C. or per °F.

The book should be useful to those who find themselves without skilled laboratory assistants and have had no training in these matters. It is to be hoped, however, that in the near future the author will provide a similar book confined to useful practical hints and tips together with well-tried formulae and recipes for the benefit of those already familiar with the elementary parts of the subject; the reviewer believes there is a real demand for an up-to-date book of this nature.

H. R. L.

Photoelements and their Applications, by B. LANGE. Translated by A. ST JOHN. Pp. 297. (New York: Reinhold Publishing Corporation; London: Chapman and Hall, Ltd.) 27*s*. 6*d*. net.

The appearance of the first book exclusively devoted to the rectifier photoelectric cell, at times designated the barrier-layer, blocking-layer or Sperrschicht cell, and here the photoelement, heralds the rapid development of the latest addition to the growing family of photoelectric cells. Following the rediscovery of the rectifier photocell in 1928, fifty years after the original work of Uljanin, Adams and Day, Fritts and others, commercial development has proceeded at such a pace that new uses are constantly being found for these cells in illumination-measurements in industrial and research laboratories throughout the world. Unquestionably, then, a book, relieving one of the labour of referring to and appraising original papers, has become a pressing need.

The book under review is a somewhat free translation of one originally published in German in 1936. No effort has been made to include later work for the English version; hence in the main only work carried out up to the end of 1935 is detailed. A further limitation has been imposed by the surprising exclusion from the German version of any references (with few exceptions) to work carried on outside Germany. There is thus no mention of the many theoretical and experimental researches made in Russia, Holland, Belgium, France, the United States of America and Great Britain. In short, the scope of the book is limited mainly to researches made in Germany; and largely to the work of B. Lange. A detailed account in English of his work is, however, not without interest.

Considerable space is devoted to the cuprous-oxide cell. In later works, this cell will doubtless be of little more than historical significance, its place having already been taken by the more sensitive selenium rectifier photocell. There are, nevertheless, common features in the characteristics of the two types of cell. Many of the properties are, however, interpreted in terms of theories which have largely been superseded by the wave-mechanical interpretation of the barrier-layer effect expounded by A. H. Wilson, Fowler, Frenkel and Joffé, Condon and others. Some of the difficulties have hence been resolved, though we have not as yet as complete an understanding of all the phenomena presented as could be desired.

The reader has to remain satisfied with a schematic diagram of the rectifier photocell reduced to its simplest terms without even a few details concerning the construction. Unpublished patent specifications are responsible for this omission. The general reader will consequently be much more interested in the very many ingenious applications fully described; this part of the book is to be commended. Here and there, Dr Lange permits his enthusiasm for his work to outweigh his usually sound judgement; an occasional tendency to belittle or minimize the errors possible in the use of these cells is apparent. The rectifier photocell always gives an answer innocently and with apparent assurance to the question "How much?" A timely warning on appropriate occasions concerning the lying-propensities of these cells would have been useful.

G. P. B.

Mathematical Tables, Vol. VI; (Bessel Functions, Part 1). Prepared by the British Association Committee for the Preparation of Mathematical Tables. Pp. xx + 288. (Cambridge: The University Press, 1938.) 40*s*.

Here we have both an achievement and a memorial. It is now half a century since the British Association first appointed a committee to consider the preparation of mathematical tables, having in mind Bessel functions in particular. To it was appointed, among others, Prof. Alfred Lodge. The work went slowly at first, though various useful tables were included in the Annual Reports of the Association from time to time. With the War the work almost came to a standstill. Then the committee was reorganized, still numbering Lodge among its personnel, and in 1931 the first volume appeared, dealing in the main with trigonometrical functions. Four more volumes were published, and then at last the committee, having cleared the ground sufficiently, was ready to issue the first of the volumes dealing with Bessel functions. At a meeting of the committee of Section A last year the members were let into the secret that the new volume was to be dedicated to Prof. Lodge, though he was not to know it until he saw it in print. He died a few days before publication, but the inscription stands.

The volume is worthy of the work spent on it. It gives only the functions of the orders zero and unity, to eight decimal places, and covers directly the range up to $x=25$, and indirectly up to 6000, whereas all previous sets of tables ceased before $x=42$; and it goes without saying that the precautions taken against misprints are as thorough as can be devised, short of the use of photographic methods of reproduction from a script typed by a calculating machine.

J. H. A.